Assessing Groundwater Impacts from Coal Combustion Products Used In Highways

by

Lin Li, Craig H. Benson, and Tuncer B. Edil

Geo Engineering Report No. 05-22

Department of Civil and Environmental Engineering
University of Wisconsin-Madison
Madison, Wisconsin 53706
USA

December 30, 2005

EXECUTIVE SUMMARY

This report describes a computer application that was developed to assess impacts to groundwater caused by leaching of trace elements from CCPs used in highway construction. Laboratory and field experiments conducted to verify the application are also described. The application, referred to as WiscLEACH, is based on three analytical solutions to the advection-dispersion-reaction equation that describe transport in the vadose zone and groundwater. The application was designed to be computationally efficient and can be used without experience in numerical modeling.

WiscLEACH was calibrated using predictions from HYDRUS-2D, a widely used and carefully verified numerical model for simulating flow and transport in variably saturated media. Identical simulations were conducted with both models, and the dispersivities in WiscLEACH were adjusted until similar distributions of concentration were predicted. Field and laboratory experiments were also conducted on CCPs to provide data for verifying WiscLEACH. Comparison of measured concentrations of trace elements with those predicted by WiscLEACH indicate that the application over-predicts measured concentrations slightly, which is a conservative error.

Predictions made with WiscLEACH indicate that maximum groundwater concentrations of trace elements leached from CCPs typically occur close to the groundwater table and near the centerline of the pavement structure. Peak groundwater concentrations decrease as the depth to groundwater increases, the thickness of the byproducts layer decreases, the seepage velocity in the vadose zone decreases, or the seepage velocity in groundwater increases. Parametric studies have shown that the variables having the greatest influence on maximum concentrations in groundwater are depth to the groundwater table, thickness of the CCP layer, hydraulic conductivity of the least conductive layer in the vadose zone, hydraulic conductivity of the aquifer material, and the initial concentration in the CCP layer.

ACKNOWLEDGEMENT

Financial support for this study was provided by the Wisconsin Department of Natural Resources Waste Reduction and Recycling Demonstration Grant Program and Alliant Energy. The findings and inferences that are reported are those solely of the authors. Endorsement by the sponsors is not implied and should not be assumed. The software application developed in this study will be available as freeware in 2006 at www.uwgeosoft.org.

TABLE OF CONTENTS

1. INTRODUCTION

Over 120 million Mg of coal combustion products (CCPs) are produced each year by coal-burning electric utilities in the US (ACAA 2003). CCPs include fly ash, bottom ash, boiler slag, flue gas desulfurization (FGD) material, and scrubber residues. In 2003, fly ash constituted 60% of the total mass of CCPs produced in the US, and bottom ash constituted 20%. Approximately 38% of CCPs are re-used in various applications. The remaining 62% is disposed in landfills and impoundments (ACAA, 2003).

There is considerable interest in finding uses for CCPs that are currently being disposed in landfills. In fact, federal and state legislation is encouraging, or even mandating the reuse of byproducts (Eighmy and Chesner, 2001). Many of the CCPs that are being disposed have desirable properties, and finding methods to use them is consistent with the principles of sustainable construction and development. Highways are of particular interest, because highway construction has potential for large volume use of CCPs. For example, fly ash can be used in concrete pavement, for stabilization of base course and subgrades, and for structural fill and embankments (Edil and Benson, 2002). Bottom ash can be used in structural fills, embankments, road base, and subbase (Kalyoncu, 2002). Using CCPs in highway construction can reduce CCP disposal costs and reduce the need for natural resources commonly used in construction.

Potential impacts on groundwater quality are an issue when industrial byproducts such as CCPs are used in highway construction. Trace elements in CCPs such As, Cd, Cr, Se, Cu, Pb, Zn, and B may leach from CCPs and migrate into underlying groundwater. The objective of this study was to develop a model that can be used to assess potential groundwater impacts caused by leaching from CCPs used as base, sub-base, subgrade, or structural fill in highway applications and to validate the model

using laboratory tests and field data collected from highway test sections constructed with CCPs. This report describes the model that was developed (WiscLEACH) and the validation using laboratory and field data. Field and laboratory data collection efforts conducted as part of this study are described in the appendix.

2. BACKGROUND

2.1. Leaching of Trace Elements from CCPs

Leaching of trace elements and their environmental impacts on surface water, groundwater, and soil is a concern when using CCPs in highway applications. Previous studies have shown that Ag, As, B, Ba, Cd, Cr, Co, Cu, Hg, Mg, Ni, Pb, Sb, Se, and Zn leach from CCPs (Kim, 2002; Praharaj et al., 2002). The release of elements from CCPs is strongly influenced by pH (Fleming et al., 1996; Ricou et al., 1998). Low pH favors leaching of elements such as Ag, Cd, Cr, Hg, Ni, Pb, and Zn (Kim, 2002). Higher pH favors leaching of elements such as As (Bin-Shafique et al., 2006). For many CCPs, trace elements are released in very low quantities due to the alkaline nature of CCPs (Bin-Shafique et al., 2006; Kim et al., 2003; Wang et al., 2004).

Release of trace elements from CCPs is largely controlled by adsorption-desorption and dissolution (Bin-Shafique et al., 2006; Mudd et al., 2004; Murarka et al., 1991; Wang et al., 2004). Murarka et al. (1991) suggests that leaching of trace elements from fly ash is solubility controlled. Bin-Shafique et al. (2006) indicate that trace element leaching from fly-ash-stabilized inorganic soils is adsorption controlled and that partitioning generally can be assumed to be instantaneous, linear, and reversible. The partitioning is a function of pH, the liquid-to-solid ratio, and the physical and chemical characteristics of the fly ash and soil (Kosson et al., 2002; Wang et al., 2004, Bin-Shafique et al., 2006).

Two distinct leaching pattern have been observed during column leach tests on CCPs and highway materials stabilized with CCPs: “first flush” and “lagged response” (Sauer et al., 2005a) (Fig. 1). The “first flush” response is characterized by a high initial concentration followed by decreasing concentrations as more water flows through the material (Bin-Shafique et al., 2006; Mudd et al., 2004). The “lagged response” is characterized by a low initial concentration, followed by an increase in concentration, and then a decrease in concentration (Creek and Shackelford, 1992; Edil et al., 1992). Creek and Shackelford (1992) indicate that the leaching pattern is related to the charge density of the elements being leached. Bin-Shafique et al. (1992) indicate that the first-flush leaching pattern from CCPs can be described mathematically by the advection-dispersion-reaction equation (ADRE) with instantaneous, linear, and reversible sorption.

In Wisconsin, the *Wisconsin Administrative Code* requires that batch water leach tests (WLTs) following ASTM D 3987 be conducted on CCPs that are used in confined geotechnical applications such as highway base, subbase, and subgrades. Concentrations of four trace elements (Cd, Cr, Se, and Ag) in the leachate must not exceed specified standards (Cd: 25 μg/L, Cr: 500 μg/L, Se: 250 μg/L, Ag: 250 μg /L). Column leach tests are also conducted in some cases to evaluate leaching from CCPs under flow-through conditions, although CLTs are not required by Wisconsin regulations. The *Wisconsin Administrative Code* also provides maximum concentrations in groundwater for the elements of concern for CCPs (Cd: 5 μg/L, Cr: 100 μg/L, Se: 50 μg/L, Ag: 50 μg /L). These groundwater standards, which are analogous to maximum contaminant levels stipulated by USEPA, must be maintained at a point of compliance, which normally is the boundary of the right-of-way for highways.

2.2. Models to Assess Impacts to Groundwater from Byproducts

Two types of computer models have been used to assess leaching behavior: geochemical models and flow and transport models. Geochemical models have been developed that simulate equilibrium dissolution/precipitation (Batchelor, 1998; Garrabrants et al., 2003; Moszkowicz et al., 1996; Moszkowicz et al., 1998; Park and Batchelor, 2002), surface complexation and surface precipitation (Dijkstra et al., 2002; Guo et al., 2004), and material heterogeneity (Sanchez et al., 2003). These models couple diffusive transport with chemical equilibrium or kinetic reactions describing partitioning of leaching contaminants between the liquid and solid phases. However, these models do not consider transport in soil or groundwater (Kosson et al., 2002).

The flow and transport models SESOIL, IMPACT, and HYRDUS-2D have been used to simulate transport of trace elements leached from byproducts in subsurface soil and groundwater (Apul et al., 2005; Bin-Shafique et al., 2002; Hesse et al., 2000). SESOIL (Seasonal Soil Compartment Theory and Model) is a screening-level one-dimensional transport model that can simulate advection, diffusion, adsorption, volatilization, biodegradation, cation exchange, and hydrolysis. The model is based on mass balance and equilibrium partitioning between phases. Output from SESOIL includes time-varying pollutant concentrations at various soil depths as well as losses to surface runoff, groundwater, volatilization, and degradation. SESOIL is integrated in Minnesota's STUWMPP model for evaluating use of byproducts in highway construction (Friend et al. 2005).

IMPACT was developed to assess the environmental impact of highway construction and repair materials on surface water and groundwater (Hesse et al., 2000). IMPACT simulates one-dimensional vertical flow and solute transport by solving the ADRE using the finite-difference method. Steady flow is assumed and all materials are assumed to be saturated. Sorption is assumed to be instantaneous and reversible. A

database of leaching parameters is included that are derived from batch leach tests, column leach tests, and flat plate leach tests conducted in the laboratory. The leaching rate is described by a power function to fit to laboratory data.

HYDRUS-2D is a widely used and verified Windows® software package for simulating water and solute movement in two-dimensional variably saturated media. Apul et al. (2005) and Bin-Shafique et al. (2002) have used HYDRUS-2D to study leaching of trace elements from highways constructed with industrial byproducts. HYDRUS-2D solves Richards' equation for two-dimensional variably saturated water flow and the advection-dispersion equation for solute transport using the finite element method (Simunek et al., 1999). Bin-Shafique et al. (2002) used HYDRUS-2D to simulate selenium (Se) leaching and transport in a fly-ash-stabilized highway subgrade in Wisconsin. Se concentrations predicted with HYDRUS-2D were found to be in good agreement with concentrations observed in pan lysimeters installed beneath the highway. Parametric simulations conducted with the model showed that the maximum concentration of leached trace elements decreases by a factor of 5 times within 1 m from a fly-ash-stabilized soil layer and then decreases more gradually at deeper depths. Apul et al. (2005) combined HYDRUS-2D and a Bayesian approach for probabilistic calibration of hydraulic parameters to reproduce measured water contents in a Minnesota highway embankment. Leaching of cadmium (Cd) from a hypothetical fly ash embankment was simulated and compared to results obtained with a percolation equation method, where the aqueous solubility is multiplied by the liquid-to-solid ratio to estimate the total release. Concentrations predicted by HYDRUS-2D were substantially lower than those predicted by the percolation equation method.

3. MODEL FORMULATION

The model developed in this study was required to (i) be relatively easy to use by designers and regulators that may not have expertise in numerical modeling, (ii) execute rapidly so that parametric simulations can be conducted efficiently, (iii) use readily available input (e.g., from climatic data bases and conventional laboratory tests), (iv) predict concentrations in the vadose zone, groundwater, and at a point of compliance (boundary of the right of way), and (v) provide predictions that are shown to be accurate or conservative. The model also needed to use routines and algorithms in the public domain so that a software application could be distributed as freeware.

The model, referred to herein as WiscLEACH, is based on a combination of three analytical solutions of the ADRE so that execution is rapid and numerical modeling expertise is not required. Input to the model consists of the annual precipitation rate (available for most locations from the National Weather Service), physical properties of the pavement layers and underlying soils (available in textbooks and in highway engineering reports), leaching characteristics of the byproducts derived from batch or column leaching tests (required for most byproducts applications), and transport parameters for the subsurface (available from textbooks or the literature). WiscLEACH was calibrated by comparison with predictions made with HYDRUS-2D and verified with monitoring data from a full-scale field study where fly-ash-stabilized subgrade and bottom ash were used for construction of a state highway.

3.1. Conceptual Model

The conceptual model consists of a CCP layer in a typical highway structure as shown in Fig. 2. The CCP layer is underlain by a subgrade and overlain by base course and pavement or shoulder material. Groundwater exists at a specified depth below the CCP layer. All materials in the profile are assumed to be homogenous and isotropic.

Precipitation falling on the pavement surface, the shoulders, and surrounding ground becomes infiltration or is shed as runoff. Steady, one-dimensional unit gradient flow is assumed in the pavement layers and the vadose zone, with the rate of flow (q_v) controlled by the least conductive layer in the profile (i.e., $q_v = K_{min}$, where K_{min} is the lowest hydraulic conductivity in the profile). The rate of vertical flow may vary across the section, but horizontal mixing of flows is not considered. The net infiltration rate is assumed to equal q_v. Evaporation from the surface of the pavement, the shoulders, and the surrounding ground is not considered (i.e., all water that infiltrates moves downward).

Trace elements leach from the CCP layer as water percolates down through the profile. This water migrates downward through the subgrade soils until the groundwater table (GWT) is reached. Leaching from the CCP layer is assumed to be sorption-controlled with linear and reversible partitioning or is defined empirically by the user. Transport in the vadose zone is assumed to follow the advection-dispersion-reaction equation (ADRE) with instantaneous, linear, and reversible sorption. Bin-Shafique et al. (2006) show that this assumption is valid for inorganic soils stabilized with fly ash and typical subgrades.

Trace elements that reach the GWT are transported horizontally and vertically, although the flow of groundwater is assumed to occur predominantly in the horizontal direction. Steady saturated groundwater flow is assumed and transport is assumed to follow the ADRE with instantaneous, reversible, and linear sorption. In both layers, chemical and biological reactions that may consume or transform trace elements are assumed to be absent.

Input to the model consists of the average annual precipitation rate, hydraulic conductivity of each of the layers, retardation factor for the CCP layer and underlying layers, geometry of the pavement structure and right of way, depth to groundwater,

retardation factors in the vadose zone and below the groundwater table, and input parameters describing leaching from the CCP layer.

3.2. Vadose Zone

Transport between the ground surface and the groundwater table (GWT) is assumed to follow the ADRE for one-dimensional steady-state vertical flow with two-dimensional dispersion and linear reversible sorption (Bear, 1979):

$$R\frac{\partial C}{\partial t} = D_x \frac{\partial^2 C}{\partial x^2} + D_z \frac{\partial^2 C}{\partial z^2} - v_z \frac{\partial C}{\partial z} \quad (1)$$

where C is the solute concentration, t is time, x is horizontal distance from the centerline of pavement, z is depth below ground surface (bgs), v_z is the seepage velocity in vertical direction, D_x and D_z are dispersion coefficients in the x and z directions, and R is the retardation factor. The seepage velocity in Eq. 1 equals $\min(q_v/n_i)$, where n_i is the effective porosity of the i^{th} layer in the profile (pavement, base, CCP layer, or subgrade). The hydrodynamic dispersion coefficients are computed assuming $D = \alpha v_z + \tau D_o$, where α is the dispersivity (vertical or horizontal), τ is the tortuosity, and D_o is the molecular diffusion coefficient for the trace element being considered. In most cases, the term τD_o is small compared to αv_z, and can be ignored.

An analytical solution to Eq. 1 provided by Leij et al. (1991) can be used for cases where the release of trace elements from the CCP layer follows a “first-flush” leaching pattern with instantaneous, linear, and reversible sorption. The solution to Eq. 1 is obtained by applying the following initial and boundary conditions

$$C(x,z,t=0)=\begin{cases} C_o & \text{at } z_T < z < z_B \text{ and } -L < x < L \\ 0.0 & \text{otherwise} \end{cases} \quad (2a)$$

$$\left(v_z C - D_Z \frac{\partial C}{\partial z} \right)\Bigg|_{z=0} = 0 \quad (2b)$$

$$\frac{\partial C}{\partial x}(\pm\infty, z, t) = 0 \quad (2c)$$

$$\frac{\partial C}{\partial z}(x, \infty, t) = 0 \quad (2d)$$

where C_o is the initial concentration in the CCP layer, z_T and z_B are the depths of the top and bottom of the CCP layer, $L = W_s + W_p/2$, W_p is the width of the pavement, and W_s is the width of the shoulder. Eq. 2a indicates that the CCP layer is the only source of trace elements and that the trace elements concentration is initially uniform in the CCP layer. Eq. 2b implies that no trace elements are transported into the CCP layer from overlying layers. Eqs. 2c and 2d indicate that transport by dispersion and diffusion is negligible at distances far from the surface of the pavement and the centerline of the profile. The solution to Eqs. 1 and 2 is (Leij et al., 1991):

$$C(x,z,t) = \frac{C_o}{4} A(z,t) B(x,t) \quad (3)$$

where

$$A(z,t) = \exp\left(\frac{v_z z}{D_z}\right)\left[\left(1+\frac{v_z}{D_z}\left(z+z_T+\frac{v_z t}{R}\right)\right)\operatorname{erfc}\left(\frac{R(z+z_T)+v_z t}{\sqrt{4RD_z t}}\right)\right] - \exp\left(\frac{v_z z}{D_z}\right)$$
$$\left[\left(1+\frac{v_z}{D_z}\left(z+z_B+\frac{v_z t}{R}\right)\right)\operatorname{erfc}\left(\frac{R(z+z_B)+v_z t}{\sqrt{4RD_z t}}\right)\right] + \operatorname{erfc}\left(\frac{R(z-z_B)-v_z t}{\sqrt{4RD_z t}}\right) -$$
$$\operatorname{erfc}\left(\frac{R(z-z_T)-v_z t}{\sqrt{4RD_z t}}\right) + \sqrt{\frac{4v_z^2 t}{\pi RD_z}}\exp\left(\frac{v_z z}{D_z}\right)$$
$$\left[\exp\left(-\frac{[R(z+z_B)+v_z t]^2}{4RD_z t}\right) - \exp\left(-\frac{[R(z+z_T)+v_z t]^2}{4RD_z t}\right)\right]$$

and

$$B(x,t) = \operatorname{erfc}\left(\frac{x-L}{\sqrt{4D_x t/R}}\right) - \operatorname{erfc}\left(\frac{x+L}{\sqrt{4D_x t/R}}\right)$$

Eq. 3 is applied from the surface of the pavement to the GWT (Fig. 2).

Leij et al. (1991) provide another solution to Eq. 1 that can be used for the "lagged response" leaching pattern. For this case, the initial and boundary conditions are assumed as follows:

$$C(x,z,t=0) = 0.0 \tag{4a}$$

$$\left(v_z C - D_Z \frac{\partial C}{\partial z}\right)\Bigg|_{z=z_B} = \begin{cases} v_z g(t) & \text{at } -L < x < L \\ 0.0 & \text{otherwise} \end{cases} \tag{4b}$$

$$\frac{\partial C}{\partial x}(\pm\infty, z, t) = 0 \tag{4c}$$

$$\frac{\partial C}{\partial z}(x, \infty, t) = 0 \tag{4d}$$

where g(t) is the trace element concentration as a function of time at the bottom of the CCP layer, z_B is the depth at the bottom of the CCP layer, and L is the half-width of the

CCP layer. Eq. 4a implies that no trace elements initially exist in the subgrade and Eq. 4b indicates that the flux of trace elements into the subgrade from the overlying CCP layer is the product of the concentration and the seepage velocity. Trace elements are assumed to be released uniformly along the base of the CCP layer. Eqs. 4c and 4d indicate that transport by dispersion and diffusion is negligible at distances far from the surface of the pavement and the centerline of the profile. The solution to Eqs. 1 and 4 for $z > z_B$ is (Leij et al., 1991):

$$C(x,z,t) = \frac{1}{4}\int_0^t g(t-\tau)\frac{v_z}{R}\left[\sqrt{\frac{R}{\pi D_z \tau}}\exp\left(-\frac{(R(z-z_B)-v_z\tau)^2}{4RD_z\tau}\right) - \frac{v_z}{2D_z}\exp\left(\frac{v_z(z-z_B)}{D_z}\right)\cdot \operatorname{erfc}\left(\frac{R(z-z_B)+v_z\tau}{\sqrt{4RD_z\tau}}\right)\right]\left[\operatorname{erfc}\left(\frac{x-L}{\sqrt{4D_x\tau/R}}\right) - \operatorname{erfc}\left(\frac{x+L}{\sqrt{4D_x\tau/R}}\right)\right]d\tau \quad (5)$$

Eq. 5 is applied from the top of the subgrade to the GWT (Fig. 2).

3.3. Groundwater

When groundwater flow occurs predominantly in the horizontal direction, transport in groundwater due to a line source at the GWT can be described with the following form of the ADRE (Leij et al., 2000):

$$R_w\frac{\partial C}{\partial t} = D_{xw}\frac{\partial^2 C}{\partial x^2} - v_h\frac{\partial C}{\partial x} + D_{zw}\frac{\partial^2 C}{\partial z^2} - v_z\frac{\partial C}{\partial z} \quad (6)$$

where C is solute concentration, t is time, v_h is the groundwater seepage velocity in the horizontal direction, v_z is the groundwater seepage velocity in the vertical direction, D_{xw} and D_{zw} are the hydrodynamic dispersion coefficients in the x and z directions, and R_w is

the retardation factor in groundwater. An implicit assumption when using Eq. 6 is that the cross-dispersion terms are negligible, which is reasonable for predominantly horizontal flow in a uniform and isotropic medium.

Leij et al. (2000) provide an analytical solution to Eq. 6 for the following initial and boundary conditions:

$$C(x,z,t=0)=0 \tag{7a}$$

$$\left(v_z C - D_{zw}\frac{\partial C}{\partial z}\right)\Bigg|_{z=z_{GW}} = \begin{cases} v_z g(x, z_{GWT}, t) & x_1 < x < x_2 \\ 0 & \text{otherwise} \end{cases} \tag{7b}$$

$$\frac{\partial C}{\partial x}(\pm\infty, z, t) = 0 \tag{7c}$$

$$\frac{\partial C}{\partial z}(x, \infty, t) = 0 \tag{7d}$$

where z_{GWT} is the depth of the GWT, g(t) is the trace element concentration at the GWT due to transport in the vadose zone, and x_1 and x_2 define the lateral extent over which g(t) applies. Eq. 7a implies that the groundwater is initially free of trace elements and Eq. 7b indicates that the flux of trace elements entering the GWT equals the advective of flux of trace elements in the vadose zone at the GWT. Eqs. 7c and 7d indicate that the diffusive and dispersive fluxes in groundwater are negligible for distances very far from the centerline of the pavement and the GWT. The solution to Eqs. 6 and 7 for $z > z_{GWT}$ is (Leij et al., 2000):

$$C(x,z,t)=\int_0^t \frac{v_z g(t-\tau)}{4R_w}\left[\operatorname{erfc}\left(\frac{R_w(x-x_2)-v_h\tau}{\sqrt{4R_w D_{xw}\tau}}\right)-\operatorname{erfc}\left(\frac{R_w(x-x_1)-v_h\tau}{\sqrt{4R_w D_{xw}\tau}}\right)\right]$$
$$\left[\sqrt{\frac{R_w}{\pi D_{zw}\tau}}\exp\left(-\frac{\left[R_w(z-z_{GWT})-v_z\tau\right]^2}{4R_w D_{zw}\tau}\right)-\right. \tag{8}$$
$$\left.\frac{v_z}{2D_{zw}}\exp\left(\frac{v_z(z-z_{GWT})}{D_{zw}}\right)\operatorname{erfc}\left(\frac{R_w(z-z_{GWT})+v_z\tau}{\sqrt{4R_w D_{zw}\tau}}\right)\right]d\tau$$

Eq. 8 accounts for solute transport from a line source at the GWT between x_1 and x_2. This feature was used to account for the horizontally varying concentration in the vadose zone that occurs in response to the different seepage velocities inside and outside the pavement and the effects of horizontal dispersion near the edges of the domain defined by x = ±L (Fig. 2). Eq. 8 was applied for a series of contiguous line sources extending along the GWT, with the combined effect obtained by superposition.

3.4. WiscLEACH Implementation

Eqs. 3, 5, and 8 are used in WiscLEACH to predict concentrations of trace elements in the vadose zone and GWT as a function of space and time. Gaussian quadrature is used for the integration in Eqs. 5 and 8. A Windows® graphical user interface is included to make entering the input and display of the output simple and straightforward. WiscLEACH is designed to predict impacts to groundwater caused by first-flush or lagged response leaching from a CCP layer in a pavement structure. However, the program can also be used to predict groundwater impacts from structural fills and embankments by adjusting the thickness and properties of the layers in the profile.

Output from WiscLEACH is presented in three ways: (i) transient concentrations at specified monitoring points, (ii) the maximum concentration at a point of compliance

(POC) located a specified distance from the centerline of the pavement (defined by the user), (iii) and two-dimensional isochors in the vadose zone and groundwater at times specified by the user. Predictions can be made for periods up to 100 yr.

A sensitivity analysis was conducted to determine the minimum horizontal and vertical dimensions of the domain so that the size of the domain does not influence the solution. The domain size was reduced systematically until the maximum concentration at the POC changed. For all conditions that were considered, the analysis showed that the minimum domain size is defined by -1.5 L to max(W_{poc}, 1.5 L) in the horizontal direction and from the ground surface to 1.5 z_{GWT} (Fig. 2). These minimum dimensions are programmed into WiscLEACH. A sensitivity analysis was also conducted to determine the temporal discretization needed to accurately integrate Eqs. 5 and 8 and the spatial discretization needed to superpose the solutions with Eq. 8 accurately. This analysis showed that the maximum time step is 0.4 yr, the maximum horizontal discretization is 2.0 m, and the maximum vertical discretization is 0.1 m. These temporal and spatial discretizations are set as defaults in WiscLEACH.

4. MODEL CALIBRATION WITH HYDRUS-2D

WiscLEACH was calibrated by comparing predictions made with WiscLEACH to predictions made with HYDRUS-2D, a widely used and verified program for simulating water and solute movement in two-dimensional variably saturated media. Predictions made with HYDRUS-2D were assumed to be the 'correct' solution to the leaching problem, whereas WiscLEACH is an approximate solution. The calibration procedure consisted of direct comparisons to check the one-dimensional solution in the vadose zone followed by iterative solutions where the dispersivities used in WiscLEACH were varied until concentrations predicted in the vadose zone and groundwater matched those predicted by HYDRUS-2D. No other parameters (besides the dispersivities)

needed to be calibrated in WiscLEACH to obtain a reasonable correspondence with the predictions made with HYDRUS-2D.

4.1. HYDRUS-2D Numerical Model

The conceptual model used for the HYDRUS-2D simulations is shown in Fig. 3. Flow in the vadose zone was assumed to be vertical and steady state and transport is assumed to follow the ADRE with instantaneous, linear, and reversible sorption. Trace elements that reach the GWT were transported horizontally and vertically in accordance with the ADRE with instantaneous, linear, and reversible sorption. Chemical and biological reactions that may consume or transform trace elements were not considered. Hydraulic properties of all materials in the profile were assumed to be homogenous and isotropic.

HYDRUS-2D simulates two-dimensional isothermal flow of water in a rigid variably saturated porous medium (Simunek et al., 1999). The air phase is assumed to have no effect on liquid flow. For these conditions, flow is described by the following modified form of Richards' equation:

$$\frac{\partial \theta}{\partial t} = \frac{\partial}{\partial x}\left[K(h)\frac{\partial h}{\partial x}\right] + \frac{\partial}{\partial z}\left[K(h)\left(\frac{\partial h}{\partial z} + 1\right)\right] - S \qquad (9)$$

where θ is the volumetric water content, h is the pressure head, t is time, x and z are spatial coordinates, K(h) is the unsaturated hydraulic conductivity, and S is a sink term. No-flow boundaries were applied on the vertical edges of the vadose zone and the bottom of the domain. Constant-head boundary conditions were applied along the upstream and downstream vertical edges of the domain below the groundwater table to establish an average hydraulic gradient of 0.01 in the longitudinal (flow) direction. A

specified flux boundary condition was applied on the top of the domain inside and outside the pavement (Fig. 3).

The form of the ADRE solved by HYDRUS-2D is:

$$\frac{\partial \theta C}{\partial t} + \frac{\partial \rho_d s}{\partial t} = \frac{\partial}{\partial x}\left[\theta D_x \frac{\partial C}{\partial x}\right] + \frac{\partial}{\partial z}\left[\theta D_z \frac{\partial C}{\partial z}\right] - \frac{\partial q_z C}{\partial z} - \frac{\partial q_x C}{\partial x} \quad (10)$$

where C and s are solute concentrations in the liquid and solid phases, q_x and q_z are the volumetric fluxes in the horizontal and vertical directions, D_x and D_z are dispersion coefficients in the horizontal and vertical directions, and ρ_d is the dry density. No flux boundaries were applied on the lateral edges of the vadose zone and on the bottom of the domain when solving Eq. 10. All other boundaries were assigned the Cauchy boundary condition with no mass influx. The initial concentration of trace elements in the domain was assumed to be zero, except in the CCP layer. The initial concentration of the CCP layer was set as the initial elution concentration (C_o) (see subsequent discussion).

A sensitivity analysis was conducted to determine the minimum longitudinal and lateral dimensions of the domain used in HYDRUS-2D so that the boundaries would not influence flow or transport near or in the CCP layer or the POC. The domain was reduced in size systematically until the distribution of velocities changed. This analysis showed that the minimum domain size is 40 m long and 12 m wide for all conditions that were considered. The domain contained 5074 finite element cells.

4.1. Validation of Vadose Zone Predictions

The solution used in WiscLEACH for the vadose zone was validated by comparing predictions from WiscLEACH and HYDRUS-2D for transport in a domain 40 m wide and 6 m deep. The CCP layer was assumed to be 5-m wide and 0.5-m thick (0.5 m to 1.0 m bgs) and was centered in the HYDRUS-2D domain. Rectangular finite element cells (0.25 m x 0.25 m) were used and a constant flux of 0.4 mm/d was assigned to the top boundary. An equivalent vertical seepage velocity of 1 mm/day was used in WiscLEACH (the subgrade was assigned a porosity of 0.4). A retardation factor of 3.5 was assumed, the longitudinal dispersivity in the vadose zone was set at 0.5 m, and the transverse dispersivity in the vadose zone was set at 0.05 m.

Relative concentrations predicted by HYDRUS-2D and WiscLEACH are shown in Fig. 8 for four locations (labeled A-D). Two locations are in the CCP layer (A and B) and two locations are outside the pavement area (A and C). The relative concentrations predicted by WiscLEACH and HYDRUS-2D are nearly identical at all four points. A series of additional simulations were conducted with different retardation factors and dispersivities. In all cases, concentrations predicted by WiscLEACH and HYDRUS-2D were essentially identical. Nearly identical agreement was expected given the close similarity of the conditions simulated by HYDRUS-2D and the underlying assumptions associated with Eq. 3 (see Sec. 3.2).

4.2. Calibration of WiscLEACH with HYDRUS-2D

WiscLEACH was calibrated by comparing predictions for transport in the vadose zone and groundwater made with WiscLEACH to predictions of the same problem made with HYDRUS-2D. For these simulations, the pavement width was set at 10.4 m, the shoulder width was 1.5 m, and the CCP layer was 13.4 m wide and 0.3 m thick (0.38 m to 0.68 m bgs). In HYDRUS-2D, a constant flux of 1 mm/d was assigned to the top

boundary. An equivalent vertical seepage velocity in the vadose zone of 3 mm/d was used in WiscLEACH, assuming the porosity in the subgrade is 0.33. The average seepage velocity in the groundwater was 0.023 m/d. The retardation factor was set at 3 in the vadose zone and 1 in groundwater. In HYDRUS-2D, the longitudinal (vertical) dispersivity in vadose zone was initially set at 10 mm and the ratio of longitudinal to transverse (horizontal) dispersivities in the vadose zone was set at 10:1. The dispersivities used in WiscLEACH were adjusted to obtain a reasonable match between concentrations predicted by WiscLEACH and HYDRUS-2D.

A comparison of predictions made with HYDRUS-2D and WiscLEACH after calibration is shown in Fig. 5. Good correspondence was obtained with WiscLEACH when the longitudinal (vertical) dispersivity in the vadose zone was 0.06 m, the longitudinal (horizontal) dispersivity in groundwater was 0.013 m, and the ratio of longitudinal to transverse dispersivity in groundwater was 6:1. For these conditions, the distribution of concentration predicted by both models is similar in the vadose zone and in groundwater. However, the peak concentrations predicted by WiscLEACH are slightly lower than those predicted HYDRUS-2D.

Concentrations predicted by WiscLEACH and HYDRUS-2D at six observation points are shown in Fig. 6 for this same simulation. Locations of the observation points are shown in Fig. 6. Four of the points (1, 3, 4, and 5) are in groundwater, one point is in the vadose zone (point 6), and one point is at the groundwater table (point 2). When the observation points are near the groundwater table (points 1, 2, and 6), the concentrations predicted from WiscLEACH and HYDRUS-2D are in general agreement, but less dispersion exists in the concentrations predicted by WiscLEACH. In groundwater (points 3-5), peak concentrations predicted by WiscLEACH are lower than those predicted by HYDRUS-2D, with greater deviations occurring for the points having lower peak concentration.

Maximum concentrations at the POC predicted by WiscLEACH and HYDRUS-2D over a 100 yr period are shown in Fig. 7. When the POC is 15 m from the centerline of the pavement, the predictions made with WiscLEACH and HYDRUS-2D are in general agreement. For a POC located 20 m from the centerline, the concentrations predicted by WiscLEACH generally are slightly higher than the concentrations predicted by HYDRUS-2D.

A series of similar simulations was conducted where the transport parameters were varied over a broad range, with the dispersivities used in WiscLEACH being adjusted in each case to obtain reasonable agreement with concentrations predicted by HYDRUS-2D (i.e., as in Fig. 5). The dispersivities obtained by calibrating WiscLEACH to HYDRUS-2D are shown in Fig. 8 (vadose zone) and Fig. 9 (groundwater). In general, the calibrated longitudinal dispersivities for WiscLEACH are less than the longitudinal dispersivities used in HYDRUS-2D (Figs. 8a and 9a). For the vadose zone, the ratio of calibrated longitudinal dispersivity to transverse dispersivity in WiscLEACH is the same as the ratio used in HYDRUS-2D (Fig. 8b). In groundwater, the calibrated ratio used in WiscLEACH is 60% of that used for groundwater in HYDRUS-2D (Fig. 9b).

Different dispersivities are required in WiscLEACH and HYDRUS-2D because the flow and transport patterns near the interface of the vadose zone and groundwater table are simplified in WiscLEACH. In HYDRUS-2D, a gradual transition exists between the vadose zone and groundwater, with flow and transport migrating horizontally and vertically near the groundwater table with spatially variable velocities. In contrast, in WiscLEACH, flow only occurs vertically in the vadose zone and no spatial variation exists in the groundwater velocity near the GWT. These differences are apparent when comparing the isochors in Fig. 5.

4.3. Computation Time

Execution times required for WiscLEACH and HYDRUS-2D for the calibration simulations were compared to confirm that the analytical modeling approach was advantageous from a computational perspective. On a desktop PC with a 2 GHz Pentium 4 processor and 512 MB of RAM, computation times for WiscLEACH were always less than 60 s, whereas those for HYDRUS-2D were hours or days. Thus, the analytical approach used in WiscLEACH is more computationally efficient, albeit with some loss in accuracy as described in Sec. 4.2.

5. MODEL VERIFICATION

5.1. Field Site

Test sections incorporating a fly ash-stabilized subgrade or a bottom ash subbase were constructed in 2000 along Wisconsin State Trunk Highway (STH) 60 between Lodi and Prairie du Sac, Wisconsin. Profiles of the test sections are shown in Fig. 10a. The pavement is 10.4 m wide and each shoulder is 1.5 m wide. The CCP layers in both test sections extend to the outer edges of the shoulders (the CCP layer is 13.4 m wide). The fly-ash-stabilized soil is 0.3 m thick (0.38-0.68 m bgs) and the bottom ash layer is 0.6 m thick (0.38-0.98 m bgs). A detailed description of the test sections can be found in Edil et al. (2002). A discussion of the field data is in Sauer et al. (2005b).

Two equal size (3.50 m x 4.75 m) lysimeters were installed beneath each test section (Fig. 10b). One lysimeter was installed along the centerline of the pavement ("inner" lysimeter) and the other along the shoulder ("outer" lysimeter). The lysimeters were constructed with 1.5-mm thick textured HDPE geomembrane overlain by a geocomposite drainage layer (geonet with a non-woven geotextile heat bonded to both sides). Water collected in each lysimeter drained to a 120-L tank buried adjacent to the pavement and below the frost depth. Six groundwater monitoring wells were also

installed in 2003-2004 along the right-of-way adjacent to the CCP test sections and the control section. The wells were constructed with 50 mm PVC casing with the screens at 2.4-2.8 m bgs. Additional information on the lysimeters can be found in Bin Shafique et al. (2002). Additional details on the monitoring well installations are in the appendix.

All of the lysimeters were monitored from 2000 to 2005, although a lapse in data collection occurred between July 2002 and June 2003 due to lack of funding. The volume of leachate collected in the tanks was recorded monthly (or more frequently) with chemical analysis of the leachate being conducted during each sampling event. Leachate samples were analyzed for concentrations of Cd, Cr, Se, and Ag. The data that were collected are compiled in the appendix along with a description of the methods used to conduct the analysis. The monitoring wells were inspected when the collection tanks were sampled. However, because the fine-grained subgrade soils at the field site have very low hydraulic conductivity, samples could not be collected from the monitoring wells during the monitoring period.

5.2 Model Input

WiscLEACH was used to predict concentrations of Cd, Cr, and Ag in the lysimeters beneath the fly ash and bottom ash test sections. Simulations were not conducted for Se because a source of Se other than the CCP layers confounded the Se concentrations measured in the lysimeters (see appendix). The seepage velocity in WiscLEACH was defined using volumetric leachate fluxes observed in the field (median and 90^{th} percentile volumetric leachate fluxes) for in the inner and outer lysimeters rather than how the software is used conventionally (i.e., with precipitation rate and hydraulic properties of the layers, as described in Sec. 3.1). Summary statistics for the volumetric fluxes are in Table 1. A detailed record of the volumetric fluxes is in the appendix along with the other monitoring data. The seepage velocity was computed from the volumetric

fluxes using the effective porosity of the subgrade (0.33), which was determined by tracer analysis (Bin-Shafique et al., 2002).

First-flush leaching was assumed for both test sections. The transport parameters used as input are summarized in Table 2. Initial concentrations (C_o) were estimated from the initial elution data from the lysimeters. Retardation factors for the fly-ash-stabilized soil were obtained from data from column tests conducted (see appendix). Retardation factors for the bottom ash were not available. Thus, the retardation factors for the fly-ash-stabilized soil were also used for the bottom ash. The molecular diffusion coefficients were computed using free solution diffusion coefficients reported in Lerman (1979) and an assumed tortuosity of 0.3. Dispersion coefficients in the vertical and horizontal directions were estimated from the seepage velocity and the dispersivity, the latter set at one-tenth the size of the transport domain.

5.3 Comparison for Fly-Ash-Stabilized Soil Section

Measured and predicted concentrations of Cd, Cr, and Ag for the fly-ash-stabilized soil are shown in Figs. 11-13. The predicted concentrations correspond to the bottom of the layer of fly-ash-stabilized soil (z_B) (Fig. 2), where the lysimeters were located. Simulations were conducted with the 50^{th} and 90^{th} percentile volumetric fluxes measured in the inner and outer lysimeters. The measured Cd, Cr, and Ag concentrations generally decrease over time, which is consistent with the “first flushing” pattern that was assumed. The exception is the Ag concentration in the inner lysimeter, which increased suddenly later in the monitoring period. The reason for this increase is unknown, and it did not occur in the outer lysimeter (see discussion in appendix).

The predicted concentrations for all three elements are in reasonable agreement with the field data when the 90^{th} percentile volumetric flux is used as input, although in many cases the predicted concentration is slightly higher than the measured

concentration. When the median (50th percentile) volumetric flux is used as input, the predicted concentrations consistently are higher than the measured concentrations. The closest agreement is for the Cd concentrations measured in the inner lysimeter and the predictions made with the 90th percentile volumetric flux. The largest deviations are for Cr concentrations measured in the inner lysimeter and predictions made with the median volumetric flux.

The reason for the over-predicted concentrations is not clear, but the disparity may be due to experimental issues rather than bias in WiscLEACH. The lysimeters installed the STH 60 site did not have sidewalls, and bypassing of some liquid may have occurred due to the contrast in texture formed by the geocomposite drainage layers used to collect leachate in the lysimeters. Given the relatively small difference between the median and 90th percentile volumetric leachate fluxes (less than a factor of 3, Table 1), bypassing is plausible. Other possible causes may be overestimated retardation factors and/or over-estimated dispersivities. Regardless of the cause, an over prediction is a conservative prediction, and therefore may not be problematic.

5.4 Comparison for Bottom Ash Section

Measured and predicted concentrations of Cd, Cr, and Ag for the bottom ash test section are shown in Figs. 14-17. The measured concentrations of Cd, Cr, and Ag follow the “first flush” elution pattern that was used as input. As was observed for the fly ash section, the measured and predicted concentrations are in closer agreement when the 90th percentile volumetric flux was used as input rather than the median volumetric flux. The closest agreement was obtained for Cr concentrations measured in the outer lysimeter, and the poorest agreement for Cd concentrations in the inner lysimeter. As was noted in Sec. 5.3, the disparity between the measured and predicted concentrations

may be due to leachate bypassing the lysimeters or overestimated retardation factors and/or dispersivities.

6. PARAMETERIC STUDIES

A series of parametric simulations were conducted to evaluate the how predictions made with WiscLEACH are affected by the geometry of the pavement and breadth of the right-of-way, the depth to groundwater, hydraulic properties of the layers, and transport properties. The analyses were conducted using the same inputs used to simulate the fly ash section at STH 60. However, the model was used in the conventional mode, with the annual precipitation rate (865 mm/yr) used as input and the hydraulic properties of the layers used to determine the seepage velocity. Se was used as the trace element of interest, although any other element exhibiting first-flush elution could have been used without loss of generality. The POC was assumed to be 20 m from the centerline of the pavement.

Hydraulic conductivity of the fly-ash-stabilized soil was set at 6.0×10^{-7} cm/s, the hydraulic conductivity of the subgrade was set at 3.2×10^{-6} cm/s, and the porosity of the subgrade was set at 0.33 based on measurements reported in Bin-Shafique et al. (2002). The overlying base and asphalt layers were assigned a hydraulic conductivity of 10^{-5} cm/s. However, these layers are much more permeable than the fly-ash-stabilized soil or the subgrade, and thus are not hydraulically important (in this case, flow is controlled by the subgrade). The depth to the top of the fly ash stabilized soil (z_T) is 0.38 m. The initial concentration and retardation factor for Se were set at 32.1 μg/L and 3.5, based on measurements reported in Bin-Shafique et al. (2002).

A sand and gravel aquifer was assumed to exist 6 m below ground surface. The aquifer material was assumed to have a saturated hydraulic conductivity of 0.01 cm/s and an effective porosity of 0.3, which are typical parameters for sand and gravel

aquifers. The regional hydraulic gradient was assumed to be 0.001. These conditions are referred to herein as the 'base case.'

Se concentrations predicted by WiscLEACH after 10, 30, and 45 yr are shown in Fig. 17, the latter time corresponding to the peak concentration being reached in groundwater (2.2 μg/L). The Se plume eluted from the CCP layer moves downward over time, and reaches the GWT between 10 and 30 yr. The highest groundwater concentrations occur at the GWT and near the centerline of the pavement, and are considerably lower than the initial concentration (32 μg/L) in the CCP layer as a result of flushing and dispersion. The effects of dispersion are evident in Fig. 17, as concentrations near the middle are higher than those near the edges in the plumes in the vadose zone and groundwater. The horizontal distribution of Se below the GWT is also indicative of flushing caused by advection in the flowing groundwater.

Se concentrations in the vadose zone and in groundwater vary spatially and temporally (Fig. 18). This effect is shown for 6 observations points in Fig. 18a. The Se concentration at each observation point gradually increases to a maximum concentration and then diminishes to background levels. When the observation point is closer to the CCP layer, the concentration increases earlier, more rapidly, and reaches a higher peak because the travel time to the observation point is shorter, which reduces the effects of dispersion and dilution.

Maximum concentrations at the POC over a 100-yr period are shown in Fig. 18b as a function of depth. The concentrations shown in Fig. 18b are the maximum concentrations at each depth over a 100-yr period. These maximum concentrations at the POC may not happen at the same time, and generally occur at different times. For this simulation, the maximum Se concentration at the POC (1.2 μg/L or 3.8% of C_o) occurs 0.9 m below the GWT at 36 yr.

6.1 Site Geometric Variables

Site geometric variables include the depth to the GWT, the CCP layer thickness and location, the pavement and shoulder width, and the location of the POC. A sensitivity analysis was conducted to assess how the maximum Se concentration at the POC is affected by the each of these variables. Each input variable was varied by 20% from the base case, while holding all others constant. Sensitivity was evaluated with the sensitivity coefficient, $S = \Delta\zeta/(\Delta\beta/\beta)$, where ζ is the response variable of interest (maximum Se concentration at the POC over 100 yr) and β is the independent variable of interest (site geometry variables). When the sensitivity coefficient has a large magnitude ($|S|$), the independent variable has a large effect on the response variable, indicating sensitivity. When the sensitivity coefficient is zero, the independent variable has no effect on the response variable. For this analysis, parameters were considered significant if the peak magnitude of the sensitivity coefficient exceeded 0.5.

Sensitivity coefficients are shown in Fig. 19 as a function of depth below ground surface (bgs) at the POC for the site geometric variables that have a peak $|S| > 0.5$. Graphs of concentration vs. depth at the POC are shown for each variable in Figs. 20-22. Concentration at the POC is most sensitive to depth to the GWT (peak $|S| = 6.0$), thickness of the CCP layer (peak $|S| = 3.0$), and distance to the POC (peak $|S| = 2.0$). Concentration at the POC is less (and equally) sensitive to the pavement and shoulder widths. Depth to the GWT and distance to the POC are both important because they affect the amount of dispersion and dilution that occurs between the CCP layer and the POC. Increasing the depth to GWT or the distance to the POC results in more dispersion and lower concentrations at the POC, as illustrated in Fig. 20. Thickness of the CCP layer is important because it affects the total mass leached (higher

concentrations occur at the POC when more mass is leached from the CCP layer) (Fig. 21a). Pavement and shoulder width are less important (Fig. 22), even though a change in either variable affects the total mass leached, because the source is distributed over a broad area.

6.2 Hydraulic Variables

Hydraulic variables include the hydraulic conductivity and porosity of the pavement, base layer, CCP layer, subgrade, and aquifer material; the regional hydraulic gradient in groundwater; and the precipitation rate. Sensitivity coefficients for hydraulic variables having peak $|S| > 0.5$ are shown in Fig. 23 as a function of depth below ground surface (bgs) at the POC. Sensitivity coefficients for porosity and hydraulic conductivity are only shown for the CCP layer in Fig. 23. Because the least conductive layer in the profile controls the seepage velocity, similar sensitivity coefficients are obtained for any of the other layers when they are the least conductive layer in the profile. The same is true for the precipitation rate; if the precipitation rate is less than the hydraulic conductivity of the least conductive layer in the profile, then the seepage velocity is controlled by the precipitation rate. Consequently, in such cases, the concentration at the POC can be equally sensitive to the precipitation rate.

Concentration at the POC is equally sensitive to the hydraulic conductivity and the porosity of CCP layer, the hydraulic conductivity and porosity of the aquifer, and the regional hydraulic gradient. Each of these variables has a peak $|S| \approx 2.0$. All are important because they control advection in the vadose zone and in groundwater, which affect dispersion and dilution. These effects are illustrated in Fig. 24, which shows concentration at the POC as a function of depth for various seepage velocities in the vadose zone or groundwater. The peak concentration at the POC decreases as the seepage velocity in the vadose zone decreases or as the seepage velocity in

groundwater increases. These seepage velocities have opposite effects because dilution of the leaching element is affected by the ratio of the seepage velocity in the vadose zone to the seepage velocity in groundwater. As this ratio decreases, more dilution occurs and the concentration at the point of compliance decreases.

6.3 Contaminant Properties

Contaminant properties include the initial elution concentration (C_o), the molecular diffusion coefficient, the dispersivities, and the retardation factors. Sensitivity coefficients for contaminant properties having peak |S| > 0.5 are shown in Fig. 25 as a function of depth below ground surface (bgs) at the POC. Concentration at the POC is only sensitive to the initial elution concentration (peak |S| = 1.2) and the dispersivity in the vadose zone. The molecular diffusion coefficient is not significant because transport in the vadose zone and groundwater is dominated by advection. The dispersivity is not important because dilution by groundwater is controlled more by advection than dispersion. Retardation factors do not affect the maximum concentration at the POC because they only affect the transit time, and not the maximum concentration.

Concentrations at the POC are shown in Fig. 26 as a function of C_o and the molecular diffusion coefficient and in Fig. 27 as a function of the dispersivities in the vadose zone and groundwater. As illustrated in Fig. 26, concentration at the POC is very sensitive to C_o, and is much less sensitive to the molecular diffusion coefficient. Similarly, as shown in Fig. 27, concentration at the POC is very sensitivity to the dispersivity in the vadose zone, and much less sensitive to the dispersivity in groundwater.

7. PRACTICAL APPLICATION

The following application is based on the STH 60 field site and illustrates how WiscLEACH can be used to assess the risks to groundwater. At the STH 60 site, groundwater quality must be maintained in accordance with standards stipulated in Section NR 140 of the *Wisconsin Administrative Code* (Wisconsin, 2004). These standards are comparable or more stringent than maximum contaminant levels (MCLs) stipulated by USEPA. The Wisconsin standards for Cd, Cr, Ag, and Se are summarized in Table 3 along with maximum concentrations recorded in the lysimeters at the STH 60 site.

Comparison of the maximum concentrations measured in the lysimeters and the maximum concentrations stipulated in the *Wisconsin Administrative Code* (Table 3) indicates that the Wisconsin groundwater standards are exceeded for of Cd, Ag, and Se. However, the lysimeters measure the concentration at the base of the pavement section and do not represent concentrations in groundwater or at a POC. Concentrations in groundwater should be lower than those in the lysimeters due to factors such as dilution and dispersion (Sec. 6). To illustrate this effect, simulations were conducted with WiscLEACH using the inputs described in Sec 5.2. Seepage velocity in the vadose zone was described using the 50^{th} and 90^{th} percentile volumetric leachate fluxes and the POC was set 20 m from the centerline of the highway, which is the limit of the right-of-way at the STH 60 site. Variables describing the groundwater characteristics were defined with the values used in Sec. 6, except the depth to the GWT, which was set at 2 m bgs. Comparisons between the model predictions and lysimeter concentrations for this case showed that WiscLEACH over-predicted the lysimeter concentrations using the 50^{th} and 90^{th} percentile volumetric fluxes, with the over-prediction being larger using the 50^{th} percentile volumetric flux. Thus, for both volumetric fluxes, groundwater concentrations will also be over-predicted.

Simulations using the 50th and 90th percentile of volumetric leaching flux were conducted for a 100 yr period. The maximum concentrations of Cd, Cr, Se, and Ag at the POC for these simulations are shown as a function of depth in Fig. 28 for the fly ash test section and Fig. 29 for the bottom ash section. The peak maximum concentrations are summarized in Table 3. For both test sections, the predicted maximum concentrations at the POC over 100-yr period are lower than the Wisconsin groundwater standards for all four trace elements.

8. SUMMARY AND CONCLUSIONS

This report has described WiscLEACH, a computer application for assessing impacts to groundwater caused by leaching of trace elements from CCPs used in highway construction. The application is based on three analytical solutions to the advection-dispersion-reaction equation that describe transport in the vadose zone and groundwater. WiscLEACH is computationally efficient and can be used without experience in numerical modeling.

WiscLEACH was calibrated by comparing identical simulations with HYDRUS-2D and adjusting the dispersivities used in WiscLEACH until both programs produced similar distributions of concentration over time. Predictions made with WiscLEACH were also compared with to concentrations of Cd, Cr, and Ag measured in lysimeters beneath two highway test sections constructed with industrial byproducts. WiscLEACH over-predicted the field concentrations slightly, which is a conservative error.

Predictions made with WiscLEACH indicate that maximum groundwater concentrations typically occur close to the groundwater table and near the centerline of the pavement structure. Peak groundwater concentrations decrease as the depth of groundwater increases, the thickness of the CCP layer decreases, the seepage velocity in the vadose zone decreases, or the seepage velocity in groundwater increases.

Parametric studies have also shown that the variables having the greatest influence on maximum concentrations in groundwater are depth to the groundwater table, thickness of the CCP layer, hydraulic conductivity of the least conductive layer in the vadose zone, hydraulic conductivity of the aquifer material, and the initial concentration in the CCP layer.

9. REFERENCES

ACAA, 2003. Coal Combustion Product Production and Use Survey, American Coal Ash Association, Aurora, CO.

Aldea, C.M., Shah, S.P. and Karb, A., 1999. Effect of microcracking on durability of high-strength concrete. Transportation Research Record, No. 1668: National Research Council, Washington D.C., 86-90.

Apul, D., Gardner, K., Eighmy, T., Benoit, J. and Brannaka, L., 2002. A Review of Water Movement in the Highway Environment: Implications for Recycled Materials Use, Recycled Materials Resource Center, University of New Hampshire, Durham, NH.

Apul, D. et al., 2005. Probabilistic modeling of one-dimensional water movement and leaching from highway embankments containing secondary materials. Environmental Engineering Science, 22(2): 156-169.

Batchelor, B., 1998. Leach models for contaminants immobilized by pH-dependent mechanisms. Environmental Science & Technology, 32(11): 1721-1726.

Bear, J., 1979. Hydraulics of Groundwater. McGraw-Hill Inc., New York.

Bin-Shafique, M.S., Benson, C.H. and Edil, T.B., 2002. Leaching of Heavy Metals from Fly Ash Stabilized Soils Used in Highway Pavements, Geo Engineering Report No. 02-14, Geo Engineering Program, University of Wisconsin-Madison.

Bin-Shafique, S., Benson, C.H., Edil, T.B. and Hwang, K., 2006. Leachate concentrations from water leach and column leach tests on fly-ash stabilized soils. Environmental Science & Technology, in press.

Bin-Shafique, S., Edil, T.B., Benson, C.H. and Senol, A., 2004. Incorporating a fly-ash stabilised layer into pavement design. Geotechnical Engineering, Institution of Civil Engineers, United Kingdom, 157(GE4): 239-249.

Chichester, D.L. and Landsberger, S., 1996. Determination of leaching dynamics of metals from municipal solid waste incinerator fly ash using a column test. Journal of the Air and Waste Management Association, 46(7): 643-649.

Creek, D.N. and Shackelford, C.D., 1992. Permeability and leaching characteristics of fly ash liner materials. Transportation Research Record, No. 1345: National Research Council, Washington D.C., 74-83.

Dijkstra, J.J., van der Sloot, H.A. and Comans, R.N.J., 2002. Process identification and model development of contaminant transport in MSWI bottom ash. Waste Management, 22: 531-541.

Edil, T.B., Acosta, H.A. and Benson, C.H., 2005. Stabilizing soft fine-grained soils with fly ash. Journal of Materials in Civil Engineering, in press.

Edil, T.B. and Benson, C.H., 2002. Use of Industrial By-Products as Geo-Materials. Geo Strata, Geo Institute, ASCE(April Issue): 28-29.

Edil, T.B. et al., 2002. Field evaluation of construction alternatives for highways over soft subgrade. Transportation Research Record, No. 1786: National Research Council, Washington D. C., 36-48.

Edil, T.B., Sandstrom, L.K. and Berthouex, P.M., 1992. Interaction of inorganic leachate with compacted pozzolanic fly-ash. Journal of Geotechnical Engineering, 118(9): 1410-1430.

Eighmy, T.T. and Chesner, W.H., 2001. Framework for Evaluating Use of Recycled Materials in the Highway Environment, FHWA-RD-00-140, U.S. DOT, Washington, D. C.

Elsayed, A.S. and Lindly, J.K., 1996. Estimating hydraulic conductivity of untreated highway bases. Transportation Research Record, No. 1519: National Research Council, Washington D. C., 11-18.

FHWA, 1990. Technical paper on subsurface pavement drainage, Technical Paper 90-01, Office of Engineering, Pavement Division, Federal Highway Administration, Washington, D. C.

Fleming, L.N., Abinteh, H.N. and Inyang, H.I., 1996. Leachant pH effect on the leachability of metals from fly ash. Journal of Soil Contamination, 5(1): 53-59.

Friend, M., Bloom, P., Halbach, T., Grosenheider, K., and Johnson, M. (2004), Screening Tool for Using Waste Materials in Paving Projects (STUWMPP), Report No. MN/RC – 2005-03, Office of Research Services, Minnesota Dept. of Transportation, St. Paul, Minnesota.

Garrabrants, A.C., Sanchez, F. and Kosson, D.S., 2003. Leaching model for a cement mortar exposed to intermittent wetting and drying. AIChE Journal, 49(5): 1317-1333.

Ghosh, A. and Subbarao, C., 1998. Hydraulic conductivity and leachate characteristics of stabilized fly ash. Journal of Environmental Engineering, 124(9): 812-820.

Guo, T.Z., Deshpande, P.S. and Rusch, K.A., 2004. Identification of dynamic leaching kinetics of stabilized, water-soluble wastes. Environmental Science & Technology, 38(2): 603-608.

Hassett, D.J. and Pflughoeft-Hassett, D.F., 2002. Evaluating coal combustion by-products (CCPs) for environmental performance. In: K.C. Vories and D. Throgmorton (Editors), Proceedings of Coal Combustion By-Products and Western Coal Mines: A Technical Interactive Forum. U.S. Department of Interior, Office of Surface Mining, Alton, Illinois & Coal Research Center, Southern Illinois University, Carbondale, Illinois, Golden, Colorado, pp. 79-82.

Hesse, T.E., Quigley, M.M. and Huber, W.C., 2000. User's Guide: IMPACT - A Software Program for Assessing the Environmental Impact of Road Construction and Repair Materials on Surface and Groundwater. NCHRP 25-09: Environmental Impact of Construction and Repair Materials on Surface and Groundwaters, Oregon State University, Corvallis, Oregon.

Huang, Y.H., 2004. Pavement Analysis and Design, Second Edition. Prentice Hall, Upper Saddle River, NJ.

Kalyoncu, R.S., 2002. Coal combustion products - production and uses. In: K.C. Vories and D. Throgmorton (Editors), Proceedings of Coal Combustion By-Products and Western Coal Mines: A Technical Interactive Forum. U.S. Department of Interior, Office of Surface Mining, Alton, Illinois & Coal Research Center, Southern Illinois University, Carbondale, Illinois, Golden, Colorado, pp. 13-24.

Kim, A.G., 2002. CCP leaching summary: Survey of methods and results. In: K.C. Vories and D. Throgmorton (Editors), Proceedings of Coal Combustion By-Products and Western Coal Mines: A Technical Interactive Forum. U.S. Department of Interior, Office of Surface Mining, Alton, Illinois & Coal Research Center, Southern Illinois University, Carbondale, Illinois, Golden, Colorado, pp. 179-196.

Kim, A.G., Kazonich, G. and Dahlberg, M., 2003. Relative solubility of cations in Class F fly ash. Environmental Science & Technology, 37(19): 4507-4511.

Kim, B., Prezzi, M. and Salgado, R., 2005. Geotechnical properties of fly and bottom ash mixtures for use in highway embankments. Journal of Geotechnical and Geoenvironmental Engineering, 131(7): 914-924.

Kim, J.Y., Edil, T.B. and Park, J.E., 1997. Effective porosity and seepage velocity in column tests on compacted clay. Journal of Geotechnical and Geoenvironmental Engineering, 123(12): 1135-1142.

Kosson, D.S., van der Sloot, H.A., Sanchez, F. and Garrabrants, A.C., 2002. An integrated framework for evaluating leaching in waste management and utilization of secondary materials. Environmental Engineering Science, 19(3): 159-204.

Leelavathamma, B. and Pandian, N.S., 2005. Effect of class C fly ash on the California Bearing Ratio behavior of soil-fly ash mixes and layered systems. Journal of Testing and Evaluation, 33(2): 88-93.

Leij, F.J., Priesack, E. and Schaap, M.G., 2000. Solute transport modeled with Green's functions with application to persistent solute sources. Journal of Contaminant Hydrology, 41(1-2): 155-173.

Leij, F.J., Skaggs, T.H. and van Genuchten, M.T., 1991. Analytical solutions for solute transport in three-dimensional semi-infinite porous media. Water Resources Research, 27(10): 2719-2733.

Lerman, A., 1979. Geochemical Processes in Water and Sediment Environments. John Wiley and Sons, New York.

Mallela, J., Titus-Glover, L. and Darter, M.I., 2000. Considerations for providing subsurface drainage in jointed concrete pavements. Transportation Research Record, No. 1709: National Research Council, Washington D. C., 1-10.

Misra, A., 1998. Stabilization characteristics of clays using class C fly ash, Stabilization and Geosynthetics. Transportation Research Record, pp. 46-54.

Moszkowicz, P., Pousin, J. and Sanchez, F., 1996. Diffusion and dissolution in a reactive porous medium: Mathematical modelling and numerical simulations. Journal of Computational and Applied Mathematics, 66(1-2): 377-389.

Moszkowicz, P., Sanchez, F., Barna, R. and Mehu, J., 1998. Pollutants leaching behaviour from solidified wastes: a selection of adapted various models. Talanta, 46(3): 375-383.

Mudd, G.M., Weaver, T.R. and Kodikara, J., 2004. Environmental geochemistry of leachate from leached brown coal ash. Journal of Environmental Engineering-ASCE, 130(12): 1514-1526.

Murarka, I.P., Rai, D. and Ainsworth, C.C., 1991. Geochemical basis for predicting leaching of inorganic constituents from coal-combustion residues, Waste Testing and Quality Assurance, ASTM Special Technical Publication, No. 1075. American Society for Testing and Materials, West Conshohocken, PA, pp. 279-287.

Ogata, A. and Banks, R.B., 1961. A solution of the differential equation of longitudinal dispersion in porous media, US Geological Survey, Washington D. C.

Pandian, N.S. and Krishna, K.C., 2003. The pozzolanic effect of fly ash on the California bearing ratio behavior of black cotton soil. Journal of Testing and Evaluation, 31(6): 479-485.

Papini, M.P., Kahie, Y.D., Troia, B. and Majone, M., 1999. Adsorption of lead at variable pH onto a natural porous medium: Modeling of batch and column experiments. Environmental Science & Technology, 33: 4457-4464.

Park, J.Y. and Batchelor, B., 2002. General chemical equilibrium model for stabilized/solidified wastes. Journal of Environmental Engineering-ASCE, 128(7): 653-661.

Parsons, R.L. and Milburn, J.P., 2003. Engineering behavior of stabilized soils. Transportation Research Record, No. 1837: National Research Council, Washington D.C., 20-29.

Praharaj, T., Powell, M.A., Hart, B.R. and Tripathy, S., 2002. Leachability of elements from sub-bituminous coal fly ash from India. Environment International, 27(8): 609-615.

Ricou, P., Lecuyer, I. and Cloirec, P.L., 1998. Influence of pH on removal of heavy metallic cations by fly ash in aqueous solution. Environmental Technology, 19(10): 1005-1016.

Sanchez, F., Massry, I.W., Eighmy, T. and Kosson, D.S., 2003. Multi-regime transport model for leaching behavior of heterogeneous porous materials. Waste Management, 23(3): 219-224.

Sauer, J.J., Benson, C.H. and Edil, T.B., 2005a. Leaching of Heavy Metals from Organic Soils Stabilized with High Carbon Fly Ash, Geo Engineering Report No. 05-01, Departmental of Civil and Environmental Engineering, University of Wisconsin-Madison.

Sauer, J.J., Benson, C.H. and Edil, T.B., 2005b. Metals Leaching from Highway Test Sections Constructed with Industrial Byproducts, Geo Engineering Report No. 05-21, Departmental of Civil and Environmental Engineering, University of Wisconsin-Madison.

Seals, R.K., Moulton, L.K. and Ruth, B.E., 1972. Bottom ash: An engineering material. Journal of Soil Mechanics - Foundation Division, 98(4): 311-325.

Simunek, J., Sejna, M. and van Genuchten, M.T., 1999. The HYDRUS-2D Software Package for Simulating the Two-Dimensional Movement of Water, Heat, and Multiple Solutes in Variably-Saturated Media, Version 2.0, U.S. Salinity Laboratory, Riverside, CA.

Stewart, B.R., Daniel, W.L., Zelazny, L.W. and Jackson, M.L., 2001. Evaluation of leachates from coal refuse blended with fly ash at different rates. Journal of Environmental Quality, 30: 1382-1391.

Trzebiatowski, B., Edil, T.B. and Benson, C.H., 2004. Case study of subgrade stabilization using fly ash: State Highway 32, Port Washington, Wisconsin. In: A. Aydilek and J. Wartman (Editors), Beneficial Reuse of Waste Materials in Geotechnical and Transportation Applications, GSP No. 127. ASCE, Reston, VA, pp. 123-136.

Van Genuchten, M.T., 1981. Analytical solutions for chemical transport with simultaneous adsorption, zero-order production, and first-order decay. Journal of Hydrology, 49(3-4): 213-233.

Wang, J.M., Teng, X.J., Wang, H. and Ban, H., 2004. Characterizing the metal adsorption capability of a class F coal fly ash. Environmental Science & Technology, 38(24): 6710-6715.

Wisconsin (2004), *Wisconsin Administrative Code*, Revisor of Statutes Bureau, Madison, WI.

TABLES

Table 1. Median (50^{th}) and 90^{th} percentile volumetric leachate fluxes for lysimeters in test sections at the STH 60 field site constructed with fly-ash-stabilized soil and bottom ash (Sept. 2000 – June 2005).

Flux Condition	Fly-Ash-Stabilized Soil		Bottom Ash	
	Inside lysimeter	Outside lysimeter	Inside lysimeter	Outside lysimeter
50^{th} percentile (q_{50}), mm/d	0.11	0.12	0.13	0.16
90^{th} percentile (q_{90}), mm/d	0.31	0.33	0.43	0.53

Table 2. Initial effluent concentrations, retardation factors, and molecular diffusion coefficients for Cd, Cr, and Ag.

	Cd	Cr	Ag
Initial effluent concentration C_o in fly ash stabilized soil section[1], μg/L	4.0	20.2	6.2
Initial effluent concentration, C_o bottom ash section[2], μg/L	21.2	32.1	15.2
Retardation factor R[3]	5.2	5.7	5.0
Molecular diffusion coefficient (free solution)[4], cm^2/s	6.0×10^{-6}	4.4×10^{-6}	1.4×10^{-5}

[1]Initial effluent concentration (C_o) from column data (see appendix).
[2]Initial effluent concentration (C_o) from lysimeters (see appendix).
[3]from Bin-Shafique et al. (2002, 2006).
[4]from Lerman (1979)

Table 3. Peak concentrations in lysimeters and predicted maximum concentration at POC for fly-ash-stabilized-soil and bottom ash test sections at STH 60 site.

Quantity	Cadmium (μg/L)	Chromium (μg/L)	Selenium (μg/L)	Silver (μg/L)
Measured peak concentration in lysimeters beneath section with fly ash stabilized soil[1]	32.1	20.2	89.0	113.0
Measured peak concentration in lysimeters beneath section with bottom ash [1]	21.2	32.1	141.0	15.2
Wisconsin groundwater standards	5	100	50	50
Simulated maximum concentration at POC over 100-yr period for fly-ash-stabilized-soil section[3]	0.2	1.2	1.5	0.3
Simulated maximum concentration at POC over 100-yr period for bottom ash section [2]	3.1	3.4	6.7	1.9

[1]Based on data combined data from inside and outside lysimeters.
[2]Point of compliance (POC) is 20 m down gradient from pavement centerline. Simulation conducted with 90th percentile volumetric leachate flux over 100 yr period. Groundwater table assumed to be 2 m below ground surface.

FIGURES

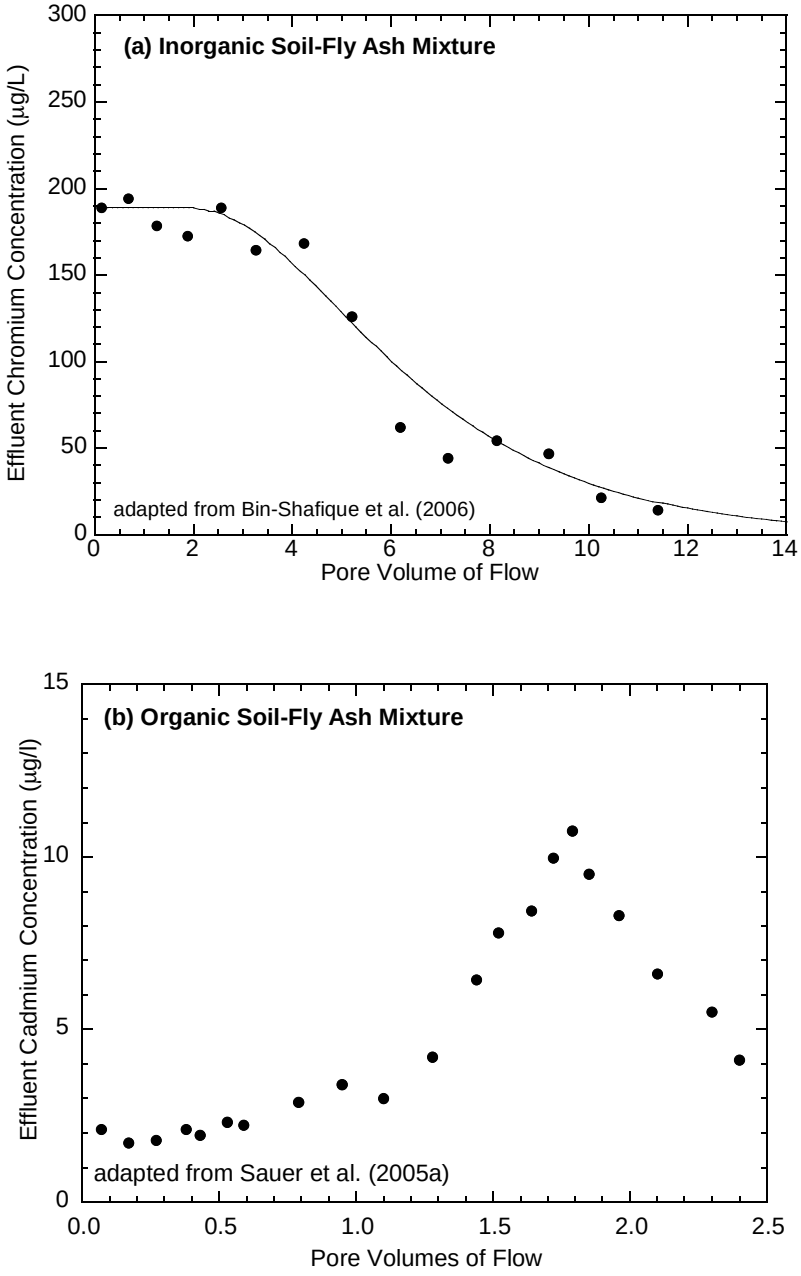

Fig. 1. Examples of first-flush (a) and lagged response (b) elution patterns. The smooth lines in (a) correspond to predictions made with the advection-dispersion reaction equation with linear, instantaneous, and reversible sorption. Graphs adapted from Bin-Shafique et al. (2002) and Sauer et al. (2005a).

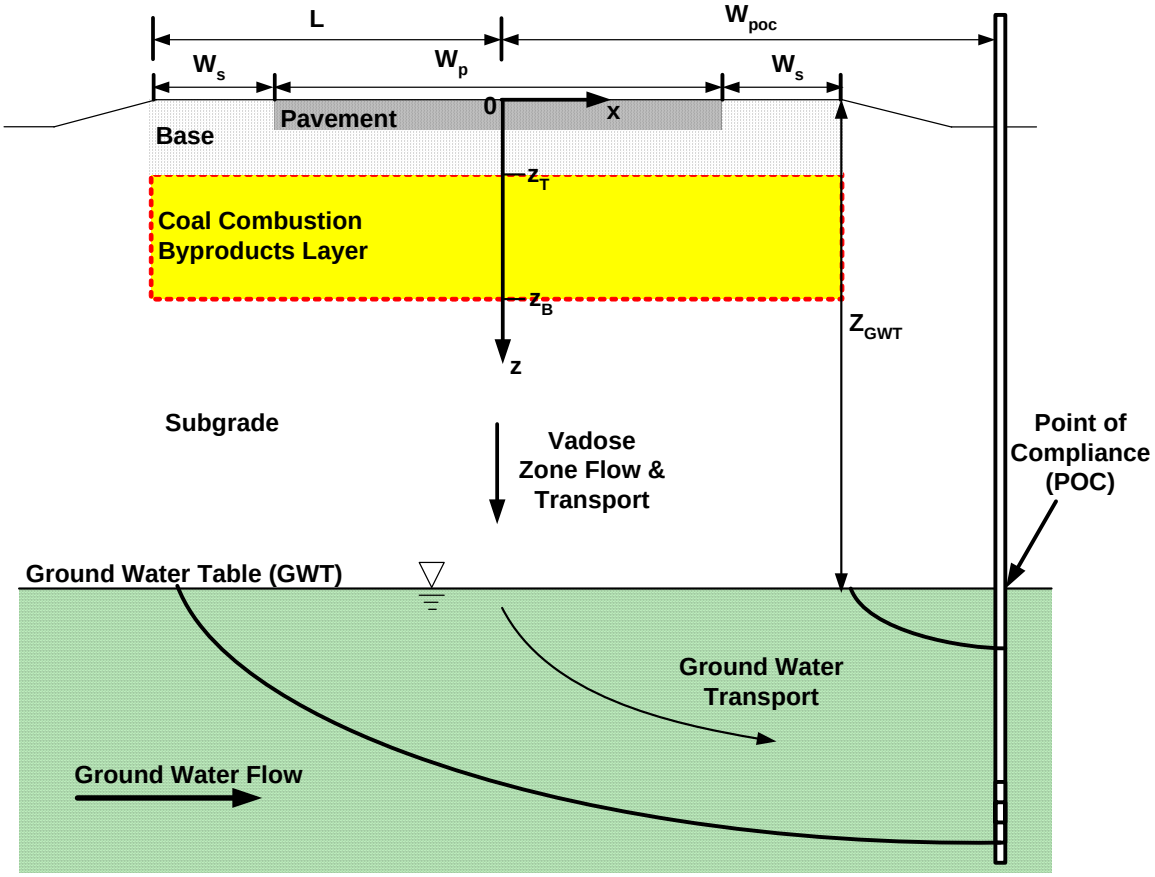

Fig. 2. Conceptual model in WiscLEACH for predicting impacts to the vadose zone and groundwater caused by leaching from a pavement structure with a CCP layer.

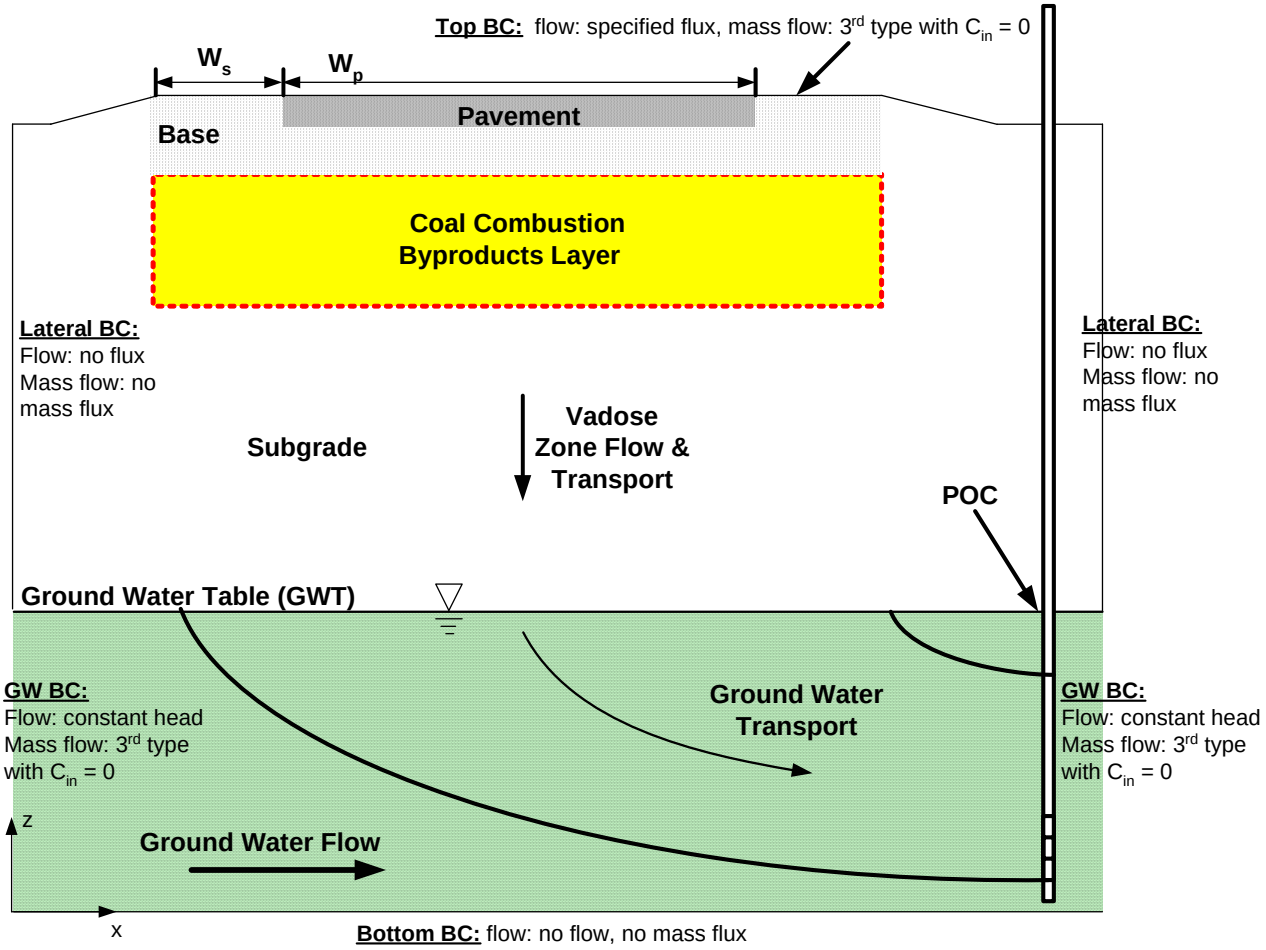

Fig. 3. Conceptual model and boundary conditions used in HYDRUS-2D for calibrating WiscLEACH.

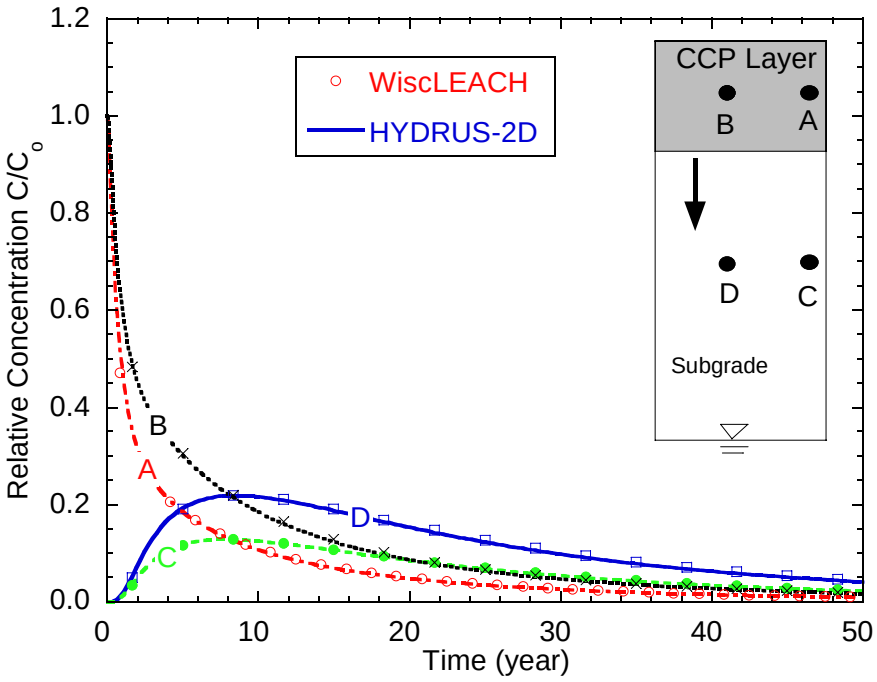

Fig. 4. Comparison of relative concentrations in vadose zone predicted by HYDRUS-2D and WiscLEACH.

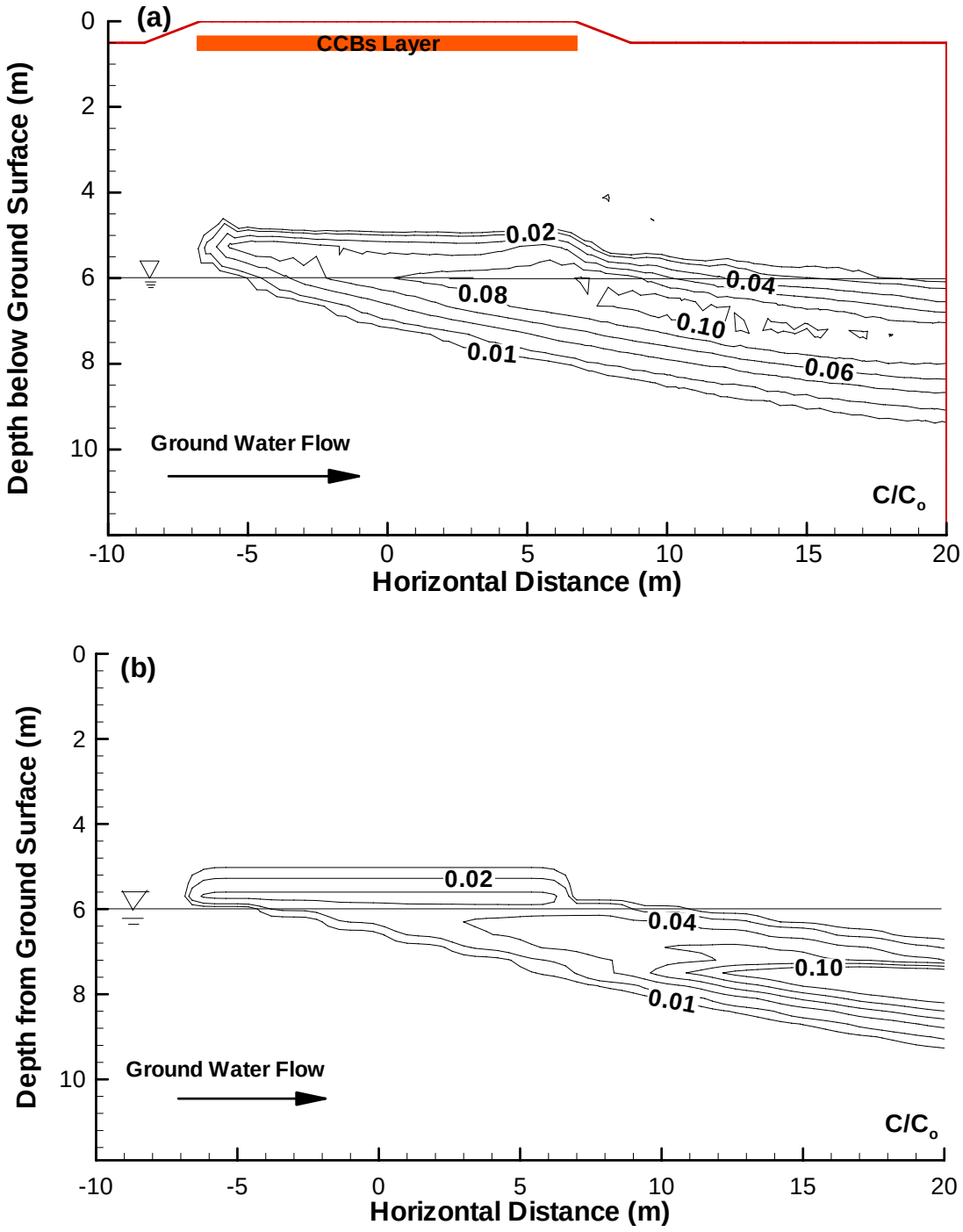

Fig. 5. Relative concentrations after 40 yr predicted by (a) HYDRUS-2D and (b) WiscLEACH. The centerline of the pavement is located at a horizontal distance of zero and the surface of the pavement is at a depth of zero.

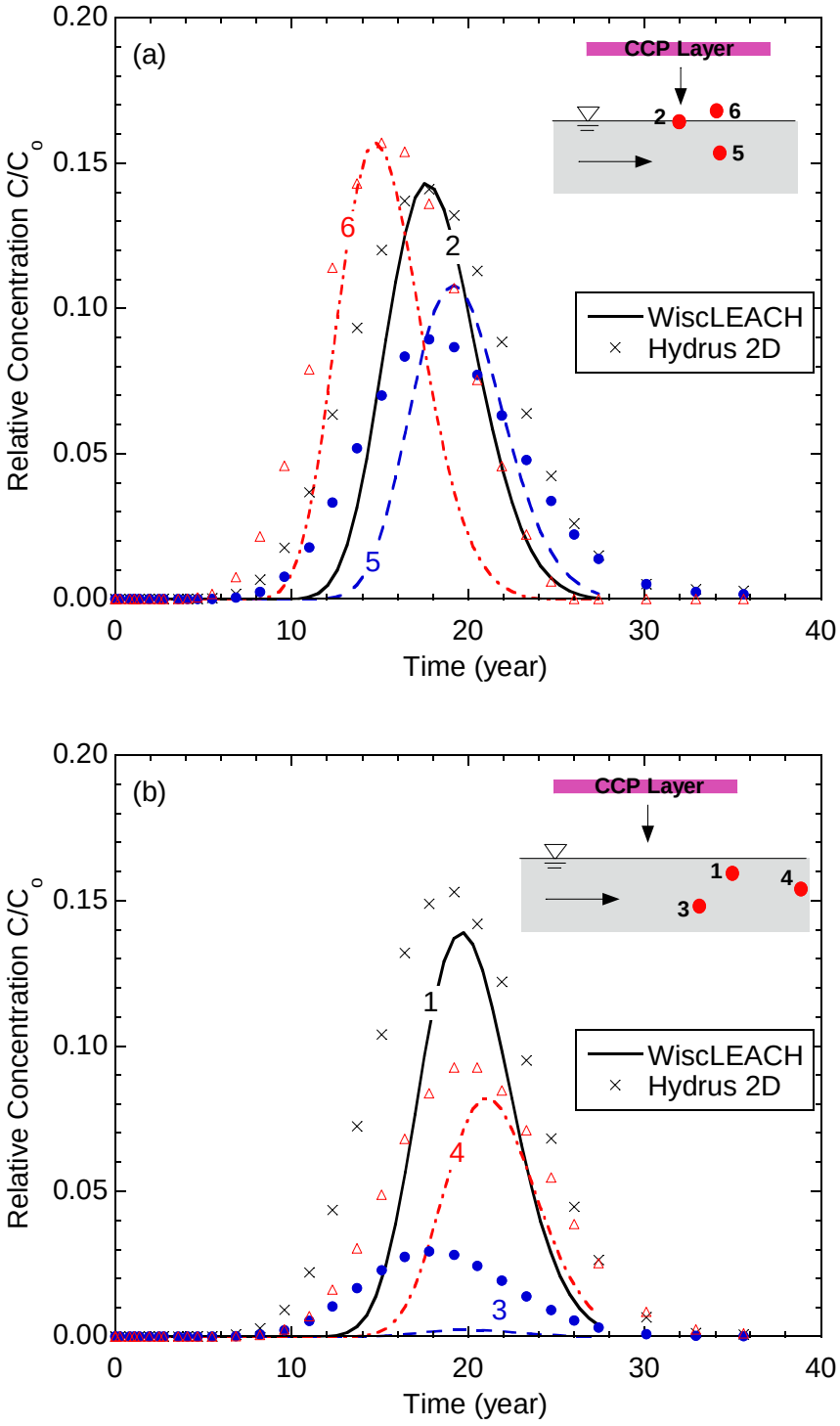

Fig. 6. Relative concentrations predicted by HYDRUS-2D and WiscLEACH at (a) observation points 2, 5, 6 and (b) at observation points 1, 3, 4.

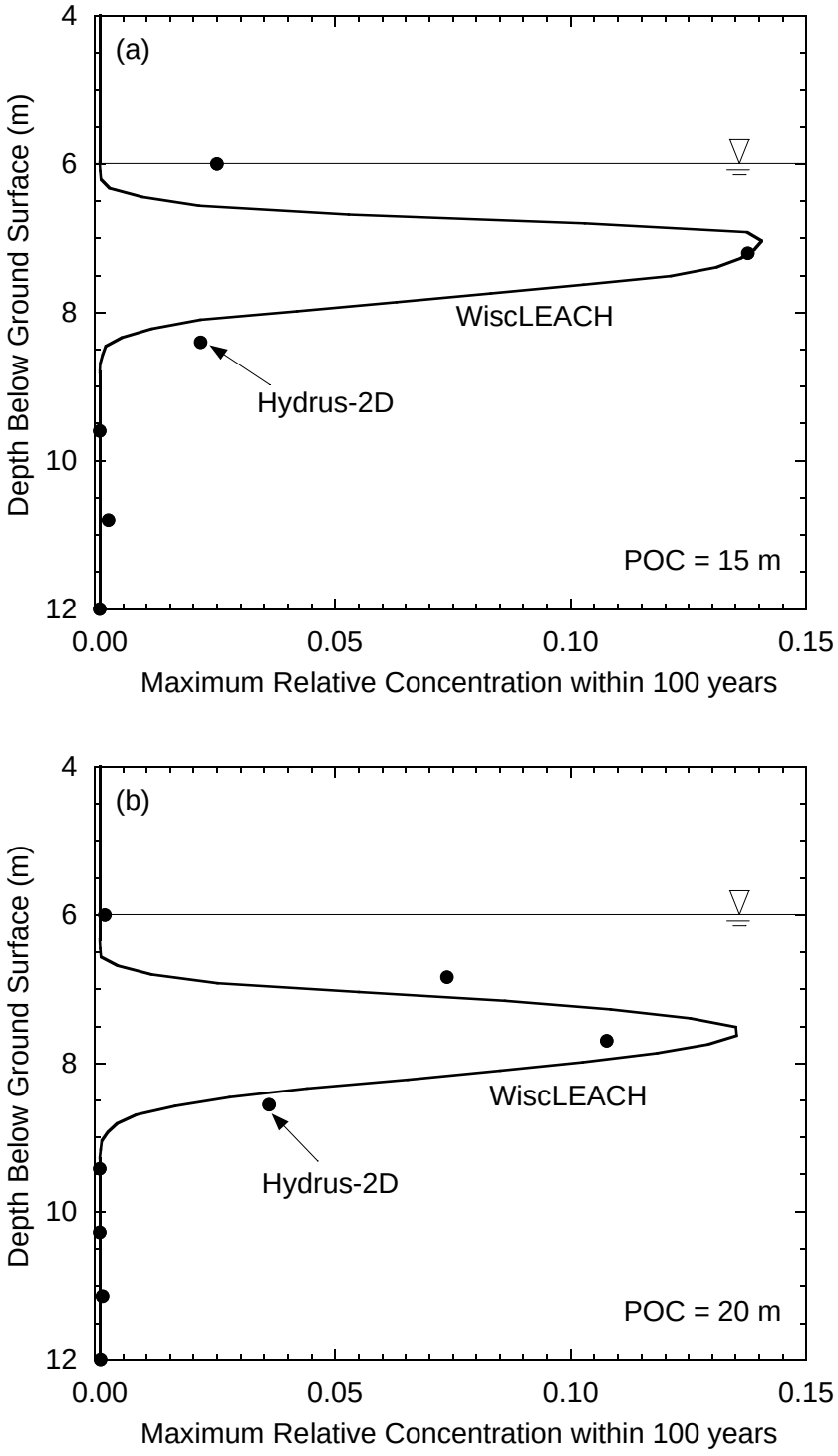

Fig. 7. Relative concentrations at POC over 100-yr period as a function of depth below ground surface predicted by HYDRUS-2D and WiscLEACH: (a) POC at 15 m and (b) POC at 20 m down gradient from pavement centerline.

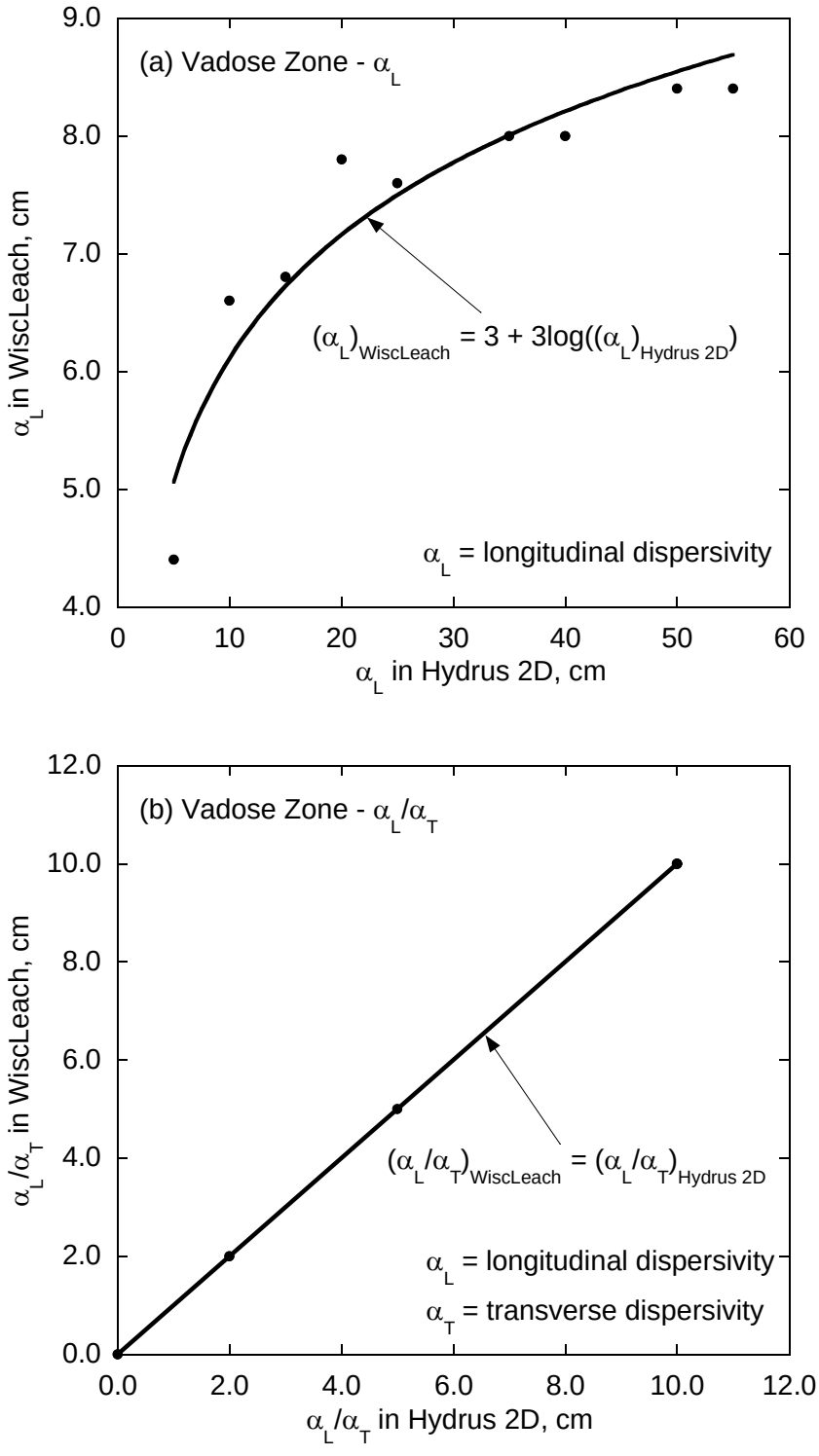

Fig. 8. Calibrated dispersivities in WiscLEACH in vadose zone required to match predictions made with HYDRUS-2D: (a) longitudinal dispersivity and (b) ratio of longitudinal dispersivity to transverse dispersivity.

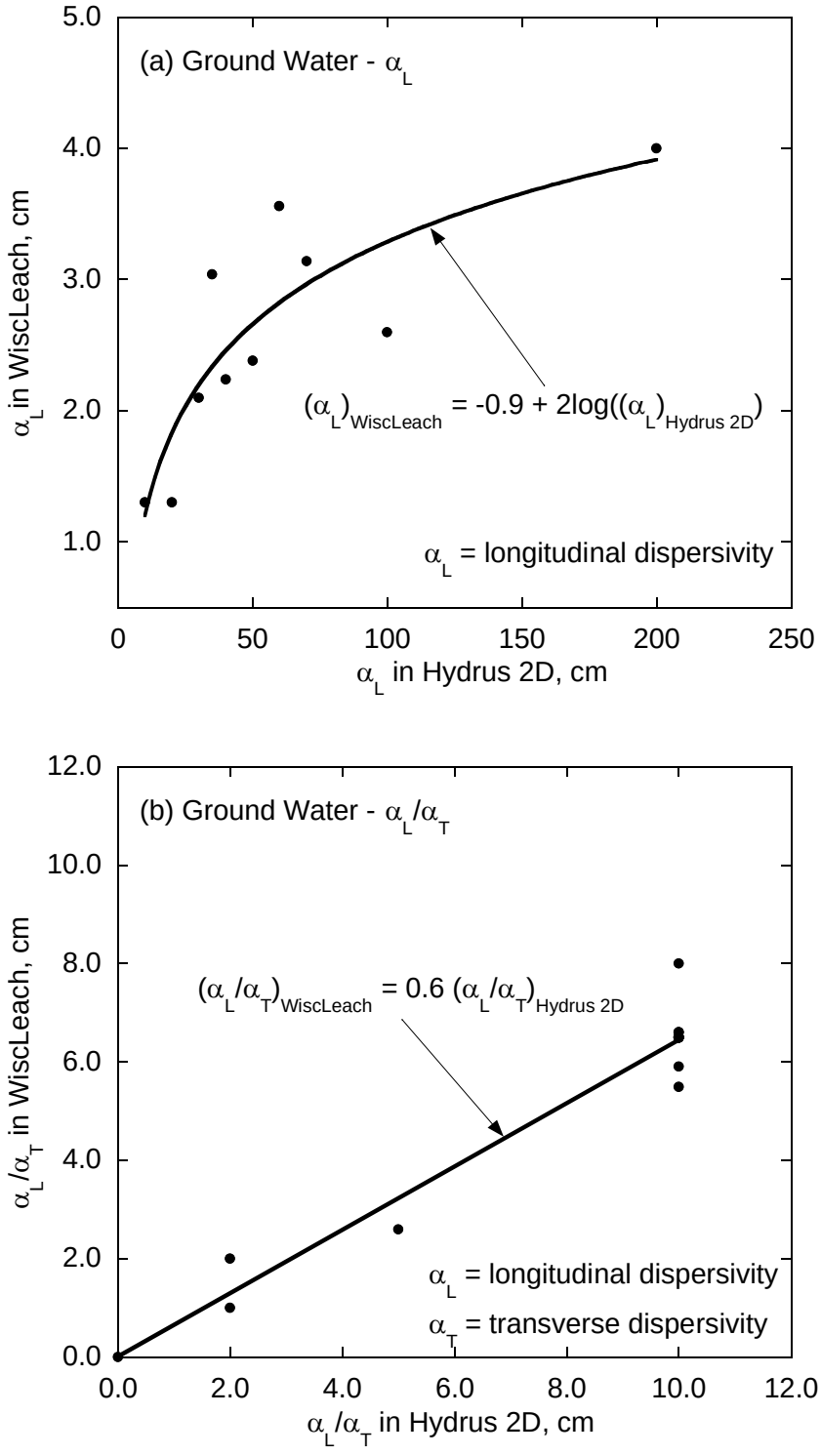

Fig. 9. Calibrated dispersivities in WiscLEACH in vadose zone required to match predictions made with HYDRUS-2D: (a) longitudinal dispersivity and (b) ratio of longitudinal dispersivity to transverse dispersivity.

(a)

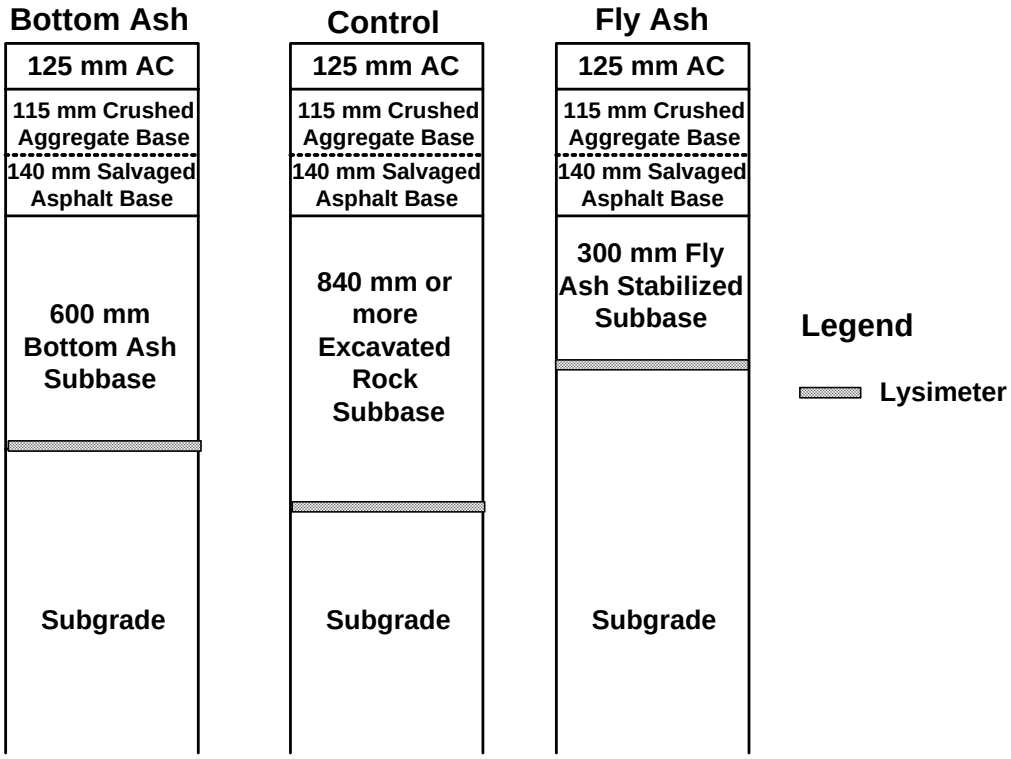

(b)

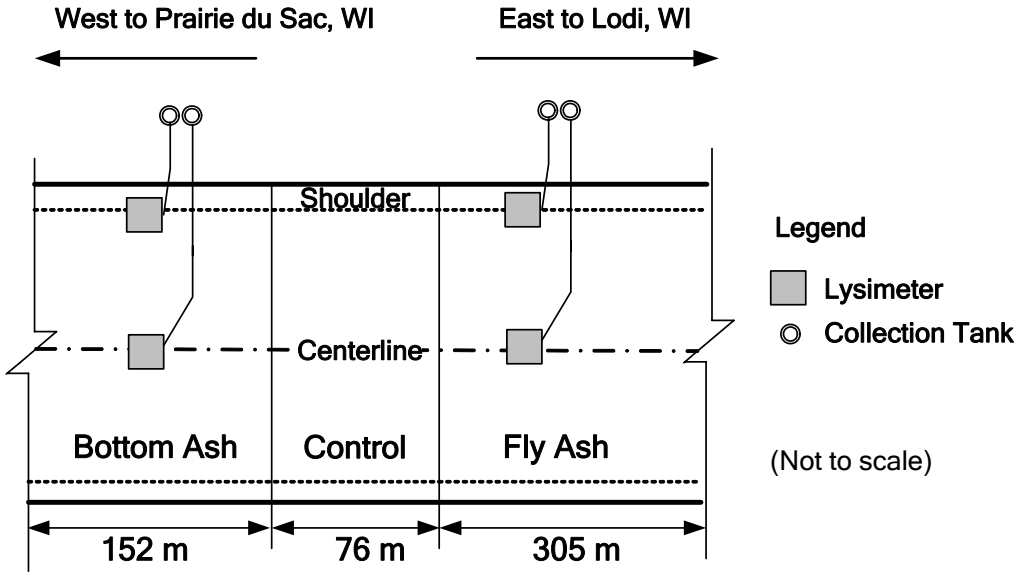

Fig. 10. CCP test sections and control section at STH 60 site: (a) profiles of pavement structures and (b) layout of lysimeters in CCP sections.

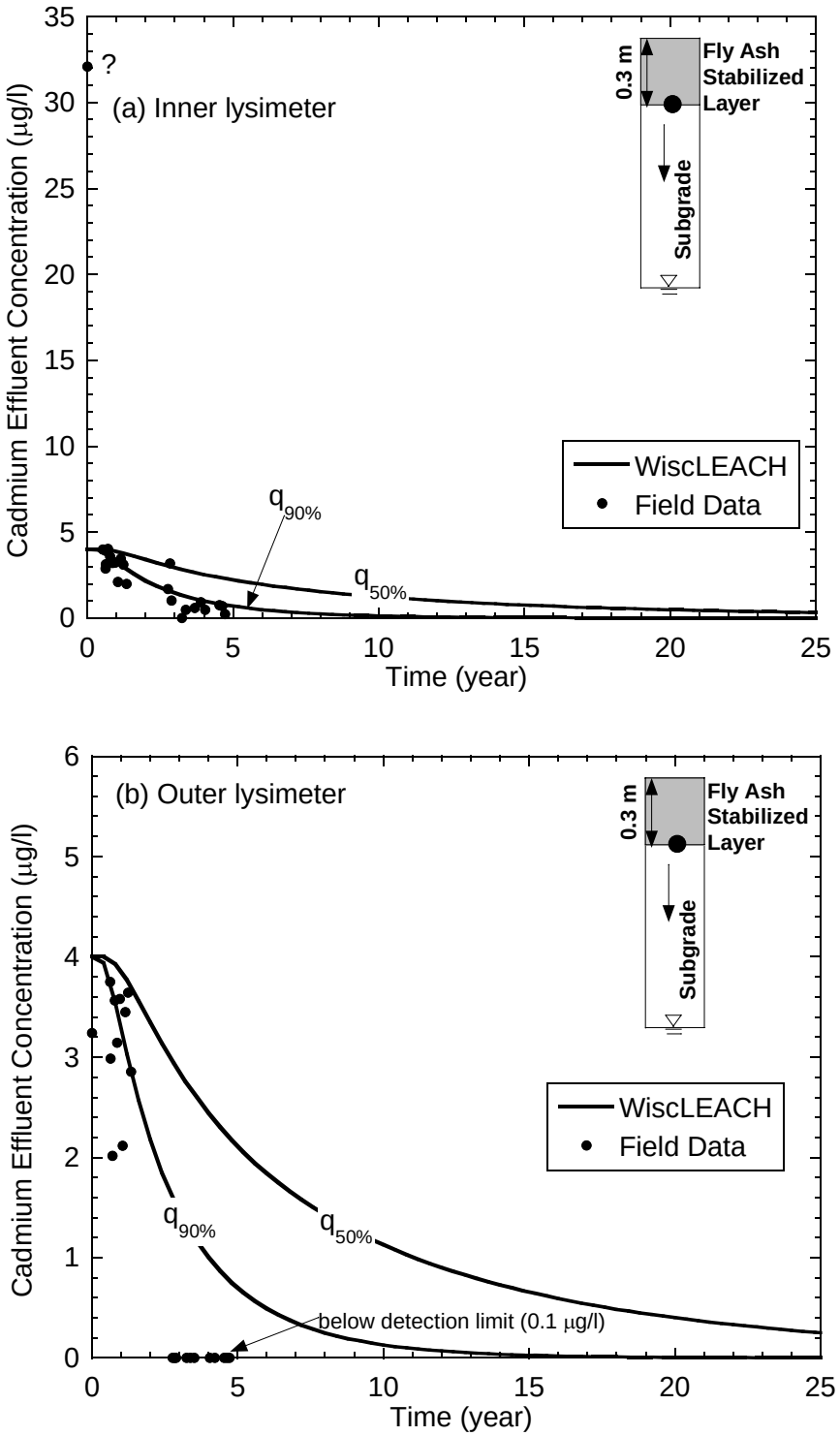

Fig. 11. Measured and predicted Cd concentrations in leachate from fly-ash-stabilized-soil section at STH 60. Simulation was conducted using volumetric leachate flux from (a) inner lysimeter and (b) outer lysimeter. $q_{50\%}$ is the 50th percentile volumetric leachate flux and $q_{90\%}$ is the 90th percentile volumetric leachate flux.

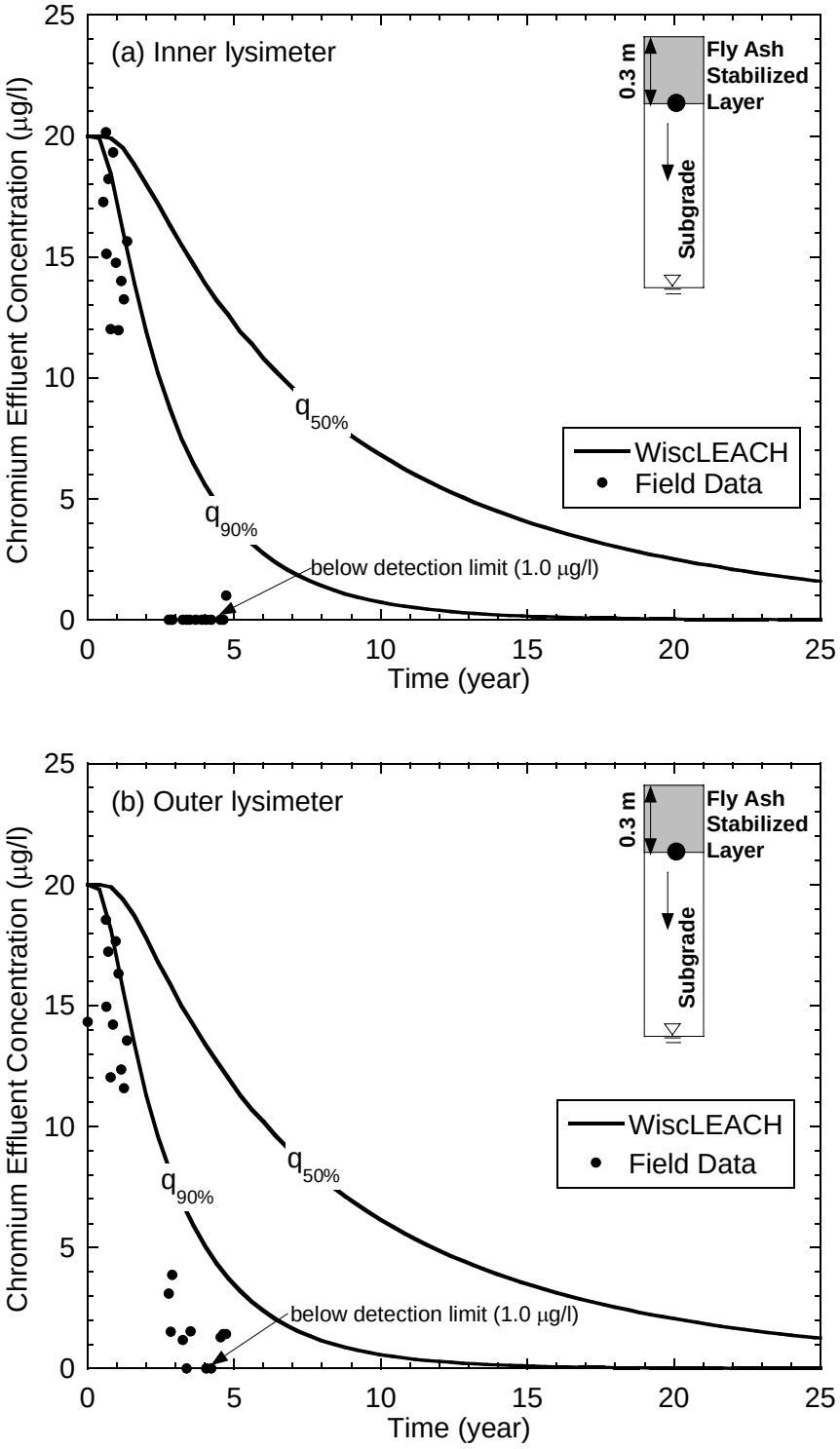

Fig. 12. Measured and predicted Cr concentrations in leachate from fly-ash-stabilized-soil section at STH 60. Simulation was conducted using volumetric leachate flux from (a) inner lysimeter and (b) outer lysimeter. $q_{50\%}$ is the 50th percentile volumetric leachate flux and $q_{90\%}$ is the 90th percentile volumetric leachate flux.

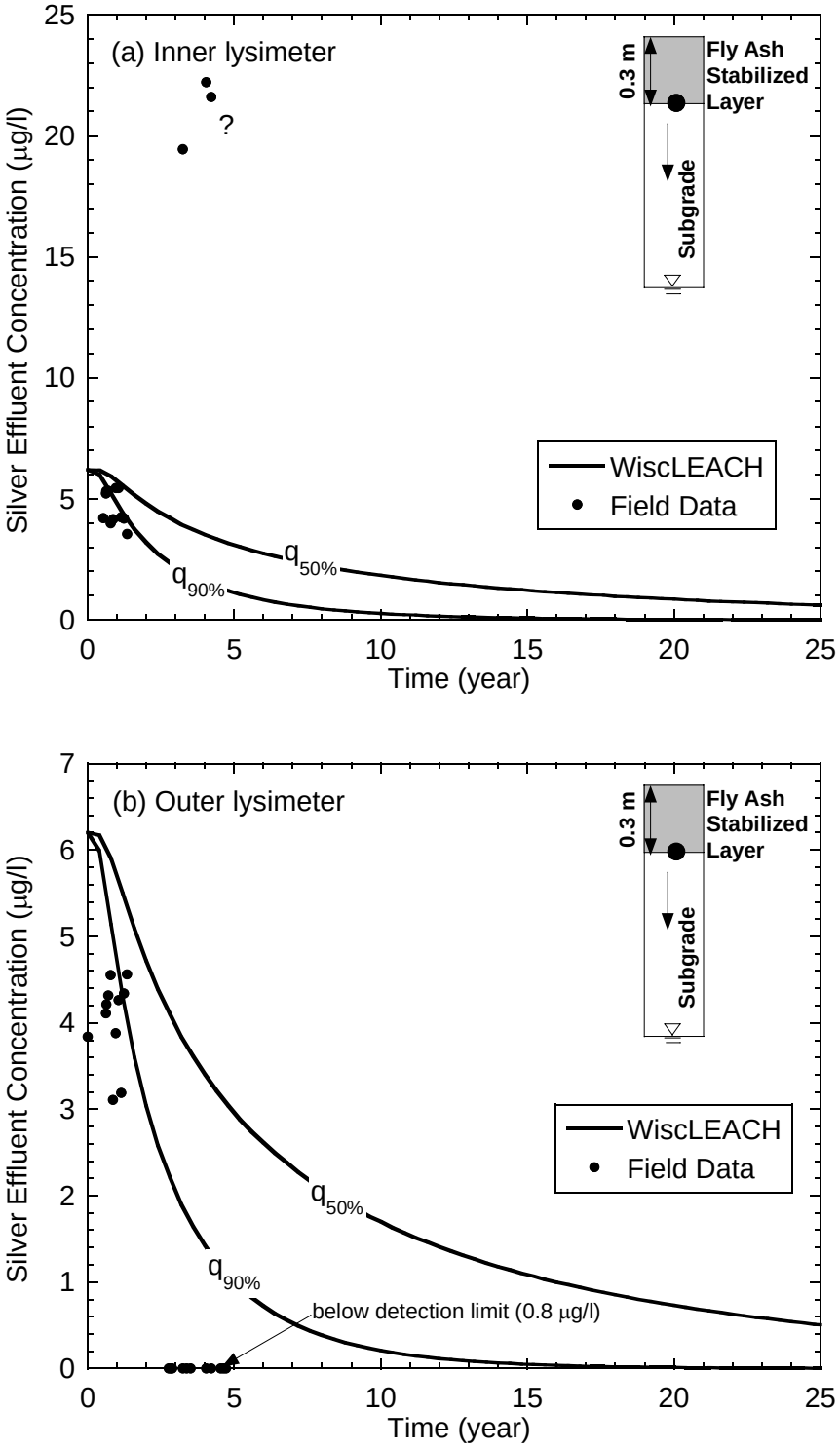

Fig. 13. Measured and predicted Ag concentrations in leachate from fly-ash-stabilized-soil section at STH 60. Simulation was conducted using volumetric leachate flux from (a) inner lysimeter and (b) outer lysimeter. $q_{50\%}$ is the 50th percentile volumetric leachate flux and $q_{90\%}$ is the 90th percentile volumetric leachate flux.

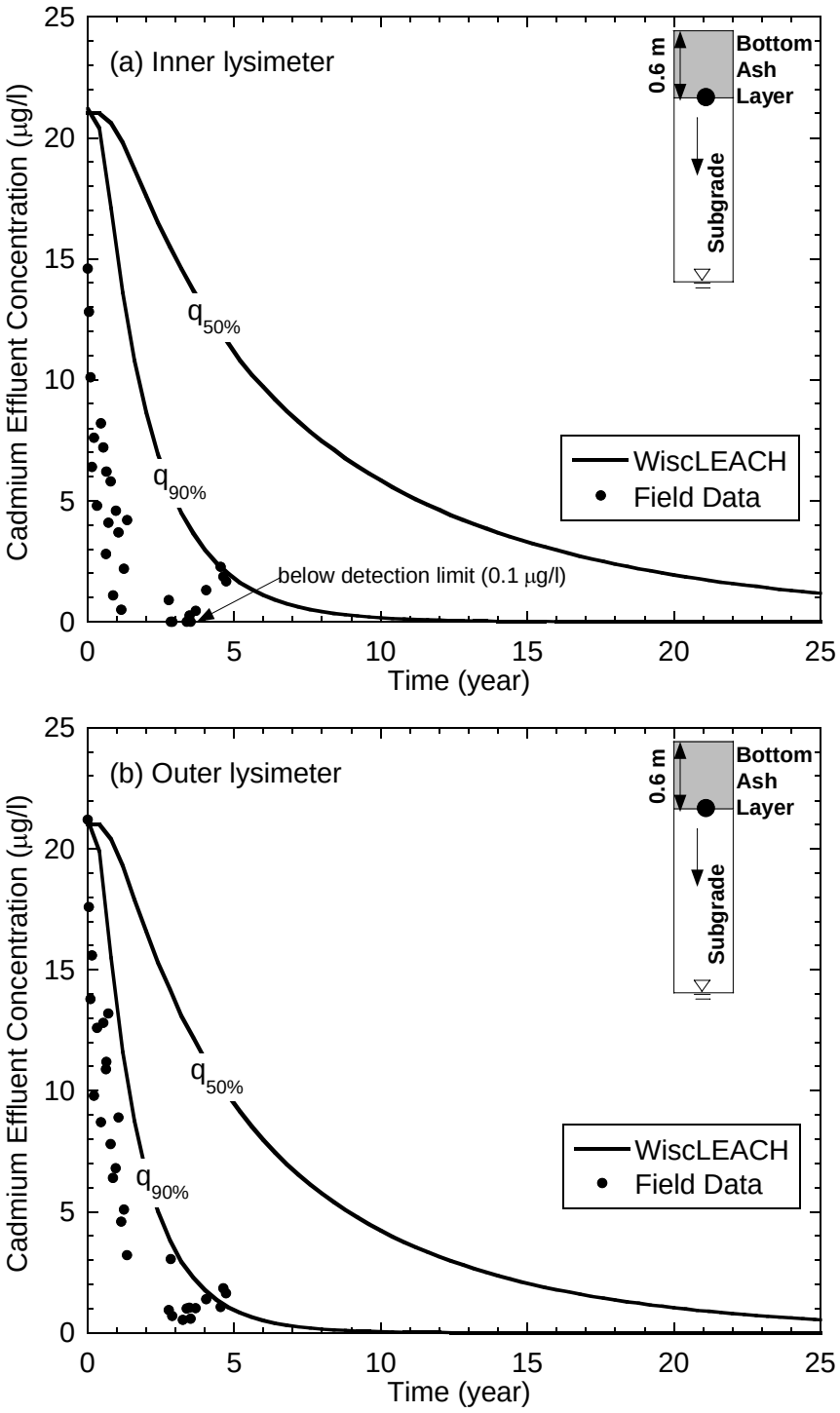

Fig. 14. Measured and predicted Cd concentrations in leachate from the bottom-ash section at STH 60. Simulation was conducted using volumetric leachate flux from (a) inner lysimeter and (b) outer lysimeter. $q_{50\%}$ is the 50th percentile volumetric leachate flux and $q_{90\%}$ is the 90th percentile volumetric leachate flux.

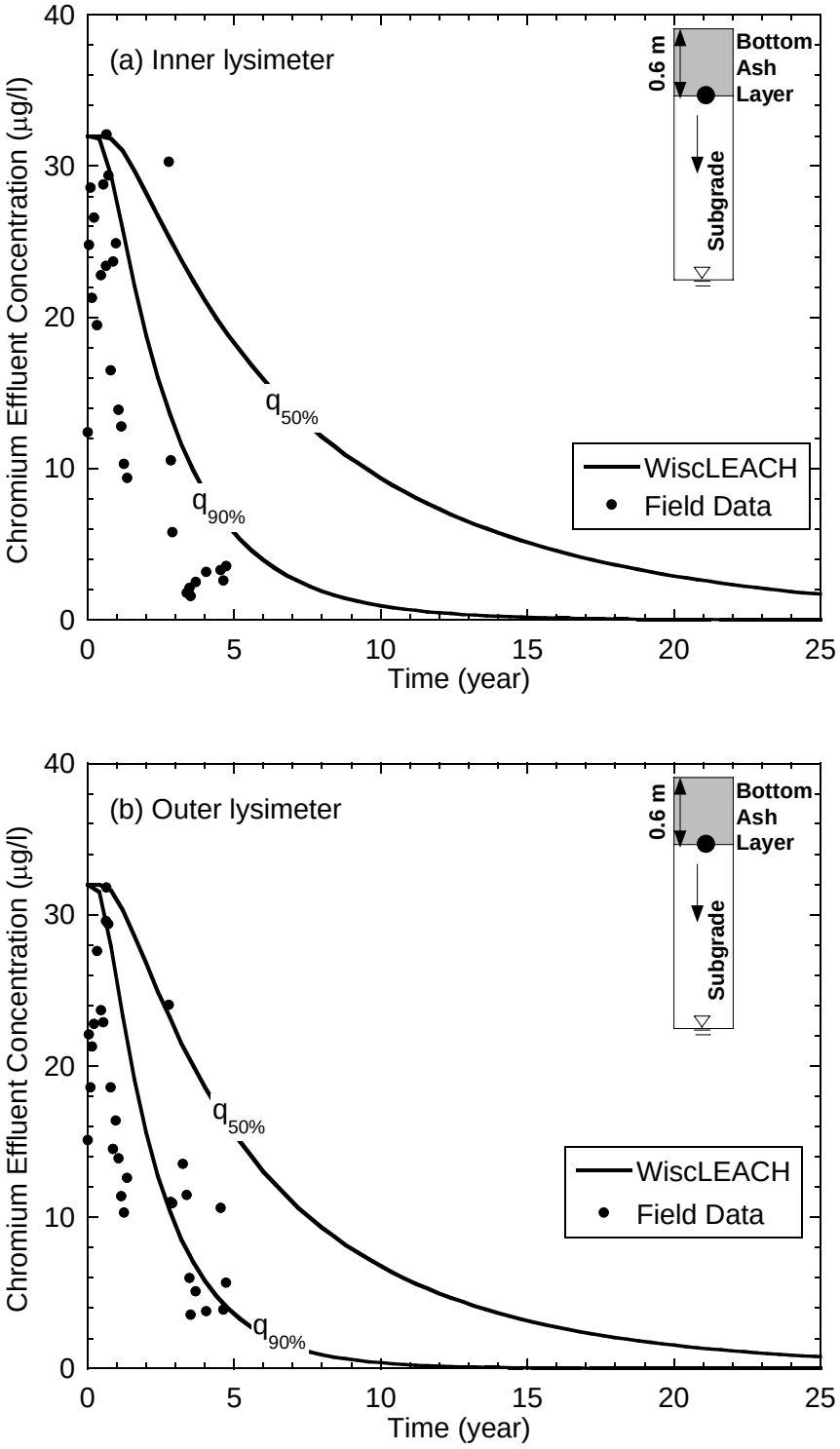

Fig. 15. Measured and predicted Cr concentrations in leachate from the bottom-ash section at STH 60. Simulation was conducted using volumetric leachate flux from (a) inner lysimeter and (b) outer lysimeter. $q_{50\%}$ is the 50th percentile volumetric leachate flux and $q_{90\%}$ is the 90th percentile volumetric leachate flux.

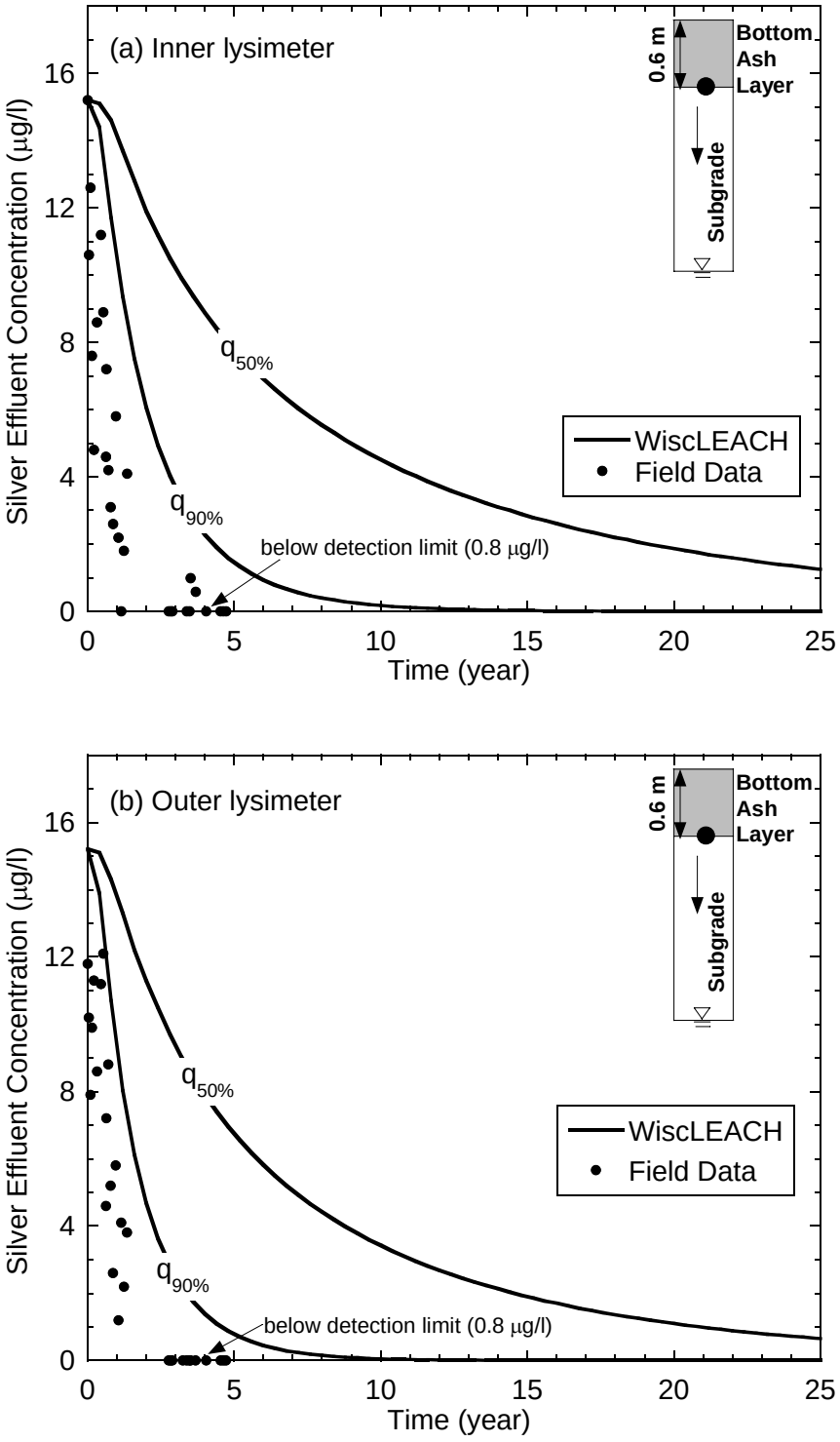

Fig. 16. Measured and predicted Ag concentrations in leachate from the bottom-ash section at STH 60. Simulation was conducted using volumetric leachate flux from (a) inner lysimeter and (b) outer lysimeter. $q_{50\%}$ is the 50th percentile volumetric leachate flux and $q_{90\%}$ is the 90th percentile volumetric leachate flux.

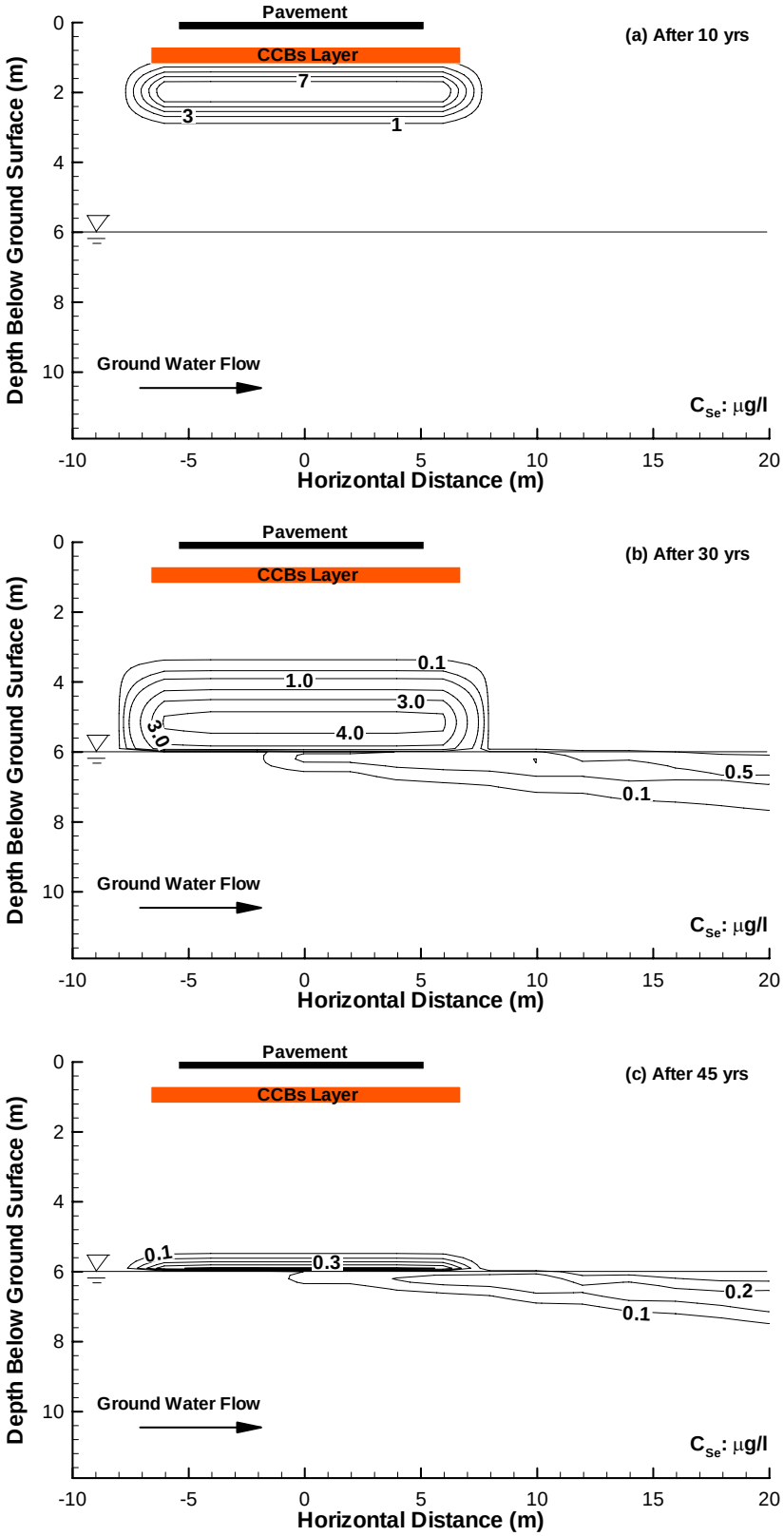

Fig. 17. Predicted Se concentrations in vadose zone and groundwater after (a) 10 yr, (b) 30 yr, and (c) 45 yr.

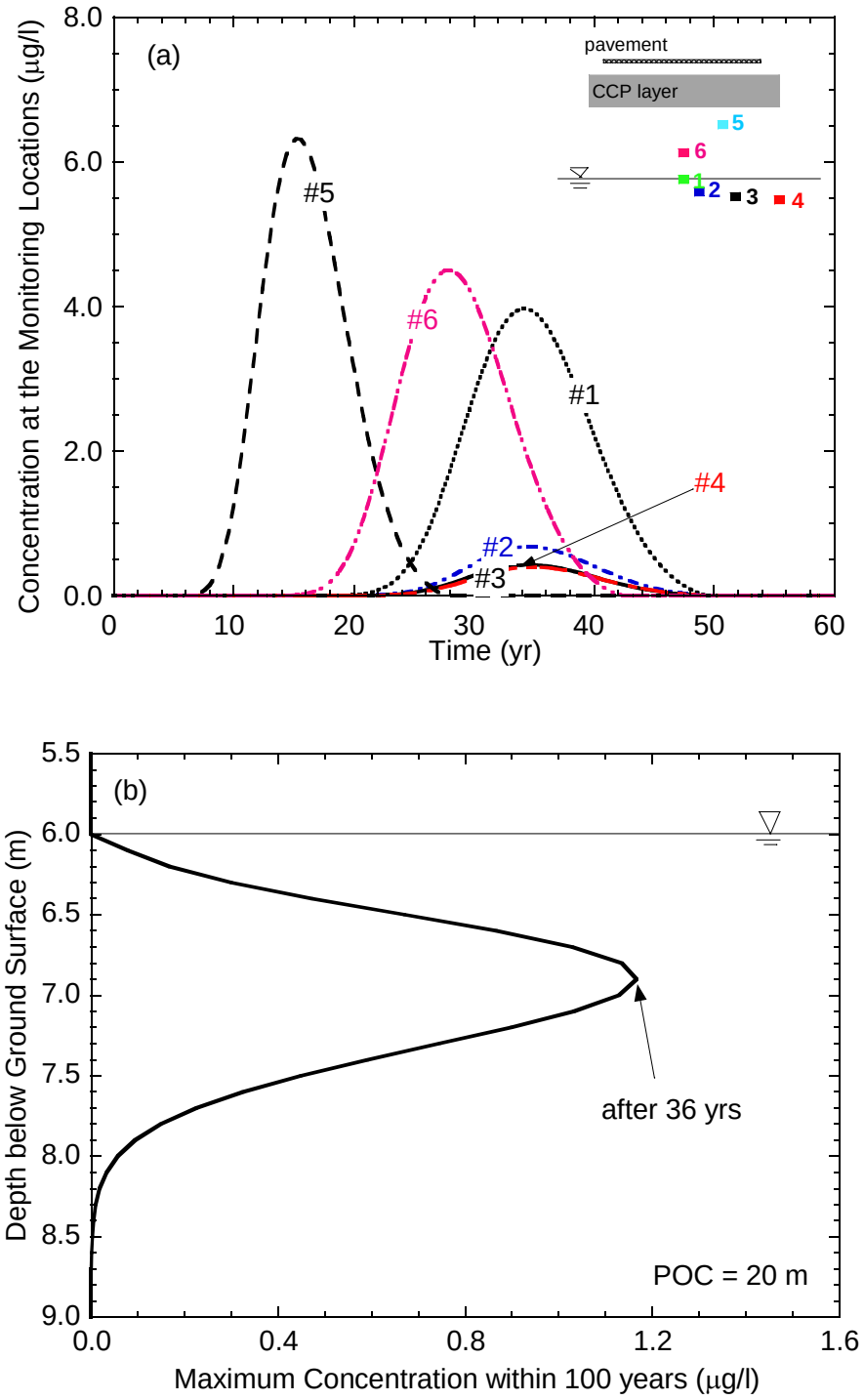

Fig. 18. Predicted Se concentrations at specified monitoring locations (a) and maximum concentration at POC over 100-yr period (b). POC located 20 m down gradient from pavement centerline.

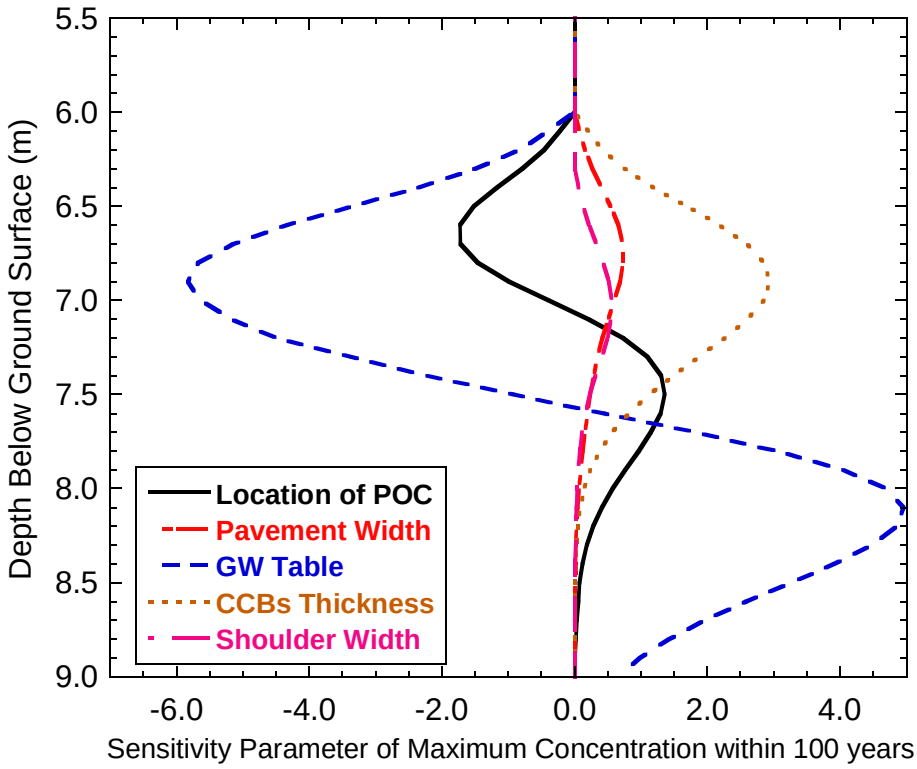

Fig. 19. Sensitivity of maximum Se concentration at POC over 100 yr to geometric variables. POC is 20 m down gradient from pavement centerline. GWT is 6 m below ground surface, except for sensitivity analyses for depth to GWT.

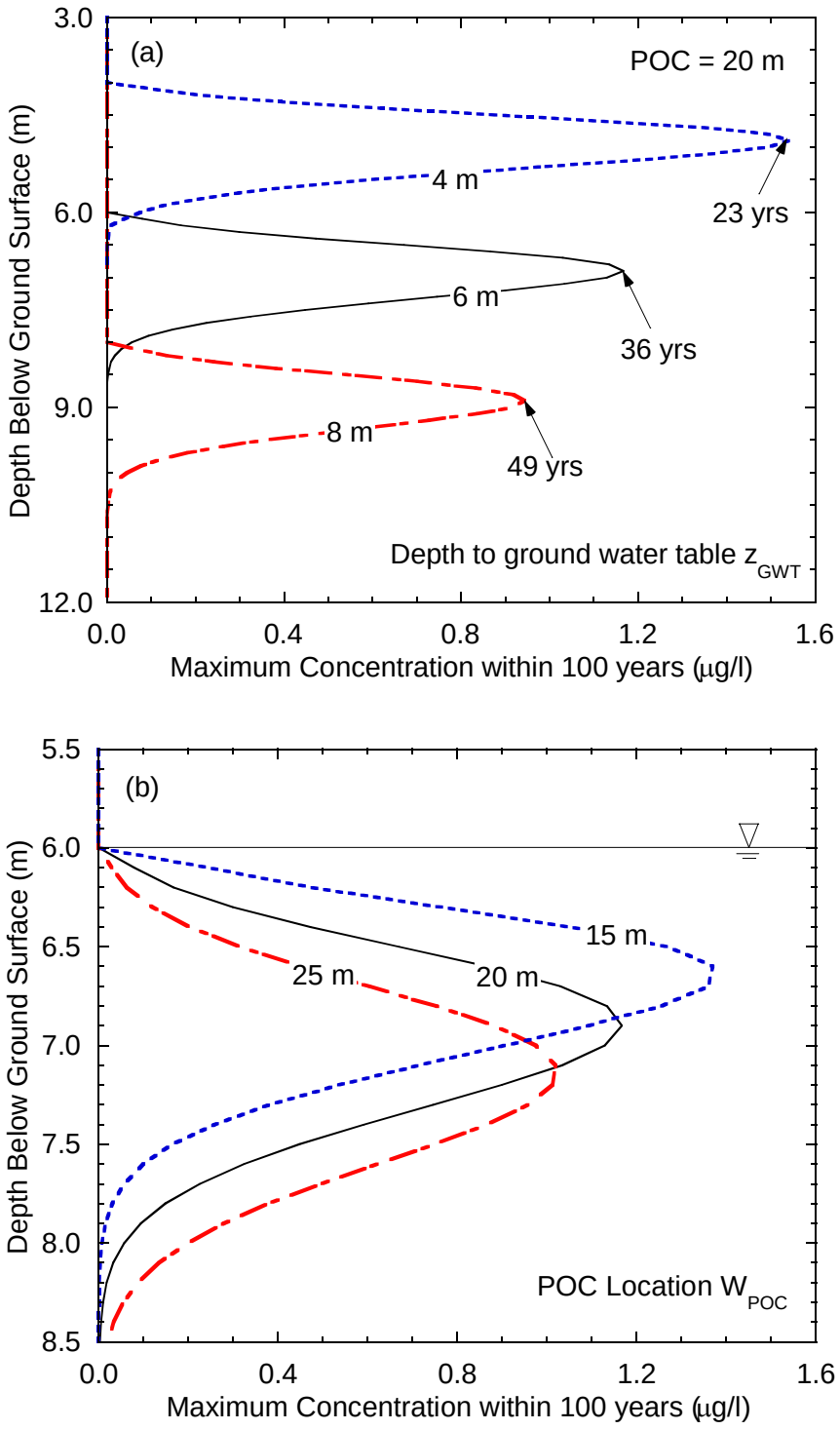

Fig. 20. Maximum Se concentration at POC over 100-yr period as a function of (a) depth to groundwater table and (b) location of POC. In (a), POC is 20 m down gradient from pavement centerline.

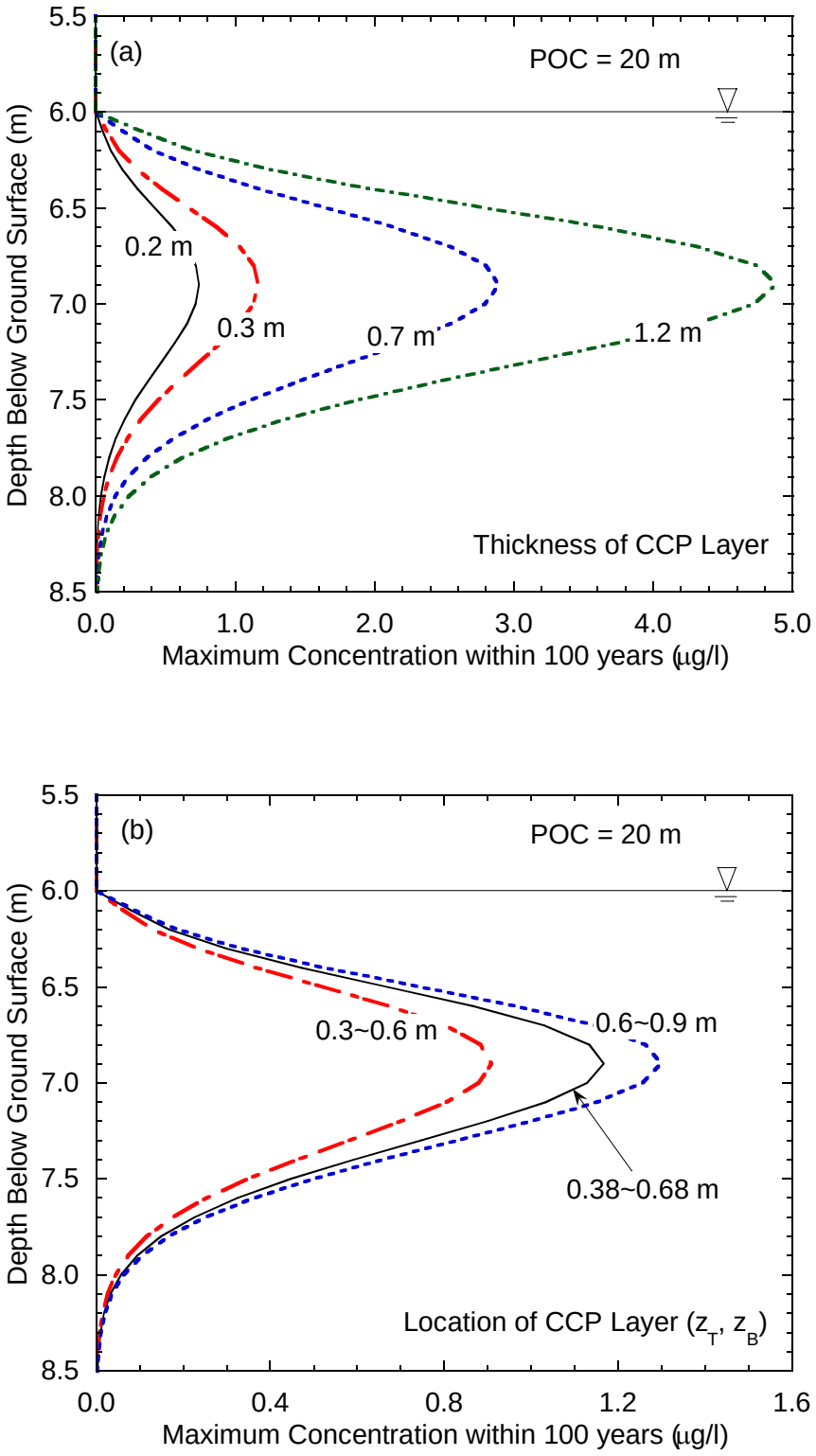

Fig. 21. Maximum Se concentration at POC over 100-yr period as a function of (a) thickness of CCP layer and (b) location of CCB layer. For (b), POC is 20 m down gradient from pavement centerline.

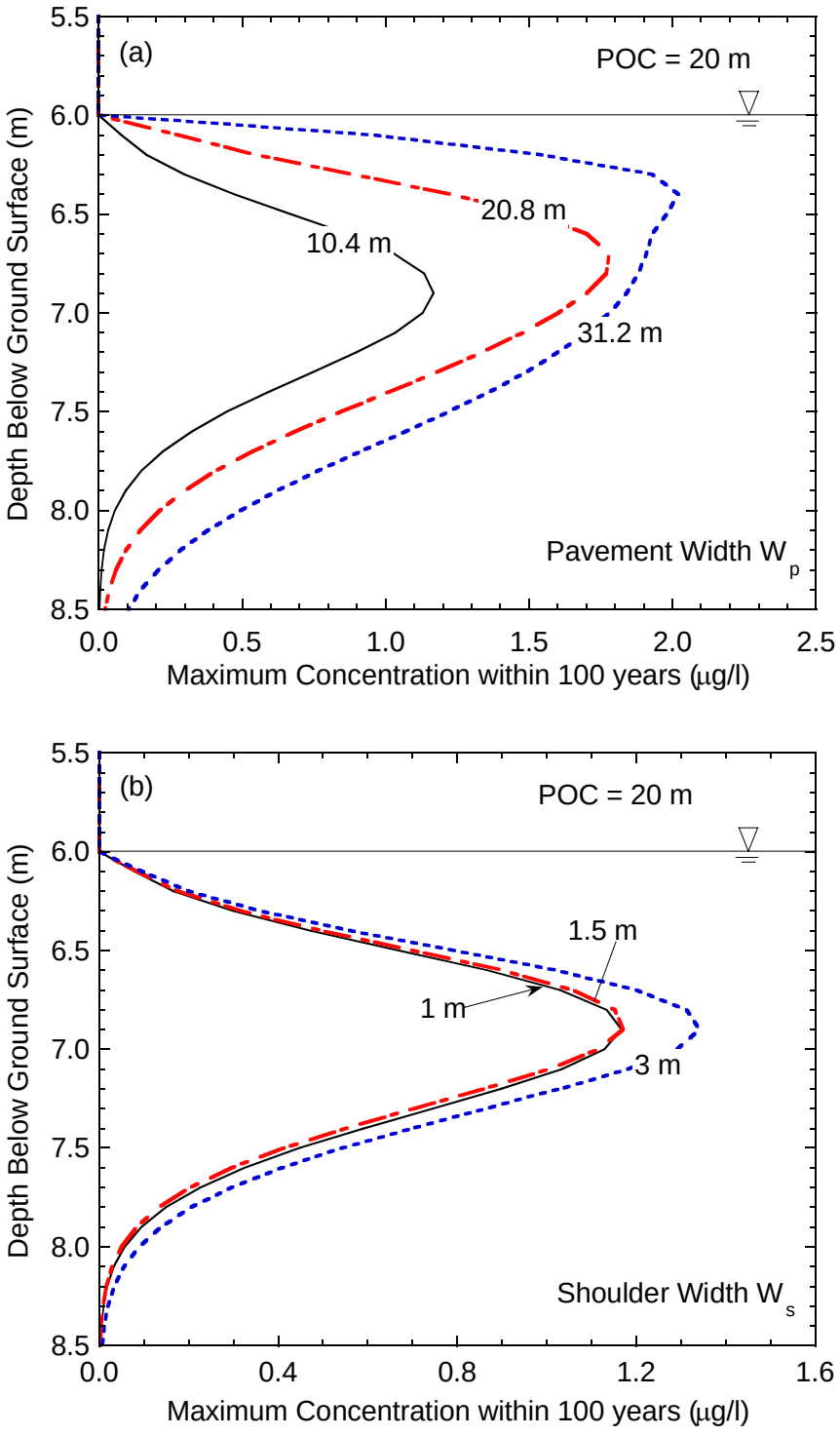

Fig. 22. Maximum Se concentration at POC over 100-yr period as a function of (a) pavement width and (b) shoulder width. POC is 20 m down gradient from pavement centerline.

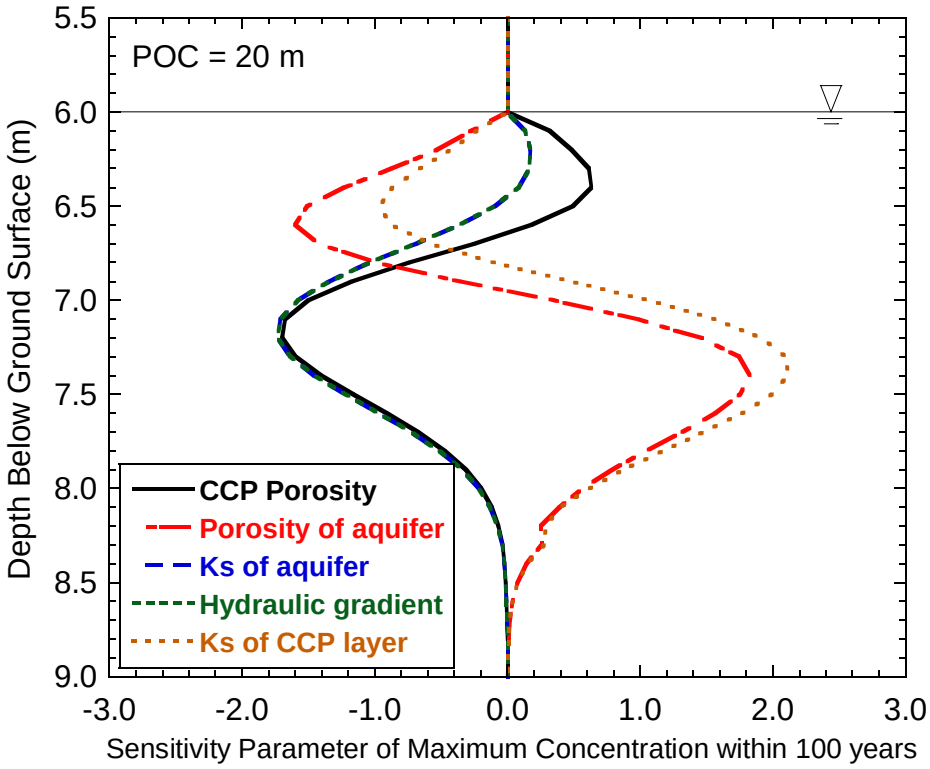

Fig. 23. Sensitivity of maximum Se concentration at POC over 100 yr to hydraulic variables. POC is 20 m down gradient from pavement centerline.

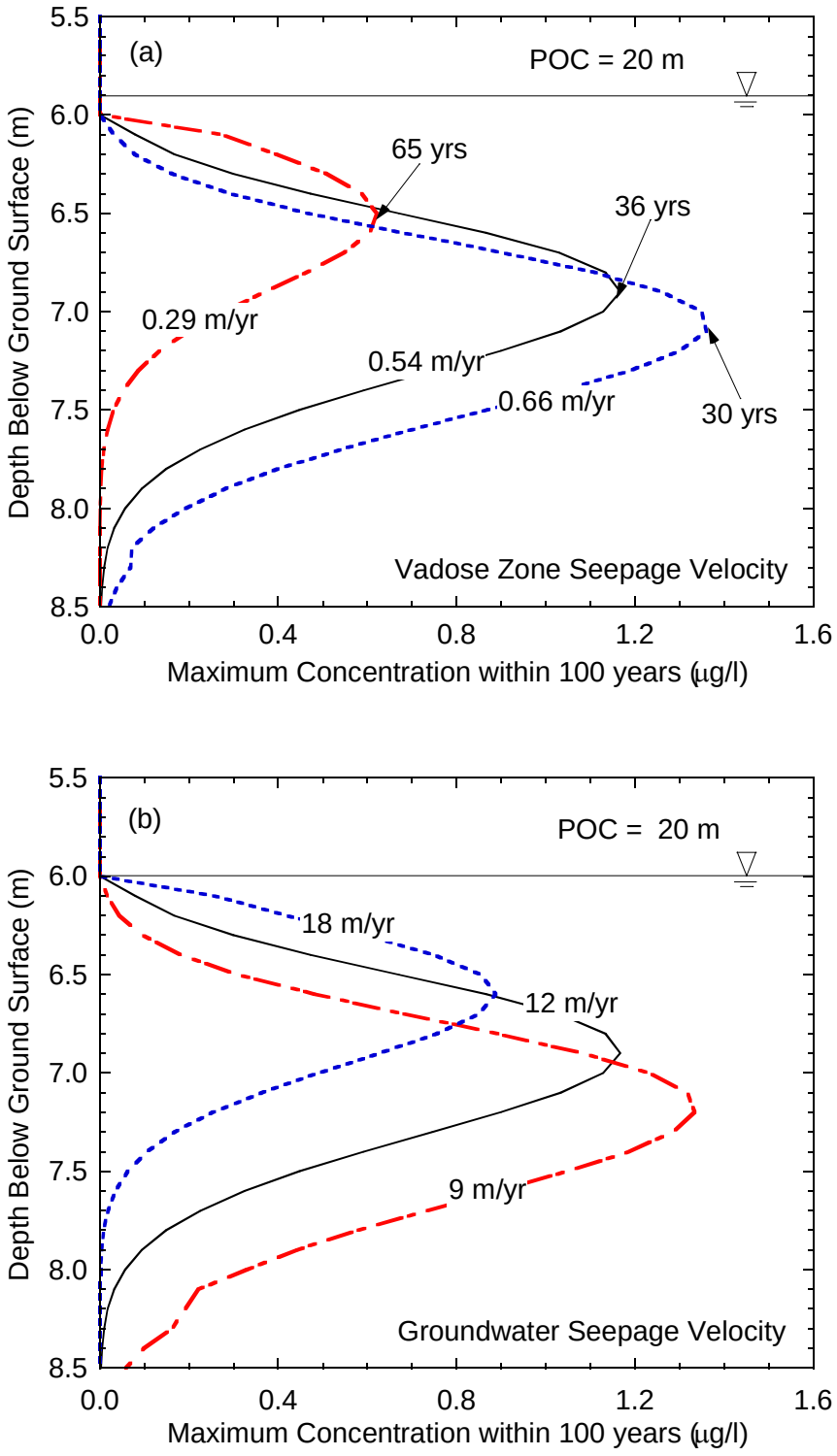

Fig. 24. Maximum Se concentration at POC over 100-yr period as a function of seepage velocity in (a) the vadose zone and (b) groundwater. POC is 20 m down gradient from pavement centerline.

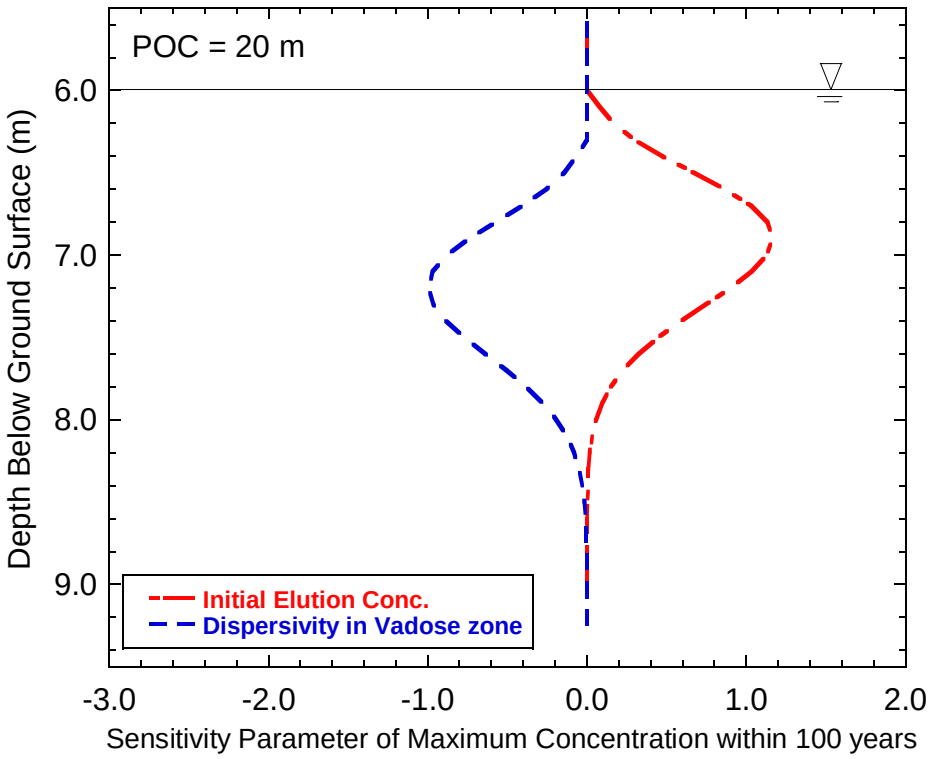

Fig. 25. Sensitivity of maximum Se concentration at POC over 100 yr to transport parameters. POC is 20 m down gradient from pavement centerline.

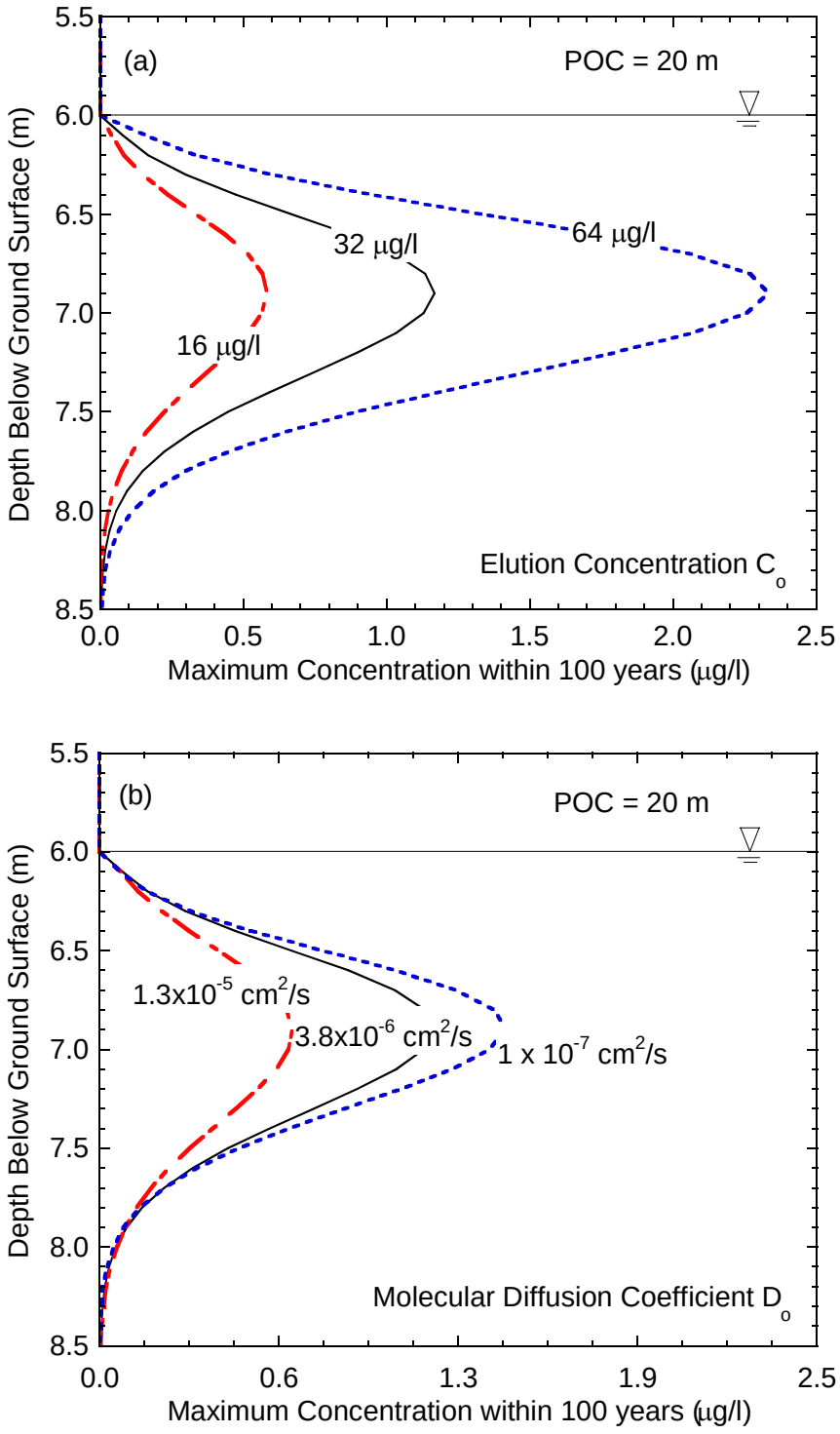

Fig. 26. Maximum Se concentration at POC over 100-yr period as a function of (a) initial elution concentration C_o and (b) molecular diffusion coefficient. POC is 20 m down gradient from pavement centerline.

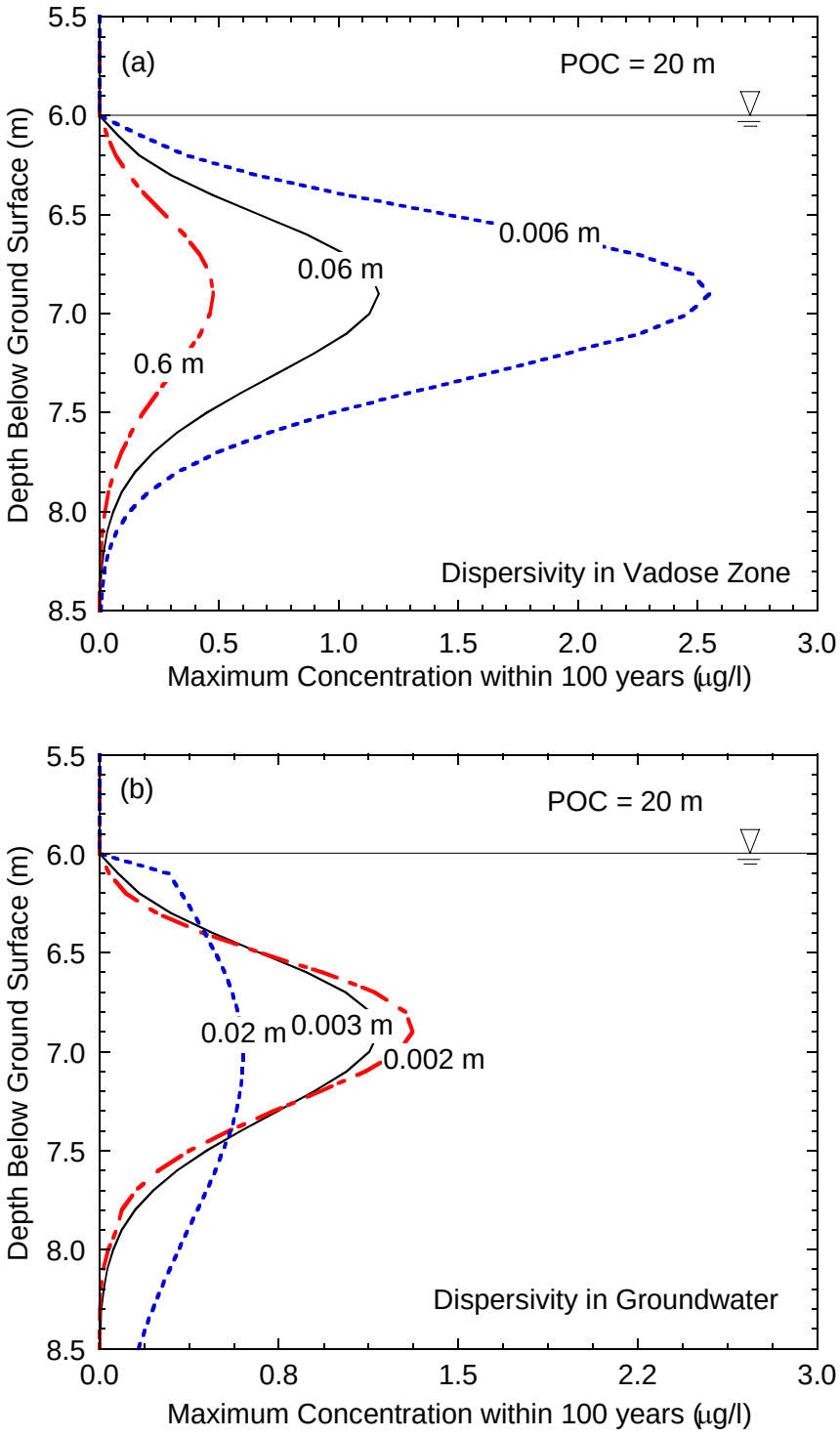

Fig. 27. Maximum Se concentration at POC over 100-yr period as a function of vertical dispersivity in vadose zone (a) and horizontal dispersivity in groundwater (b). POC is 20 m down gradient from pavement centerline.

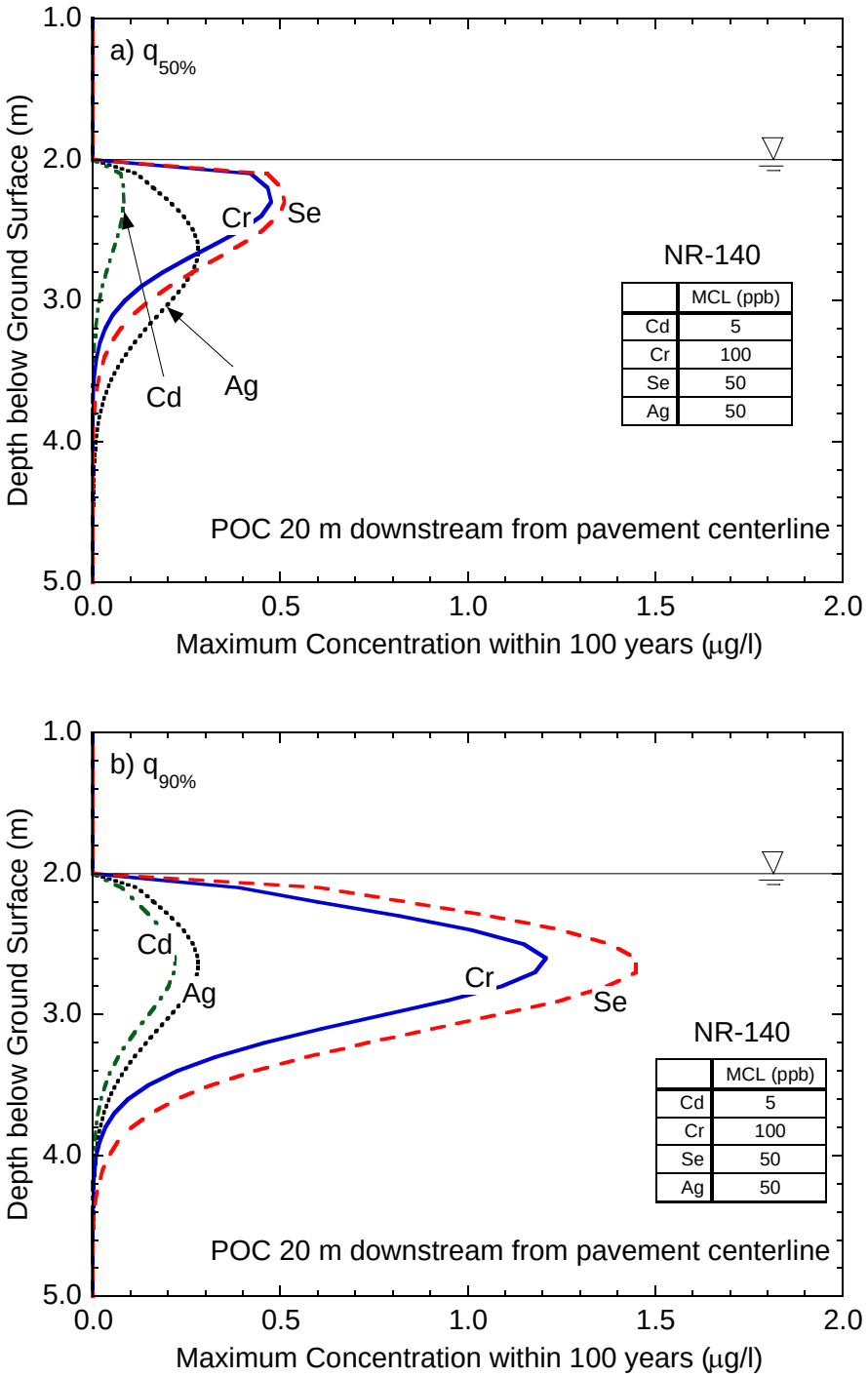

Fig. 28. Predicted maximum concentrations at POC in fly-ash-stabilized-soil section at STH 60. Simulation was conducted using volumetric leachate flux from (a) inner lysimeter and (b) outer lysimeter. $q_{50\%}$ is 50th percentile of measured volumetric leachate flux and $q_{90\%}$ is 90th percentile of measured volumetric leachate flux.

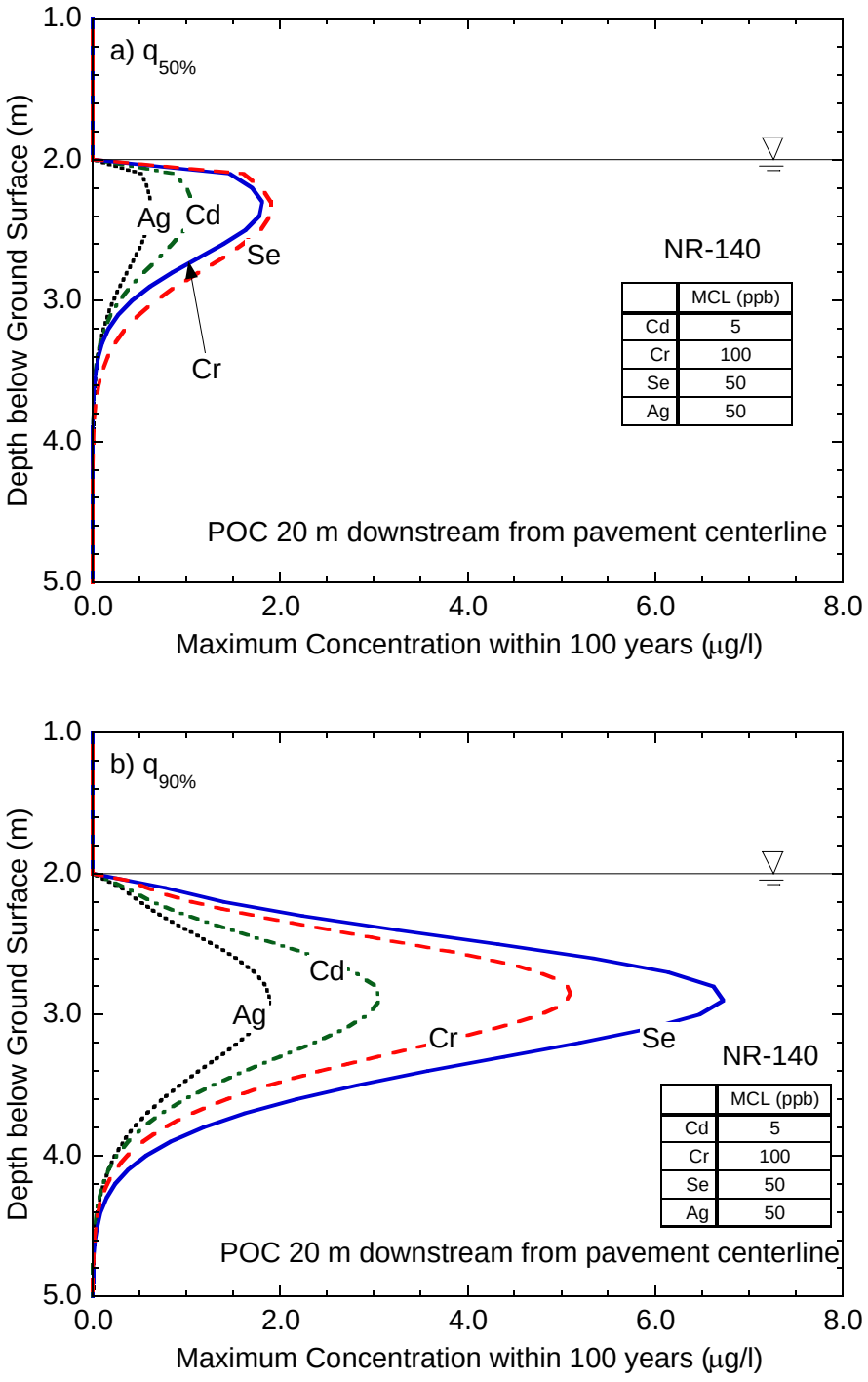

Fig. 29. Predicted maximum concentrations at POC in bottom ash section at STH 60. Simulation was conducted using volumetric leachate flux from (a) inner lysimeter and (b) outer lysimeter. $q_{50\%}$ is 50th percentile of measured volumetric leachate flux and $q_{90\%}$ is 90th percentile of measured volumetric leachate flux.

APPENDIX

FIELD AND LABORATORY DATA FROM STH 60 TEST SECTIONS

A1. INTRODUCTION

Five test sections were constructed along a 1.4 km stretch of Wisconsin State Highway (STH) 60 near Lodi, Wisconsin (USA) to evaluate alternative working platforms for highway construction on soft subgrades. One of the test sections was constructed with bottom ash and another with fly-ash-stabilized subgrade (a mixture of existing subgrade and 10% fly ash by dry weight blended *in situ*). A control section was also constructed with crushed dolostone (Fig. A1).

During construction, two pan lysimeters were placed beneath each test section to monitor the quality and quantity of water discharged from the base of the pavement. Samples were collected from these lysimeters over a 5-year period and analyzed for concentrations of cadmium (Cd), chromium (Cr), selenium (Se), and silver (Ag). Laboratory tests were also conducted on the byproducts using batch water leach tests (WLTs) and column leach tests (CLTs), both of which are commonly used to assess the suitability of byproducts for re-use. This appendix describes and compares the elution patterns and concentrations observed in field and from the WLTs and CLTs. Peak concentrations observed in the field are also compared with ground water quality standards stipulated by the State of Wisconsin. The focus is on the test sections constructed with bottom ash and fly ash. A complete summary of data from all test sections can be found in Sauer et al. (2005).

A2. MATERIALS

A summary of the index and physical properties of the byproducts and the subgrade soil at the field site can be found in Table A1 along with classifications of these materials according to the Unified Soil Classification System (USCS) and the AASHTO classification system. Particle size distribution curves for the materials are shown in Fig. A2.

The fly ash and bottom ash used in this study are from a dry bottom furnace at Alliant Energy's Columbia Power Station that burns sub-bituminous coal from the Wyoming Powder River Basin. The bottom ash is coarse-grained material that classifies as well-graded sand (SW) in the USCS and A-3 in the AASHTO system. The fly ash contains 98% fines and classifies as elastic silt (ML) in the USCS, A-4 in the AASHTO system, and Class C in ASTM C 618.

The test section with a fly-ash-stabilized subgrade was constructed by blending fly ash into the existing subgrade (10% fly ash by dry weight) to a depth of 300 mm using a reclaimer. The subgrade soil classifies as low plasticity clay (CL) in the USCS and A-6 in AASHTO. Immediately after blending, the mixture was compacted to 15.4 kN/m^3 using a tamping foot, steel drum, and rubber tire compactors. The water content was 21% $\pm$ 2% when the mixture was compacted. Details on the construction can be found in Edil et al. (2002).

Water leach tests (WLTs) were conducted on the bottom ash, fly ash, and the soil-fly ash mixture following the procedure in ASTM D 3987. Based on these analyses, the byproducts meet the requirements in Section NR 538 of the *Wisconsin Administrative Code* for use in confined geotechnical applications. Results of the WLTs are discussed in Section 4.

A3. METHODS

A3.1 Field Lysimeters

Two pan lysimeters (3.75 m x 4.75 m) were installed beneath each section at the STH 60 site to collect leachate draining from the bottom of the profile. A schematic of a typical set of lysimeters is shown in Fig. A3. One lysimeter was located directly under the centerline of the highway and the other was located at the edge, with one-half of the lysimeter under the highway shoulder. The lysimeters

were constructed with 1.5-mm-thick textured HDPE geomembrane overlain by a geocomposite drainage layer. Water collected by the lysimeters drains to 120-L HDPE drums located below ground surface adjacent to the highway. Additional information on the lysimeters can be found in Bin Shafique et al. (2002).

Samples were collected from the drums periodically. The sampling frequency depended on the rate of drainage from the lysimeters, which varied seasonally. Sampling was least frequent in the winter when freezing occurred and most frequent in the spring when snowmelt and rainfall are more common. During each sampling event, water contained in each drum was removed with a pump, the total volume of water in the drum was recorded, and samples were collected for chemical analysis.

Monitoring wells were also installed adjacent to the sections constructed with fly ash and bottom ash and the control section. However, because the fine-grained subgrade soils at the field site have very low hydraulic conductivity, samples could not be collected from the monitoring wells during the monitoring period. A description of the monitoring wells is attached.

A3.2 Water Leach Tests

Water leach tests (WLTs) were conducted on the byproducts following the methods in ASTM D 3987, where 70 g of dry solid is mixed with 1400 ml of ASTM Type II water (L-S ratio = 20:1) in 2 L HDPE bottles that are rotated continuously for 18 hr at 29 rpm. After rotation, the solution was allowed to settle for 5 min and the supernatant was collected, filtered, and the pH was recorded. Samples of the supernatant were stored in sealed HDPE bottles with no headspace.

A3.3 Column Leach Tests

Column leach tests (CLTs) were conducted on each of the industrial byproducts to evaluate leaching under flow-through conditions. A rigid-wall procedure was used for the bottom ash and a flexible-wall permeameter was used for the soil-fly ash mixture. Methods described in Lee and Benson (2006) were used for the bottom ash and methods described in Bin Shafique et al. (2006) were used for the soil-fly ash mixture. Upward flow was imposed using a peristaltic pump set at 7 mL/hr (2 mm/d).

A 0.1 M LiBr solution was used as the influent for all CLTs. The solution was prepared by dissolving LiBr salt (99+% pure, from Aldrich Chemical Company) in de-ionized water followed by exposure to the atmosphere until pH 6 was reached. The concentration was selected so that the ionic strength was similar to pore water in pavement layers (Karczewska et al. 1996). Effluent from the columns was collected in sealed Teflon bags that were emptied after approximately 30~60 mL of flow accumulated (≈ 0.1 PVF). Volume and pH of the effluent were recorded each time a bag was emptied and a 45 mL sample was collected for chemical analysis.

The bottom ash was tamped into a compaction molds in 3 lifts using a standard Proctor hammer until the dry unit weight in the field (17.1 kN/m^3) was reached. The soil-fly ash mixture (10% ash) was prepared at a molding water content approximately 2% dry of optimum water content to simulate conditions that existed during construction of the test sections (Bin Shafique et al. 2002). The mixture was blended by hand until uniform and then sprayed with deionized water until the desired water content (17.3%) was reached. The mixture was compacted one hour after mixing to simulate the delay between mixing and compaction that occurs during construction. After compaction, the specimens were extruded from the compaction molds, sealed in plastic, and cured for 7 days in a 100% humidity

environment prior to testing to simulate the condition existing in the field (Edil et al. 2002). The specimen was compacted to a dry unit weight 15.4 kN/m^3, which is the same dry unit weight obtained in the field.

A3.4 Chemical Analysis of Effluent

Procedures described in Bin Shafique et al. (2002) were followed for sample handling, preservation, analysis, and quality control. All samples were filtered through a 0.45-μm membrane filter as required in ASTM D 3987, acidified to pH < 2 using metals-grade nitric acid, and stored in sealed HDPE bottles at 4°C prior to testing. Blanks were prepared and handled using the same protocol used for the other samples.

All samples from the CLTs and lysimeters were analyzed for Cd, Cr, Se, and Ag. The samples were analyzed by atomic adsorption (AA) spectrometry or inductively coupled plasma optical emission spectrometry (ICP-OES). AA was used earlier in the study and ICP-OES later in the study. A switch was made to ICP-OES to make testing more efficient.

The AA analyses were conducted using a Varian SpectrAA-800 atomic adsorption (AA) spectrometer equipped with a GTA-100 graphite tube atomizer, an automated sample dispenser, and a Varian SpectAA-800 Data Station. Procedures described in USEPA Standard Methods 213.2, 218.2, 270.2, and 272.2 were followed for the AA analyses. The AA was calibrated using 4 standard dilutions to create a calibration curve. Samples were analyzed using ICP-OES following USEPA Method 6010B using a Perkin Elmer Optima 4300 DV ICP-OES or a Thermo Jarrell Ash ICAP 61E Trace Analyzer. The detection limits for the AA and ICP-OES analyses are in Table A2.

Duplicate tests were conducted on each sample and samples with a relative standard deviation (RSD) > 5% were re-tested. Blanks were included every 10 to 20 analyses and the calibration was verified every 10 analyses. A reagent blank was tested every 20 samples and a spiked sample was analyzed every 10 samples.

A4. RESULTS AND DISCUSSION

A4.1 Lysimeters

A4.1.1 Hydrologic Data

Volumetric flux in each lysimeter over the 5-year monitoring period is shown in Fig. A4 along with precipitation data from the National Oceanic and Atmospheric Administration (NOAA) station in Prairie du Sac, WI (≈ 16 km from the site). The gap between July 2002 and June 2003 occurred due to a lapse in funding. The volumetric flux from each test section varies seasonally, with higher fluxes typically occurring in spring and summer when precipitation rates are higher and temperatures are above freezing. The lowest volumetric fluxes occur during winter, when frozen ground conditions are common

A4.1.2 Metals Concentrations

Metals concentrations in leachate from the lysimeters over the monitoring period are shown in Figs. A5-8. Peak concentrations observed in the lysimeters along with the number of pore volumes of flow to reach the peak concentration are summarized in Table A3.

Cd and Cr concentrations in leachate (Figs. A5 and A6) generally are highest in the early portion of the monitoring period and then steadily decrease, a pattern referred to as “first-flush” leaching (Edil et al. 1992). Peak concentrations of

Cd and Cr in leachate from the bottom ash and fly-ash-stabilized-soil sections are higher than the peak concentrations in leachate from the control section. After 3 years, the Cd and Cr concentrations are comparable for all test sections (<5 μg/L for Cd, <10 μg/L for Cr).

The elution pattern for Se (Fig. A7) sharply contrasts the patterns for Cd and Cr (Figs. A5 and A6). Se concentrations are low (or are decreasing) during the first 18 mos and much higher during the final 24 mos. Peak Se concentrations from each section were similar, although the fly-ash-stabilized-soil test section typically had lower Se concentrations than the other test sections throughout the monitoring period. At the end of the monitoring period, Se concentrations from all sections were comparable. The one exception is the Se concentration in the leachate from the inner lysimeter in the fly-ash-stabilized-soil section, which dropped below detection limits (<10 μg/L) after 3 yr.

A possible explanation for the elevated Se concentrations in the latter portion of the monitoring period is that another material in the pavement structure is eluting Se. The similarity of the Se elution patterns and concentrations in leachate from each of the test sections during the latter portion of the monitoring period is consistent with this hypothesis. All of the test sections used the same base course material (recycled asphalt and crushed limestone), which could be the source of Se. Alternatively, changing redox conditions may be occurring, resulting in transformation of Se(IV) to Se(VI). Se(IV) is cationic, more strongly adsorbed by soil solids, and less mobile, whereas Se(VI) forms anionic complexes that are weakly sorbed and more mobile. However, no tests were conducted to identify the Se species present in leachate, and the redox conditions present in the field are also unknown.

Ag followed a first-flush elution pattern for the bottom ash and control sections, with concentrations beginning to drop within 18 mos and 0.5 PVF and decreasing to less than 3 μg/L during the final two years of the monitoring period. The two lysimeters in the fly-ash-stabilized-soil section yielded remarkably different Ag elution patterns. Ag concentrations in leachate from the outer lysimeter never exceeded 5 μg/L and followed a first-flush pattern. In contrast, Ag concentrations in the inner lysimeter increased to over 100 μg/L after 3 yr, and remained above 20 μg/L for the remainder of the monitoring period. The peak Ag concentration in the leachate from the inner lysimeter in the fly-ash-stabilized soil section occurred after 1.9 PVF.

Peak concentrations in each test section constructed with byproducts were divided by peak concentrations from the control section to define normalized peak concentrations. The normalized concentrations are summarized in Table A3. One of the cases (fly-ash-stabilized soil – Se) has a normalized peak concentrations less than unity (i.e., metals eluted at a lower peak concentration from the fly-ash-stabilized soil section than from the control section). In all other cases, the normalized peak concentrations are greater than unity. The normalized peak concentrations typically are highest for Cr and lowest for Se.

A4.2 Comparison of Peak Concentrations in Lysimeters and WLTs

Cd, Cr, Se, and Ag concentrations in the leachate from the WLTs are summarized in Table A4 along with peak concentrations from the lysimeters and CLTs. Concentrations from the WLTs are below detection limits many cases, whereas peak concentrations in the lysimeters are always above detection limits (Table A4). A graph of peak concentrations from the lysimeters vs. corresponding concentrations from the

WLTs is shown in Fig. A9. Peak concentrations from the lysimeters generally are higher than those from the WLTs; in only one case is the peak concentration from the WLT higher than the peak concentration from the lysimeters (Cr from fly-ash-stabilized soil).

Differences in liquid-solid ratio may be responsible for the disparity between the peak field concentrations and the concentrations from the WLTs. A dilution calculation based on the PVF at the peak lysimeter concentration indicates that the L-S ratio in the field (at peak concentration) ranges between 0.5-2.2, whereas a L-S ratio of 20 was used in the WLTs (i.e., 9.1 – 40 times larger than the L-S ratio at peak concentration in the field). Differences in pH and redox conditions may also have contributed to the disparity, but cannot be quantified with the data that are available.

A4.3 Comparison of Elution in Lysimeters and CLTs

Peak concentrations from the CLTs are summarized in Table A5. A comparison of peak concentrations from the lysimeters and peak concentrations from the CLTs is shown in Fig. A10. Many of the peak lysimeter and CLT concentrations differ by less than a factor of 10. Peak Se and Cd concentrations in the lysimeters tend to be higher than those from the CLTs, Ag concentrations from the lysimeters and the CLTs tended to be more comparable, and peak Cr concentrations from the lysimeters tend to be lower than those form the CLTs.

Elution curves for Cd from the test sections and CLTs are shown in Fig. A11. Similar elution patterns for Cd were obtained in the field and the CLTs for the test section constructed with fly-ash-stabilized soil (first-flush leaching). In fact, for the fly-ash-stabilized soil, the Cd elution patterns in the field and CLTs are nearly identical.

Elution curves for Cr from the test sections and CLTs are shown in Fig. A12. The elution curves from the CLTs on bottom ash and fly-ash-stabilized-soil exhibit a similar

pattern as those from the field, although the peak Cr concentrations from the CLTs were larger than those in the field.

Elution curves for Se from the test sections and CLTs are shown in Fig. A13. Similar curves were obtained from the CLTs and the field only for the fly-ash-stabilized-soil. For the other bottom ash, Se concentrations from the CLTs were nearly always less than the detection limit (4.0 μg/L), whereas peak concentrations of Se in the field ranged from 89 μg/L to 151 μg/L. The large discrepancy between Se concentrations from the CLTs and those measured in the field also supports the hypothesis that another material in the pavement structure, which was not tested in the CLTs, is the source of Se.

Elution curves for Ag from the test sections and CLTs are shown in Fig. A14. Similar elution patterns were obtained from the field and CLTs for bottom ash and fly-ash-stabilized soil. For the fly-ash-stabilized soil, however, Ag concentrations increased in one lysimeter and decreased in the other during the latter portion of the monitoring period, whereas the CLT concentrations decreased slightly over the same range of PVF.

A5. IMPLICATIONS FOR GROUNDWATER QUALITY

Groundwater quality standards applicable to the field site are defined in Section NR 140 (Groundwater Quality) of *Wisconsin Administrative Code*. The Wisconsin standards are the same as or lower than USEPA MCLs. A comparison of the Wisconsin standards for Cd, Cr, Se, and Ag and peak concentrations from the test sections is in Table A6. Cd concentrations in the leachate from the bottom ash and control sections exceeded the Wisconsin standard (5 μg/L) by a factor of 1.2-6.4 for the first 18 mos of the field test. However, in all cases, the Cd concentrations were below the Wisconsin standard after 16 mos and 0.6 PVF. Se concentrations exceeded the Wisconsin standard (50 μg/L) for all test sections by a factor of 1.8 to 3.0. Moreover, except for the fly-ash-stabilized soil, the Se concentrations increased and

then leveled off at a concentration exceeding the Wisconsin standard over the last 24 months of monitoring.

In contrast to Cd and Se, leachate concentrations exceeding the Wisconsin standard for Ag (50 μg/L) were only observed in the fly-ash-stabilized soil section (peak = 96 μg/L). Ag concentrations of this magnitude were only recorded in one lysimeter in the fly-ash-stabilized soil section, and the concentration in this lysimeter fluctuated between 19 and 113 μg/L over the last 24 months of the monitoring period. None of the test sections had Cr concentrations exceeding the Wisconsin standard (100 μg/L).

Leachate collected in the lysimeters is representative of pore fluid at the bottom of the pavement profile and represents water reaching groundwater only if the groundwater table is at the base of the pavement profile. In many roadways, the groundwater table will be deeper. Processes such as sorption, diffusion, dispersion, and dilution occurring in soils between the base of the pavement and the groundwater table will result in lower concentrations by the time the groundwater table is reached.

Bin Shafique et al. (2002) conducted a modeling study to simulate the transport of contaminants from working platforms constructed with byproducts to the groundwater table using a variably saturated model of flow and transport that was validated using data from field lysimeter studies. Their findings indicate that the maximum concentration 1 m below the pavement layer is approximately 20% of the peak concentration at base of the byproduct layer. At 5 m, the maximum concentration is approximately 10% of the peak concentration at the base of the byproduct layer.

Concentrations at the groundwater table obtained by applying these “dilution” factors are summarized in Table A6. In all cases, the estimated concentrations of Cd, Cr, Se, and Ag at the groundwater table are below Wisconsin standards when the groundwater table is at least 5 m below the byproduct layer. For cases where the groundwater table is 1 m below the byproduct

layer, the Wisconsin standards for Cd, Cr, Se, and Ag would be met for the bottom ash section. However, for the test section with fly-ash-stabilized soil, the Cd concentration modestly exceeds the Wisconsin standard, whereas the Cr, Se, and Ag concentrations are at least 40% lower than the Wisconsin standards.

A6. SUMMARY AND CONCLUSIONS

Leaching data from test sections constructed along a stretch of Wisconsin State Highway 60 near Lodi, WI have been presented and discussed in this report. Two of these test sections were constructed with coal combustion products (bottom ash or fly-ash-stabilized soil). One of the test sections was a control and was constructed with a layer of crushed dolostone instead of industrial byproducts. Both byproducts met the criteria in the *Wisconsin Administrative Code* for re-use in confined geotechnical fills.

Leachate draining from the test sections was collected in pan lysimeters and analyzed for concentrations of Cd, Cr, Se, and Ag. Batch water leach tests (WLTs) and column leach tests (CLTs) were also conducted on each of the byproducts using typical procedures used to evaluate the suitability of byproducts for use in earthwork applications. Concentrations of Cd, Cr, Se, and Ag from the WLTs and CLTs were compared with concentrations measured in the leachate collected in the field and with groundwater quality standards in the *Wisconsin Administrative Code*.

Leachate collected in the lysimeters had Cd, Se, and Ag concentrations exceeding Wisconsin groundwater quality standards. However, application of dilution factors to account for the reduction in concentration expected between the bottom of the pavement structure and the groundwater table showed that concentrations exceeding groundwater quality standards would not occur if the byproducts layer is at least 5 m above the groundwater table. For a separation distance of 1 m, only Cd would modestly exceed the groundwater quality standard directly beneath the centerline of the pavement.

Comparison of peak concentrations from the lysimeters and concentrations obtained from the WLTs indicated that WLTs generally underestimate peak field concentrations. Dilution caused by the large liquid-solid ratio used in the WLTs is partly responsible for the disparity between the field and WLT concentrations, although differences in pH and redox conditions may have been important as well.

Peak concentrations from the CLTs were closer to peak concentrations in the field than the concentrations from the WLTs. The elution patterns in the field and the CLTs (first flush or delayed response) generally were similar, although the magnitude of the concentrations differed. An exception is the fly-ash-stabilized soil, for which both concentrations and elution patterns from the field and the CLTs were similar.

An unusual rise in Se concentration was observed in all of the field lysimeters (including the control) later in the monitoring period, but in none of the CLTs. The presence of elevated Se concentrations in all lysimeters (and at similar concentration) suggests that Se is leaching from another source within the pavement structure, and not the byproducts. One potential source is the crushed rock or recycled asphalt in the base course layer. This observation illustrates that leaching from pavement structures is not limited to byproducts layers, and that other potential sources of contaminants should be considered when evaluating impacts to groundwater attributed to the use of industrial byproducts in highway construction.

A7. REFERENCES

Bin Shafique, S., Benson, C. H., and Edil, T. B. (2002). "Leaching of Heavy Metals from Fly Ash Stabilized Soils Used in Highway Pavements." Geo Engineering Report No. 02-14, Dept. of Civil and Environmental Engineering, University of Wisconsin-Madison.

Bin Shafique, S., Benson, C., Edil, T., and Hwang, K. (2006), Leachate Concentrations from Water Leach and Column Leach Tests on Fly-Ash Stabilized Soil, *Environmental Engineering Science*, 23(1), 51-65.

Edil, T. B., Benson, C. H., Bin Shafique, S., Tanyu, B. F., Kim, W. H., and Senol, A. (2002). "Field Evaluation of Construction Alternatives for Roadway Over Soft Subgrade." Geo Engineering Report No. 02-04, Dept. of Civil and Environmental Engineering, University of

Wisconsin-Madison.

Karczewska, A., Chodak, T., and Kaszubkiewicz, J. (1996). “The Suitability of Brown Coal as Sorbent for Heavy Metals in Polluted Soils,” *Applied Geochemistry*, Vol. 29, 343-349.

Lee, T. and Benson, C. (2006), Leaching Behavior of Green Sands from Gray-Iron Foundries Used for Reactive Barrier Applications, *Environmental Engineering Science*, 23(1), 153-167.

Sauer, J., Benson, C., and Edil, T. (2005). “Metals Leaching from Highway Test Sections Constructed with Industrial Byproducts.” Geo Engineering Report No. 05-21, Dept. of Civil and Environmental Engineering, University of Wisconsin-Madison.

Wisconsin (2004), *Wisconsin Administrative Code*, Revisor of Statutes Bureau, Madison, WI.

FIGURES

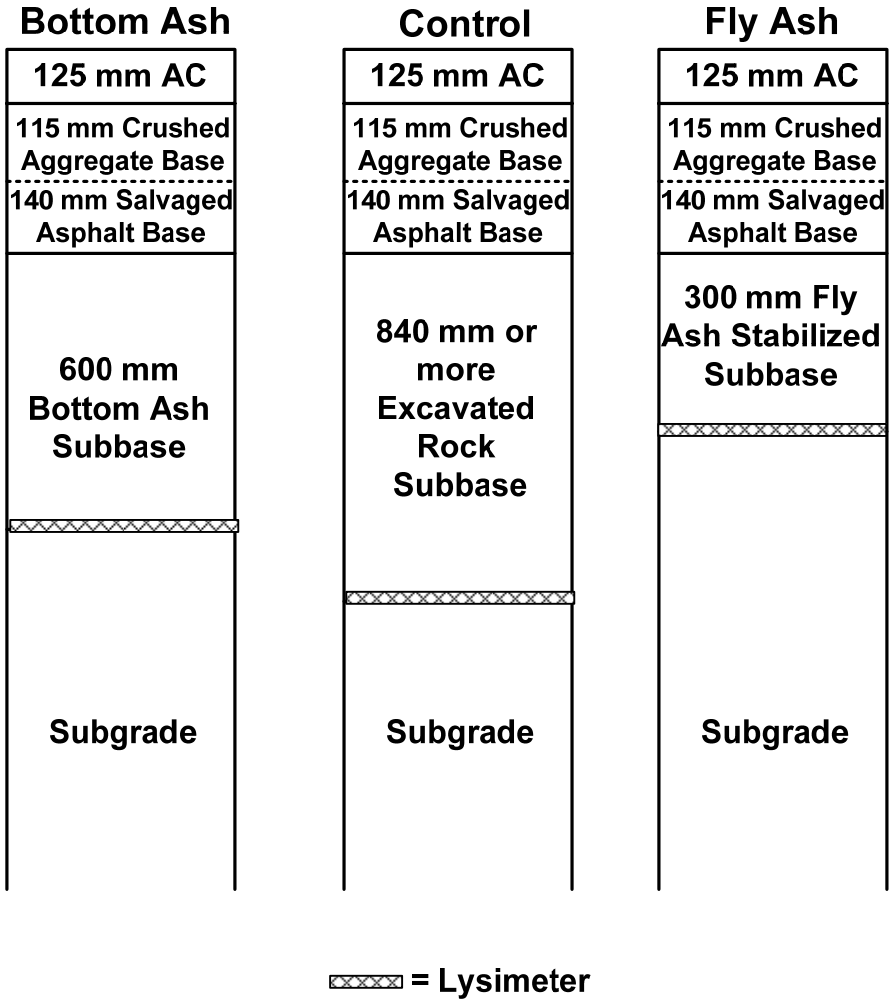

Fig. A1. Profiles of the test sections constructed using bottom ash, fly ash, and crushed rock (control) at STH 60 near Lodi, WI (AC = asphalt concrete).

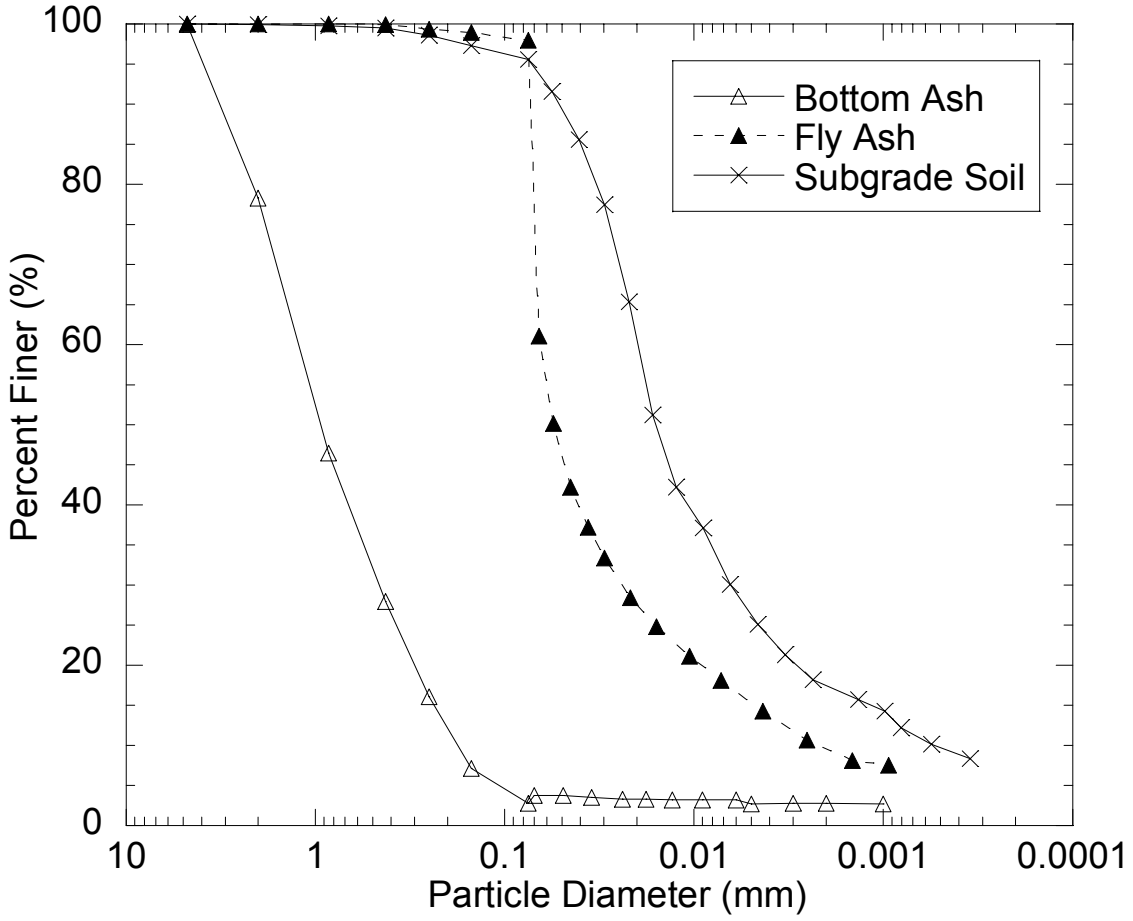

Fig. A2. Particle size distribution curves for bottom ash, fly ash, and subgrade soil used at STH 60 and for the laboratory tests.

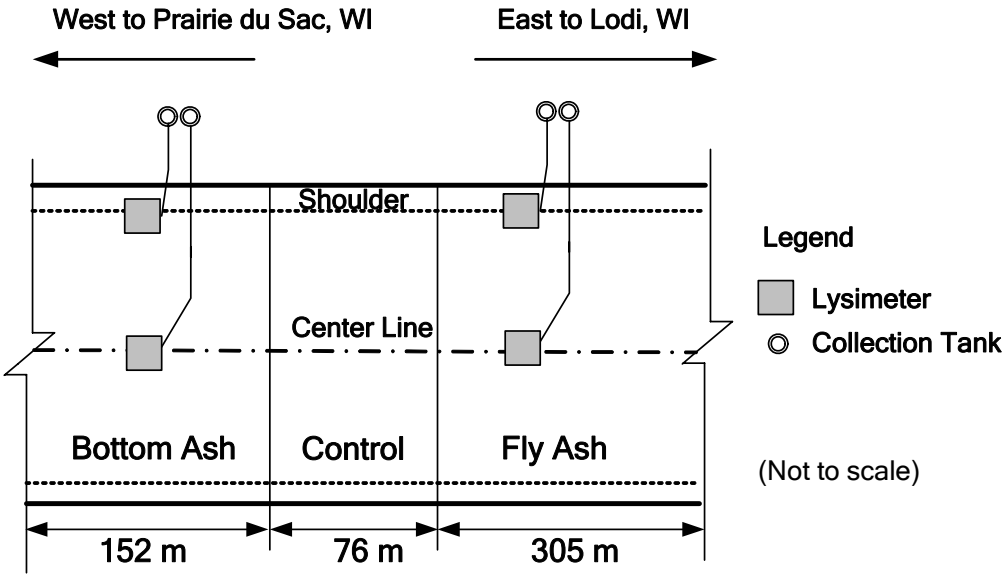

Fig. A3. Plan view of lysimeter layout for fly ash and bottom ash sections.

.

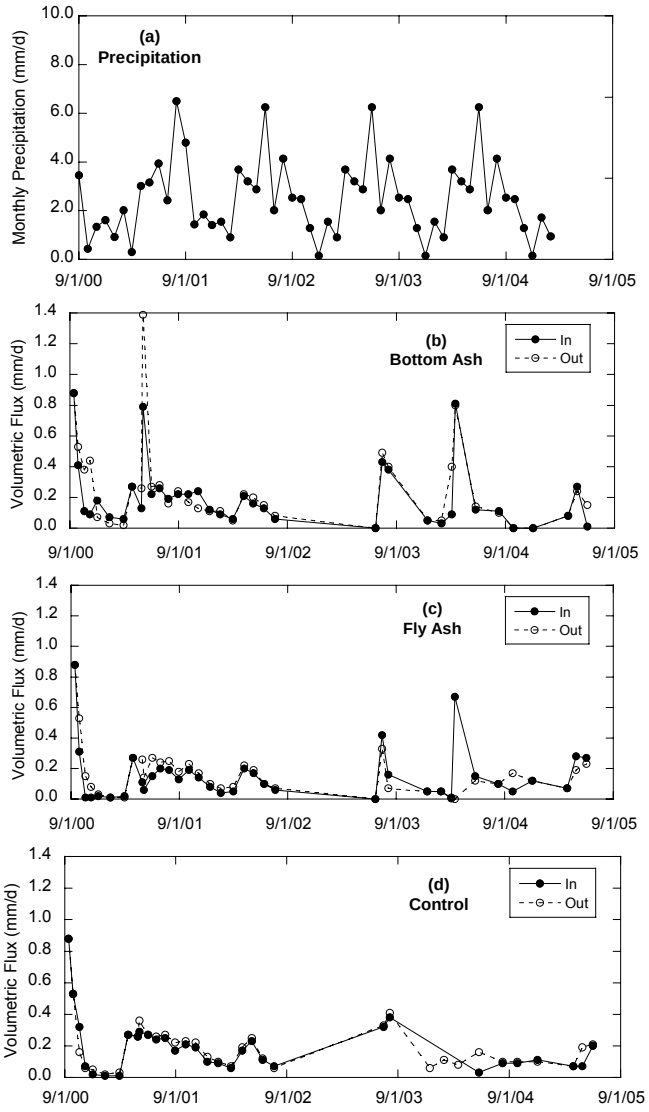

Fig. A4. Precipitation (a) and volumetric flux from (b) bottom ash, (c) fly-ash-stabilized-soil, and (d) control sections.

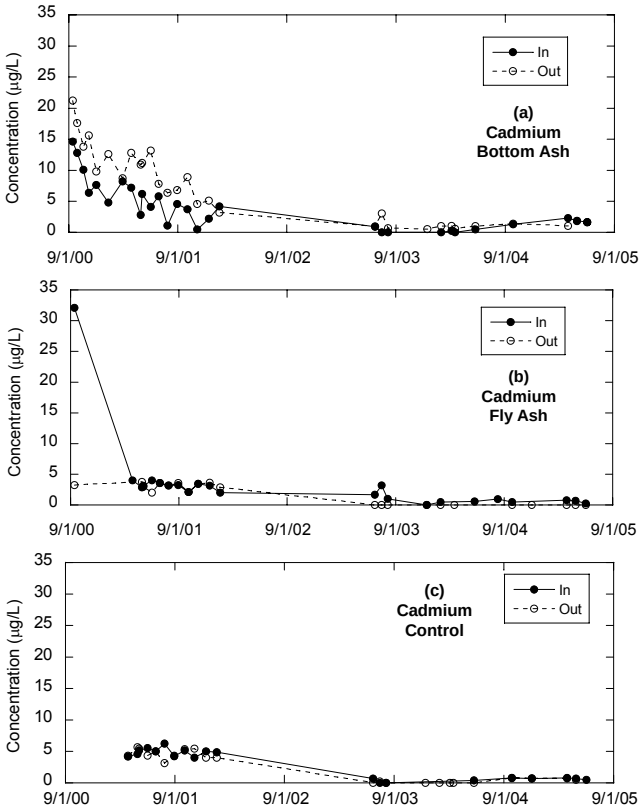

Fig. A5. Cd concentrations in leachate from lysimeters in (a) bottom ash, (b) fly-ash-stabilized-soil, and (c) control sections.

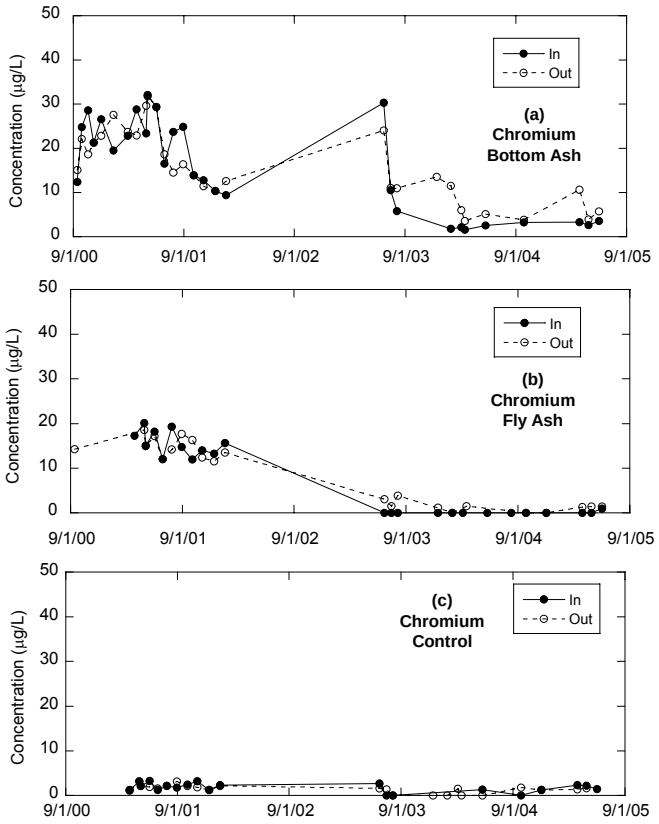

Fig. A6. Cr concentrations in leachate from lysimeters in (a) bottom ash, (b) fly-ash-stabilized-soil, and (c) control sections.

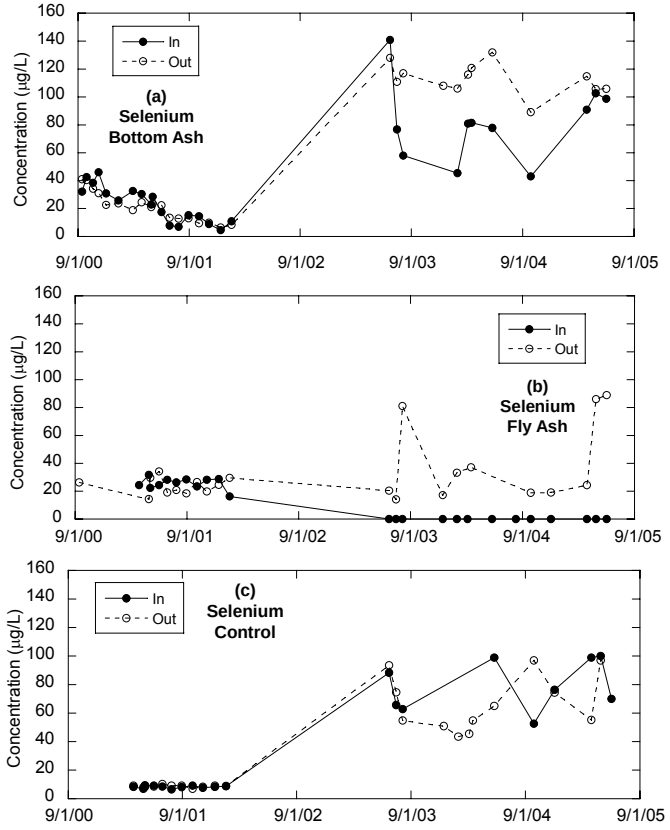

Fig. A7. Se concentrations in leachate from lysimeters in (a) bottom ash, (b) fly-ash-stabilized-soil, and (c) control sections.

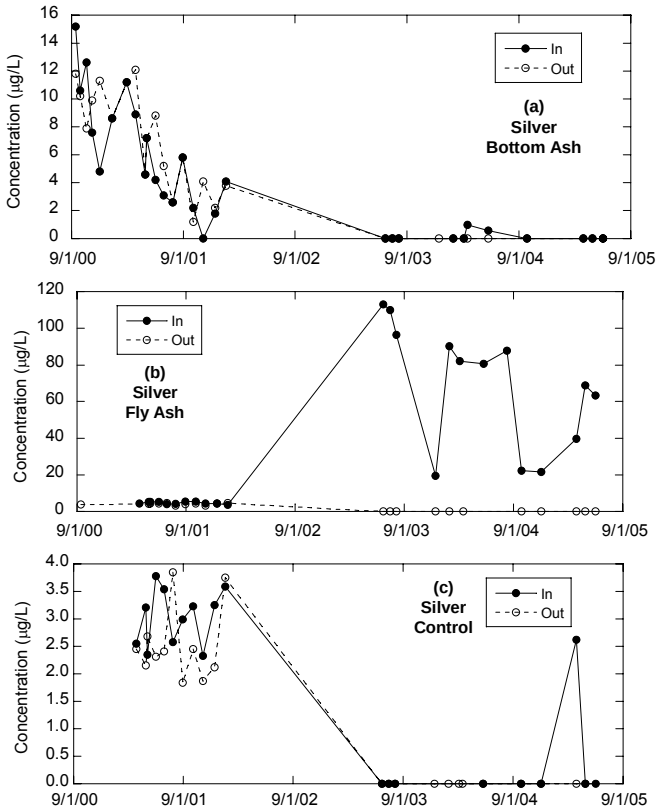

Fig. A8. Ag concentrations in leachate from lysimeters in (a) bottom ash, (b) fly-ash-stabilized-soil, and (c) control sections.

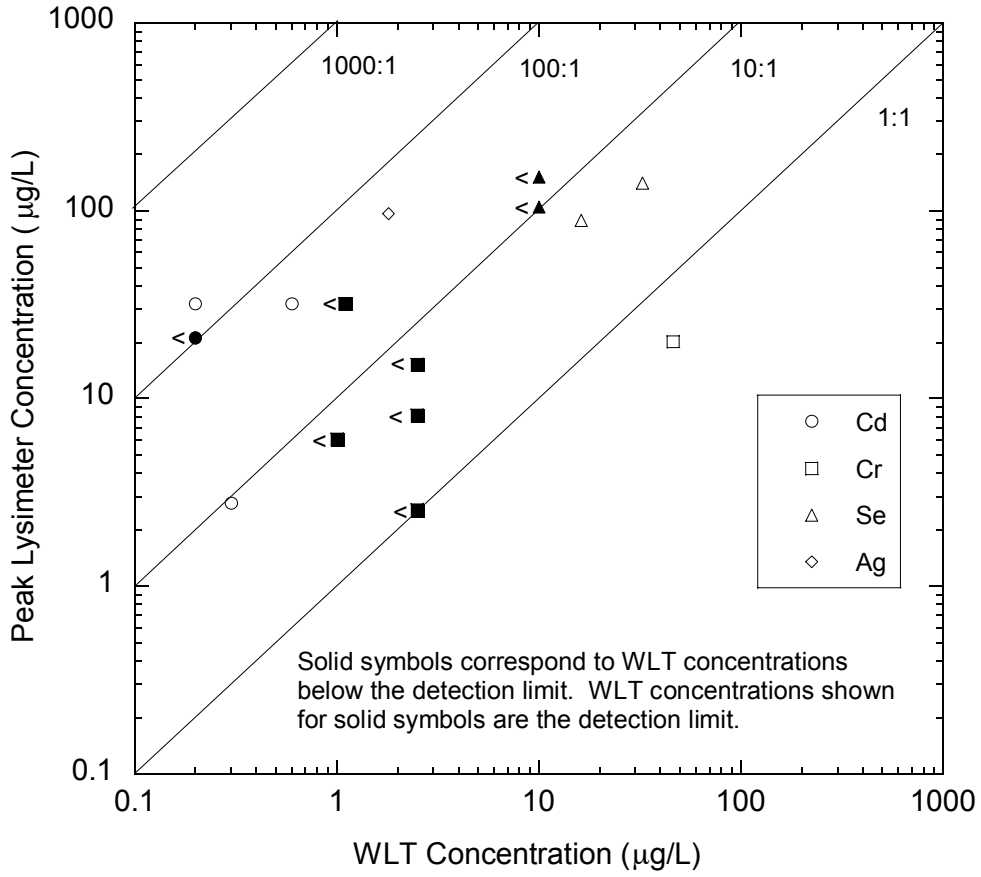

Fig. A9. Comparison peak concentrations found in the leachate from lysimeter tests to Cd, Cr, Se, and Ag concentrations from WLTs.

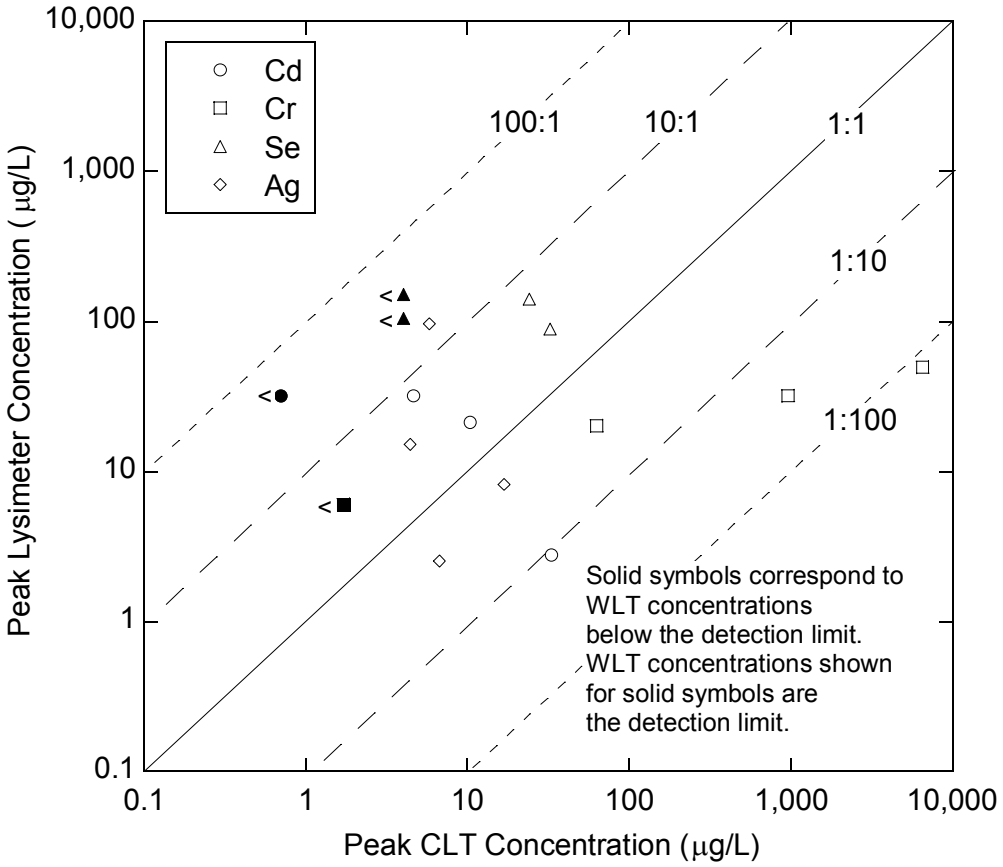

Fig. A10. Comparison of peak Cd, Cr, Se, and Ag concentrations in leachate from lysimeters to peak CLT concentrations.

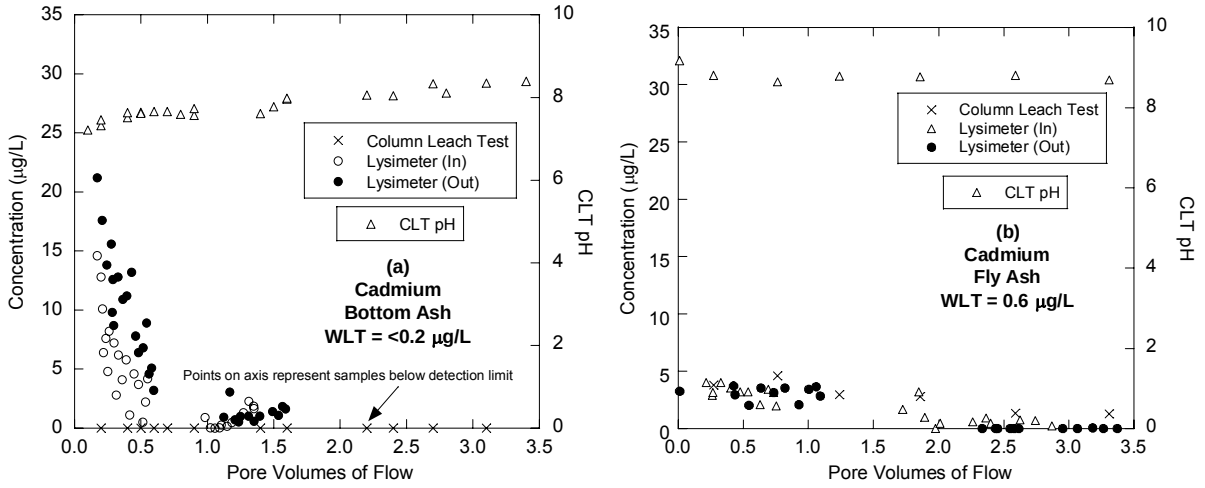

Fig. A11. Cd elution curves from CLTs and lysimeters: (a) bottom ash and (b) fly ash stabilized soil.

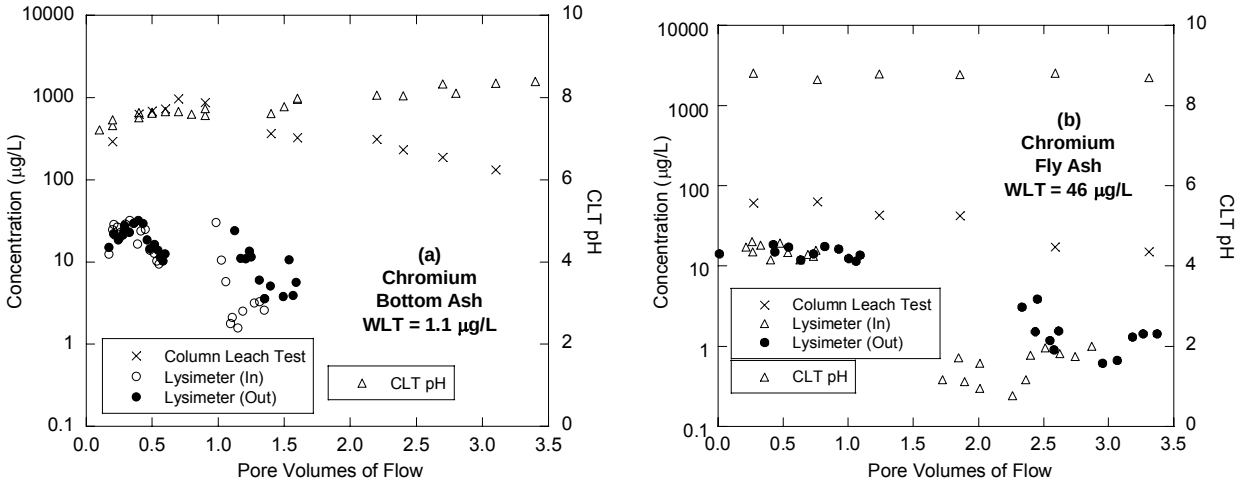

Fig. A12. Cr elution curves from CLTs and lysimeters: (a) bottom ash and (b) fly ash stabilized soil.

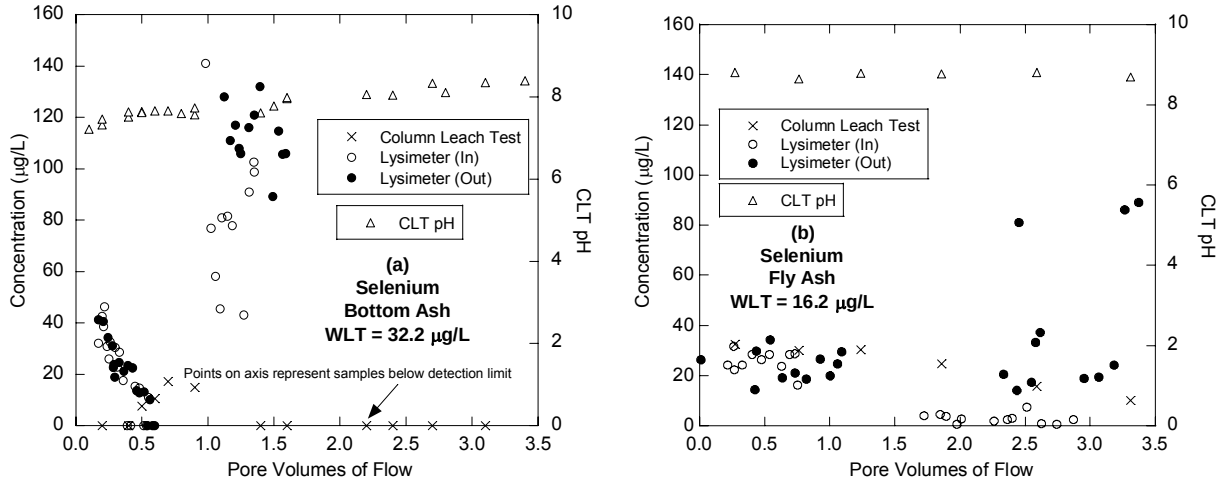

Fig. A13. Se elution curves from CLTs and lysimeters: (a) bottom ash and (b) fly ash stabilized soil.

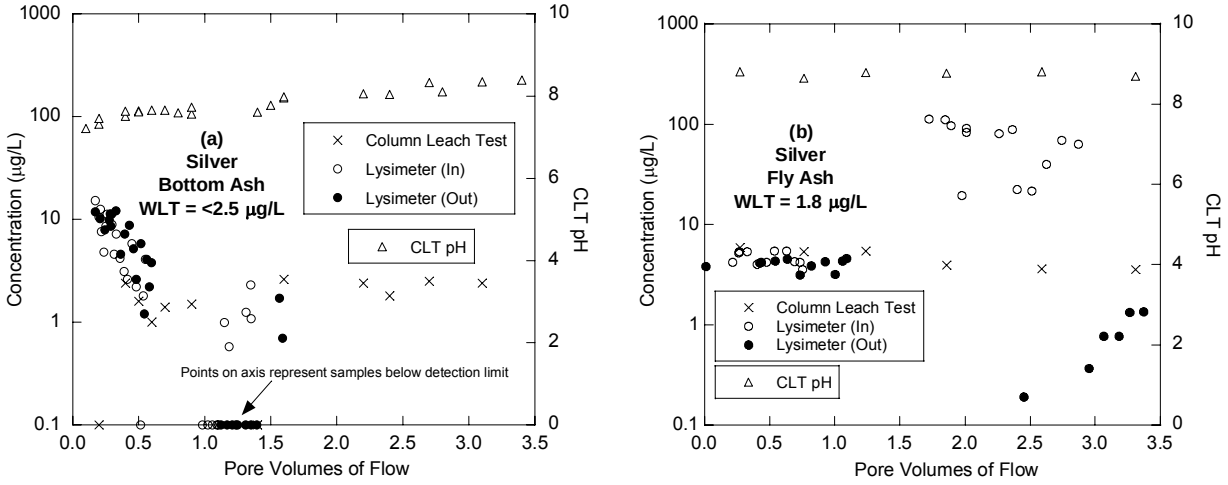

Fig. A14. Ag elution curves from CLTs and lysimeters: (a) bottom ash and (b) fly ash stabilized soil.

TABLES

Table A1. Physical properties and USCS and AASHTO classifications of the bottom ash, fly ash, and soil used in the study.

Material	Specific Gravity	D_{10} (mm)	D_{60} (mm)	C_u	Percent Fines (%)	USCS Symbol	AASHTO Symbol
Bottom Ash	2.65	0.2	1.5	8	3	SW	A-3
Fly Ash	2.70	0.001	0.07	70	98	ML	A-4
Subgrade Soil	2.70	0.0006	0.02	33	96	CL	A-6

Table A2. Limits of detection for ICP-OES and AA analysis.

Element	Detection Limit (μg/L)	
	ICP-OES	AA
Cd	0.2 or 0.7	0.1
Cr	1.0 or 1.7	2.0
Se	4.0 or 10.0	2.0
Ag	0.8 or 2.5	0.2

Note: Detection limits for the ICP-OES analyses differ depending on the instrument that was used for analysis.

Table A3. Peak Cd, Cr, Se and Ag concentrations found in the leachate from lysimeter tests on bottom ash, fly-ash-stabilized soil, and crushed rock (control), along with the PVF to reach the peak concentration.

Material	Cd			Cr			Se			Ag		
	Peak Lysimeter Conc. (μg/L)	Normalized Conc.	PVF to Peak Conc.	Peak Lysimeter Conc. (μg/L)	Normalized Conc.	PVF to Peak Conc.	Peak Lysimeter Conc. (μg/L)	Normalized Conc.	PVF to Peak Conc.	Peak Lysimeter Conc. (μg/L)	Normalized Conc.	PVF to Peak Conc.
Bottom Ash	21.2	3.42	0.17	32.1	9.73	0.33	141	1.41	0.98	15.2	3.90	0.17
Fly-Ash-Stabilized Soil	32.1	5.18	0.01	20.2	6.12	0.26	89	0.89	3.37	96.4	24.72	1.89
Control	6.2	1.00	0.51	3.3	1.00	0.44	100	1.00	1.23	3.9	1.00	0.51

Table A4. Cd, Cr, Se, and Ag concentrations in leachate from lysimeters, CLTs, and WLTs on bottom ash, and fly-ash-stabilized soil.

Material	Peak Lysimeter Conc. (μg/L)				Peak CLT Conc. (μg/L)				WLT pH and Concentration (μg/L)				
	Cd	Cr	Se	Ag	Cd	Cr	Se	Ag	Cd	Cr	Se	Ag	pH
Bottom Ash	21.2	32.1	141	15.2	10.3	961	24.1	4.4	<0.2	1.1	32.5	<2.5	10.3
Fly-Ash-Stabilized Soil	32.1	20.2	89.0	96.4	4.6	62.9	32.4	5.8	0.6	46	16.2	1.8	11.0
Fly Ash Alone	-	-	-	-	-	-	-	-	0.7	95	26	2.2	11.8

Note: Hyphen indicates that test was not conducted. <X.Y indicates concentration is below the detection limit (X.Y μg/L).

Table A5. Peak Cd, Cr, Se, and Ag concentrations, leachate pH, and PVF to peak concentration from CLTs on bottom ash and fly-ash-stabilized soil.

Material	Cd			Cr			Se			Ag		
	Peak CLT Conc. (μg/L)	pH at Peak Conc.	PVF to Peak Conc.	Peak CLT Conc. (μg/L)	pH at Peak Conc.	PVF to Peak Conc.	Peak CLT Conc. (μg/L)	pH at Peak Conc.	PVF to Peak Conc.	Peak CLT Conc. (μg/L)	pH at Peak Conc.	PVF to Peak Conc.
Bottom Ash	10.3	8.5	22.9	961	7.7	0.7	24	9.1	16.5	4.4	8.5	6.9
Fly-Ash-Stabilized Soil	4.6	8.6	0.8	62.9	8.6	0.8	32.4	8.6	0.3	5.8	8.6	0.3

Table A6. Peak lysimeter concentrations and estimated concentrations after 1 m and 5 m of migration from the byproduct layers based on analysis reported in Bin Shafique et al. (2002).

Material	Peak Lysimeter Conc. (μg/L)				Conc. after 1 m migration (μg/L)				Conc. after 5 m migration (μg/L)			
	Cd	Cr	Se	Ag	Cd	Cr	Se	Ag	Cd	Cr	Se	Ag
Bottom Ash	21.2	32.1	141	15.2	4.2	6.4	28.2	3.0	2.1	3.2	14.1	1.5
Fly-Ash-Stabilized-Soil	32.1	20.2	89	96.4	6.4	4.0	17.8	19.3	3.2	2.0	8.9	9.6
Wisconsin Standard	5	100	50	50	5	100	50	50	5	100	50	50

MONITORING WELLS

Well Profile:

Well ID: BA #1
Well Location: 20 ft South of STH 60, 50 ft West of Dettman Rd
Installation Date: 1/16/04

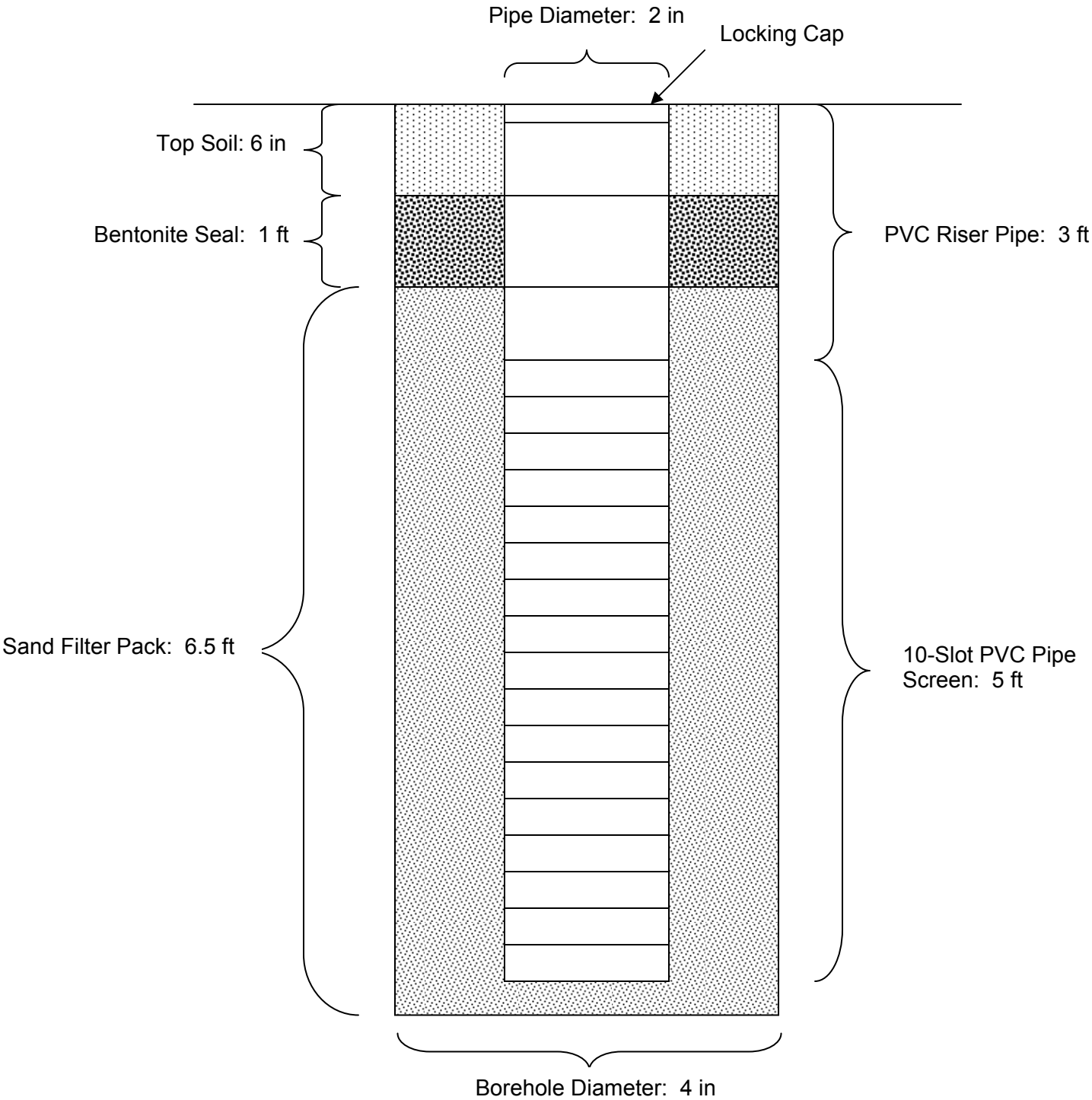

Well Profile:

Well ID: BA #2
Well Location: 15 ft North of STH 60, 50 ft West of Dettman Rd
Installation Date: 10/27/03

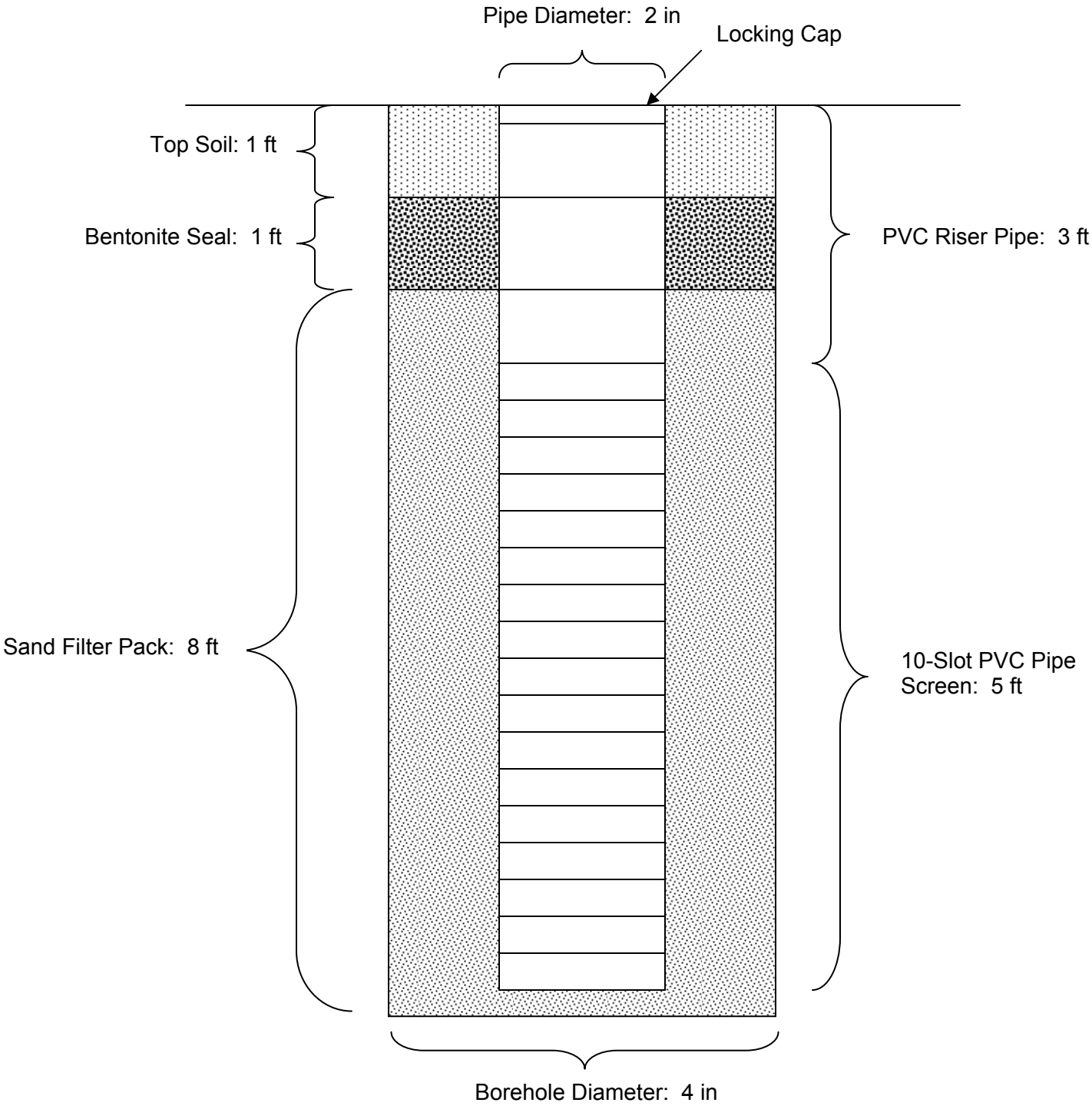

Well Profile:

Well ID: Control #1
Well Location: 20 ft South of STH 60, 50 ft East of Dettman Rd
Installation Date: 1/16/04

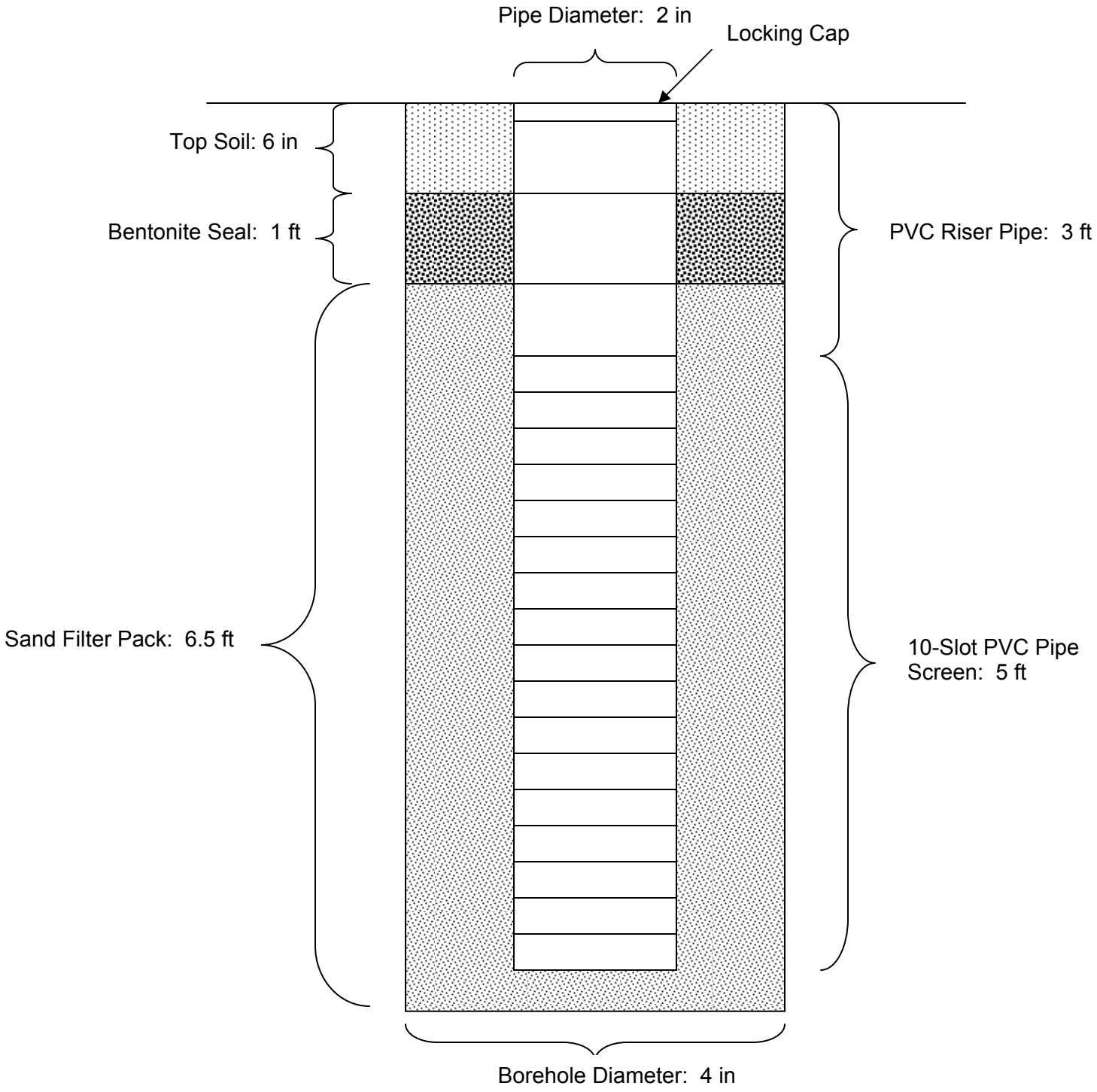

Well Profile:

Well ID: Control #2
Well Location: 20 ft North of STH 60, 50 ft East of Dettman Rd
Installation Date: 10/27/03

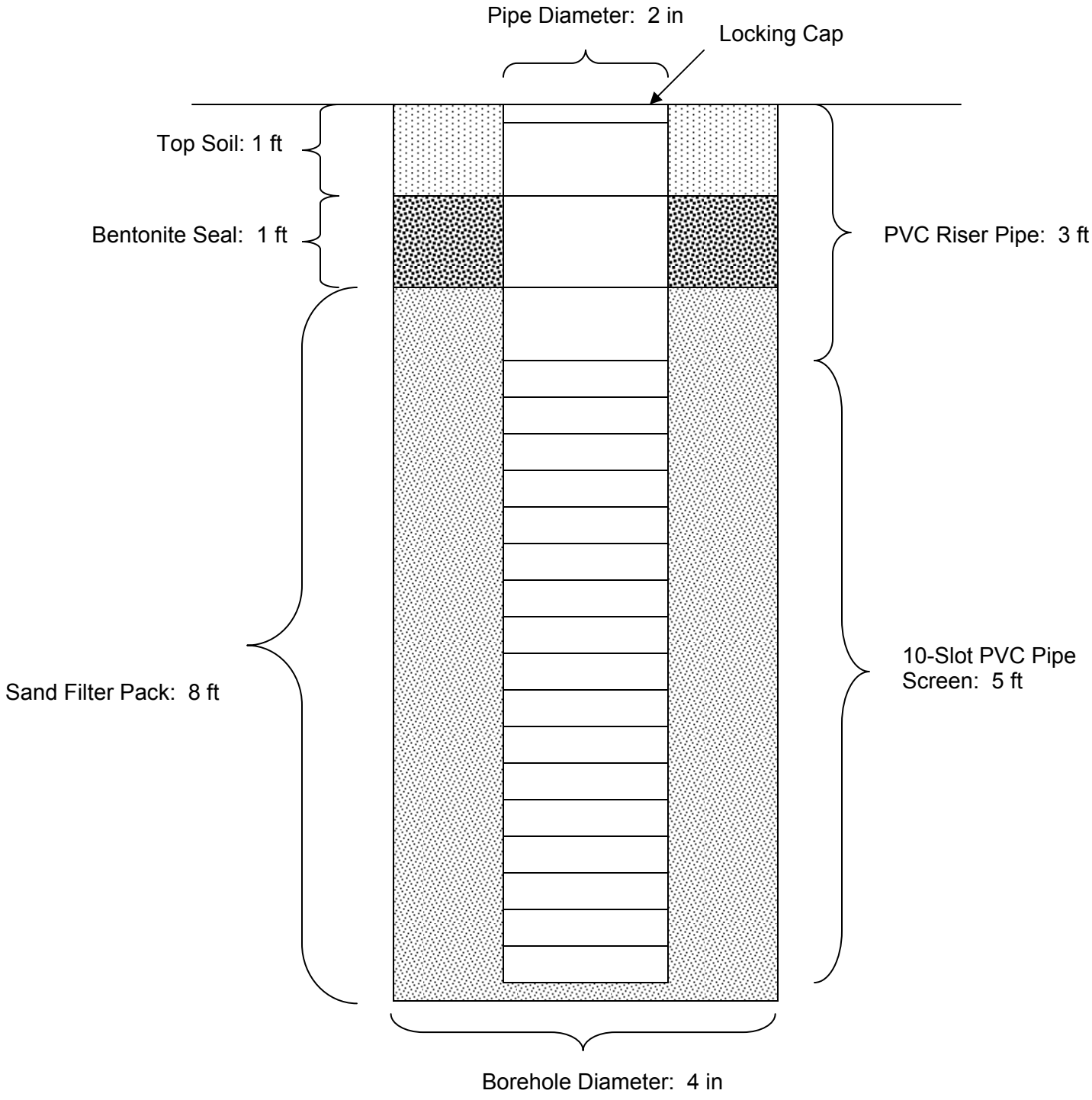

Well Profile:

Well ID: FA #1
Well Location: 20 ft South of STH 60, 350 ft East of Dettman Rd
Installation Date: 1/16/04

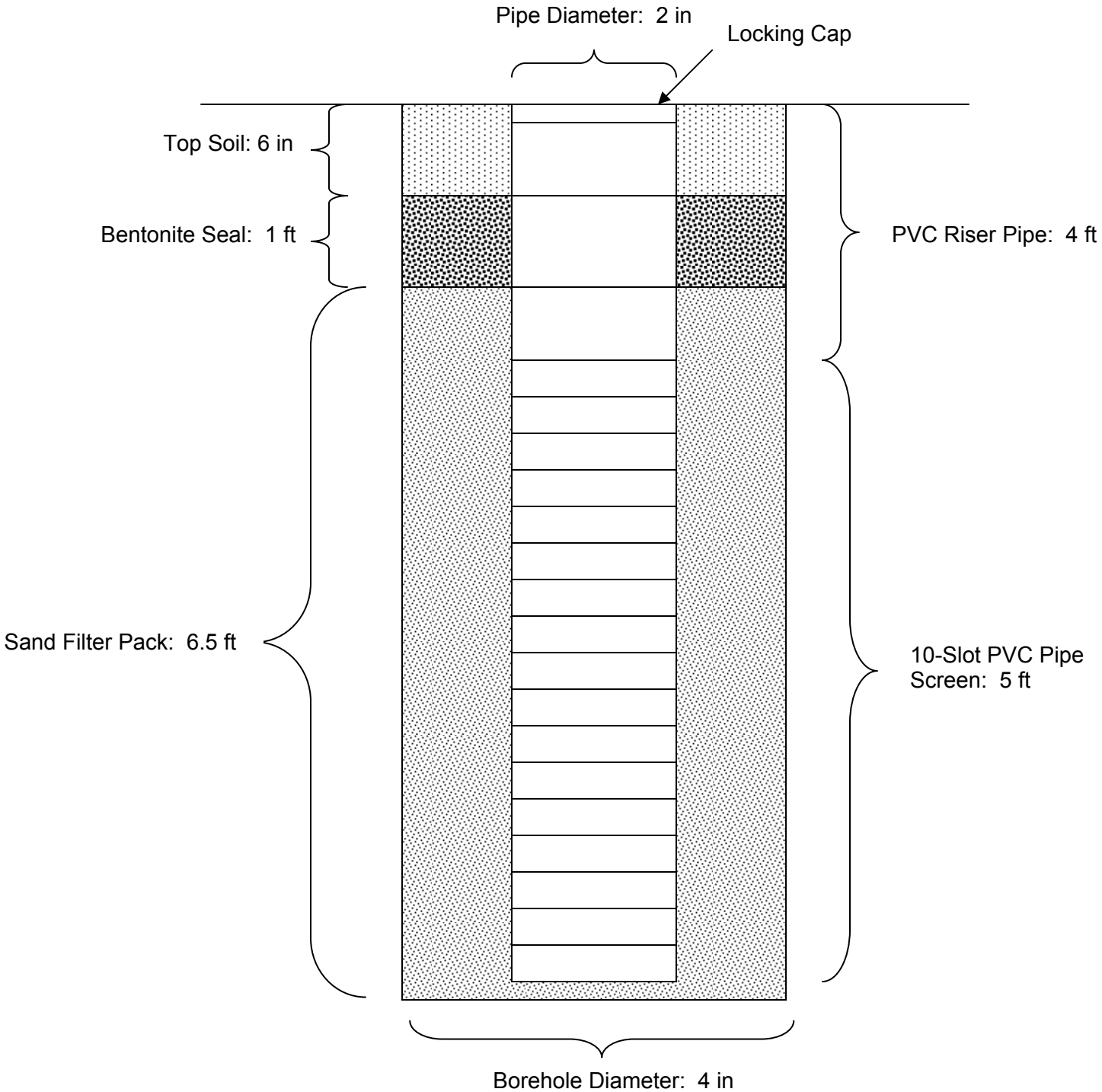

Well Profile:

Well ID: FA #2
Well Location: 20 ft North of STH 60, 350 ft East of Dettman Rd

Installation Date: 10/27/03